

Copyright
by
Jourdan Andersson
2017

**The Dissertation Committee for Jourdan Andersson Certifies that this is the
approved version of the following dissertation:**

**Combating Plague: Fighting a War on Two Fronts Through Vaccine
Design and New Therapeutic Intervention**

Committee:

Ashok Chopra, PhD, CSc, Mentor, Chair

Johnny Peterson, PhD

Juan Olano, MD

Vladimir Motin, PhD

Jason Rosenzweig, PhD

Dean, Graduate School

**Combating Plague: Fighting a War on Two Fronts Through Vaccine
Design and New Therapeutic Intervention**

by

Jourdan Alexandra Olga Andersson, B.S.

Dissertation

Presented to the Faculty of the Graduate School of
The University of Texas Medical Branch
in Partial Fulfillment
of the Requirements
for the Degree of

Doctor of Philosophy

**The University of Texas Medical Branch
November, 2017**

Dedication

To my family and friends who have supported me throughout this journey. Without their constant support and encouragement this would not have been possible.

Acknowledgements

I would first like to acknowledge and thank my mentor, Dr. Ashok Chopra, for his guidance, patience, and encouragement throughout my graduate studies. I would also like to thank my advisory committee, Drs. Johnny Peterson, Vladimir Motin, Juan Olano, and Jason Rosenzweig, for their guidance, ideas, valuable critiques, and encouragement. Special thanks to all members of Dr. Chopra's laboratory, both past and present, for providing help, advice, and support throughout my years in the lab. I would like to especially thank Michelle Kirtley for providing me with training, advice, and help throughout all my projects and Dr. Jian Sha for providing help and advice in the day to day challenges of research. I wish to give sincere thanks to Dr. Sara Dann and Dr. Sadhana Chauhan for their assistance with various aspects of this project. I am grateful to the Graduate School and the Human Pathophysiology and Translational Medicine Program, particularly the program director, Dr. Mark Hellmich, and the program coordinators, Donna Adams and Jennifer Ruiz-Betacourt. I sincerely thank all members of the Sealy Center for Vaccine Development, McLaughlin Endowment Fund, and T32 biodefense training grant committees for providing me with fellowships and travel awards to support my research project. I owe my deepest gratitude to my parents, Matts and Tammy Andersson, who have always been there to support and encourage me. And, finally, I would like to thank my fiancé, Greg Morano, for his love and support throughout this journey.

Combating Plague: Fighting a War on Two Fronts Through Vaccine Design and New Therapeutic Intervention

Publication No. _____1_____

Jourdan Alexandra Olga Andersson, PhD
The University of Texas Medical Branch, 2017

Supervisor: Ashok K. Chopra

Assumed by many to be a disease of the past, plague continues to be a globally prevalent disease, with thousands of cases estimated to occur annually. With no FDA-approved vaccine and therapeutics limited to antibiotics, there is an imperative need to develop new prophylactics as well as therapeutics against plague infection. Identification of new virulence factors of *Y. pestis* and understanding their role during the infection process is imperative in designing a better vaccine candidate. By using high-throughput signature-tagged mutagenic approach, we screened 5,088 mutants of *Y. pestis* CO92 to identify clones with impairment in dissemination to the spleen. In subsequent screens, 20/118 mutants exhibited attenuation when individually tested in a mouse model of bubonic plague. Upon sequencing, 3 of the attenuated mutants carried interruptions in genes encoding hypothetical type VI secretion system components. Through the generation of several T6SS associated gene deletion mutants, we have shown significant attenuation of the bacterium in pneumonic models of plague. Combinatorial deletions of T6SS associated genes resulted in further augmenting attenuation as well as providing protection against subsequent re-challenge with wild-type (WT) bacteria. For therapeutic development, traditional drug discovery is an inefficient and costly process; however,

systematic screening of Food and Drug Administration (FDA)-approved therapeutics for other indications in humans offers a rapid alternative approach. Utilizing this approach, we screened a library of 780 FDA-approved drugs to identify molecules that rendered RAW 264.7 murine macrophages resistant to cytotoxicity induced by the highly virulent *Yersinia pestis* CO92 strain. Following *in vitro* screening, a total of 17 prioritized drugs were chosen for further evaluation in a murine model of pneumonic plague to delineate if *in vitro* efficacy could be translated *in vivo*. Three drugs, doxapram (DXP), amoxapine (AXPN), and trifluoperazine (TFP), increased animal survivability despite not exhibiting any direct bacteriostatic or bactericidal effect on *Y. pestis in vitro* and having no modulating effect on crucial *Y. pestis* virulence factors, suggesting that DXP, AXPN, and TFP may modulate host cell pathways necessary for disease pathogenesis. Taken together, these results provide potential new tools in the arsenal to combat plague infection.

TABLE OF CONTENTS

List of Tables	xii
List of Figures	xiii
List of Abbreviations	xv
Chapter 1 <i>Yersinia pestis</i>	17
Introduction.....	17
Bacteriology.....	18
Factors contributing to bacterial virulence	19
Type III secretion system.....	19
F1 capsule	21
Plasminogen-activator protease	22
Type VI secretion system	22
History	25
Pandemics	25
Use as a biological warfare agent	26
Plague epidemiology and the challenges faced today	27
Global epidemiology and plague in the United States.....	27
Clinical disease, current treatments, and limitations	28
Where do we stand with plague vaccines?	30
Chapter 2: Characterization of the Type VI Secretion System (T6SS) as a Virulence Mechanism of <i>Yersinia pestis</i> CO92	33
Introduction.....	33
Materials and Methods.....	35
Bacterial strains and cell culture.....	35

Construction of T6SS cluster, single gene, and combinatorial deletion mutants.....	35
Testing for attenuation with <i>Y. pestis</i> CO92 T6SS mutant strains in a mouse model of pneumonic plague infection.....	38
Complementation of attenuated Hcp-encoding gene homolog deletion mutant strains.....	38
Production and purification of recombinant Hcp6 protein	39
Western blot analysis for detecting the T6SS effector Hcp6 and type III secretion system (T3SS) function in <i>Y. pestis</i> CO92 mutant strains	39
Assessing growth kinetics, cytotoxicity on host cells, phagocytosis, and intracellular survival of <i>Y. pestis</i> CO92 strains in RAW 264.7 murine macrophages	40
Statistical analysis.....	41
Results.....	42
Deletion of putative T6SS clusters and effectors resulted in varying levels of attenuation in pneumonic plague mouse model	42
Generation of combinatorial T6SS deletion mutants further augments attenuation in a murine model of pneumonic plague and provide some protection against re-challenge with WT CO92	45
Characterization of growth kinetics and expression of effectors by attenuated T6SS mutant strains of <i>Y. pestis</i> CO92 <i>in vitro</i>	47
Role of T6SS host cell cytotoxicity following <i>Y. pestis</i> infection.....	52
Quantification of phagocytosis and intracellular survival of T6SS deletion mutant strains	52

Discussion.....	55
Chapter 3: Development and Testing of New Therapeutics Targeting Host Genes	
to Combat Plague Infection	60
Introduction.....	60
Materials and Methods.....	61
Bacterial strains and cell culture.....	61
Reagents.....	62
Screening for macrophage cell viability	62
Screening for inhibition of <i>Y. pestis</i> CO92 intracellular survival.....	64
Testing lead drugs in <i>Y. pestis</i> CO92 pneumonic plague model	64
Screening for dose response effects on macrophage viability following drug treatment and infection with <i>Y. pestis</i>	65
Growth kinetics and sensitivity of <i>Y. pestis</i> CO92 to TFP, DXP and AXPN	67
Evaluation of <i>Y. pestis</i> CO92 virulence factor expression and plasminogen activator (Pla) protease activity in response to TFP, DXP, and AXPN.....	67
Testing TFP, AXPN, and DXP as therapeutics in a murine model of pneumonic plague infection alone or in combination with levofloxacin	68
Resistance of <i>Y. pestis</i> CO92 to DXP- and AXPN-treated serum.....	69
Bacterial proliferation in murine lungs following infection and treatment with DXP	70
Statistical analyses	70
Results.....	70
A high-throughput <i>in vitro</i> screen identified FDA-approved drugs that are effective at inhibiting host cell cytotoxicity during <i>Y. pestis</i> CO92 infection	70

Quantification of bacterial survival <i>in vitro</i> identified 3 drugs capable of limiting host cell death and decreasing intracellular <i>Y. pestis</i> CO92 survival	73
Three drugs exhibited protection in the murine pneumonic plague infection model	73
TFP, DXP, and AXPB exhibited a dose-response effect on macrophage viability after <i>Y. pestis</i> CO92 infection	78
TFP, DXP, and AXPB exhibited no bactericidal or bacteriostatic effects on <i>Y. pestis</i> CO92	79
TFP, DXP, and AXPB exhibited no effects on <i>Y. pestis</i> CO92 virulence factors.....	80
TFP, AXPB, and DXP exhibit therapeutic efficacy in a murine model of pneumonic plague infection.....	82
Animals treated with TFP, AXPB, or DXP during initial infection exhibit some protection upon re-challenge with <i>Y. pestis</i> CO92.....	86
Treatment of AXPB or DXP does not alter serum resistance of <i>Y. pestis</i> CO92	88
Treatment with DXP inhibits <i>Y. pestis</i> proliferation in the lungs of infected animals	88
Discussion.....	90
Chapter 4: Broad applicability of identified drugs	99
Introduction.....	99
Materials and Methods.....	100
Bacterial strains	100
Testing TFP as a therapeutic in models of <i>S. Typhimurium</i> and <i>C. difficile</i> infections and AXPB as a therapeutic in a model of <i>C. difficile</i> infection	100
Growth kinetics and sensitizing of <i>S. Typhimurium</i> to TFP	102

Evaluation of TFP, AXPN, and DXP effect on autophagy in RAW 264.7 macrophages	102
Statistical analysis.....	102
Results.....	103
TFP exhibited protection in a murine model of <i>S. Typhimurium</i> infection with no direct bactericidal or bacteriostatic effects	103
TFP, but not AXPN or DXP, treatment with and without infection resulted in an increase in autophagy in murine macrophages	105
TFP and AXPN exhibited protection in a murine model of <i>C. difficile</i> infection	106
Discussion.....	108
Chapter 5: Conclusions and Future Directions	110
Conclusions.....	110
Future Directions	114
Appendix A Primers used in this study.....	116
Table 1A: Sequences of primers used in these studies	116
Appendix B Names, therapeutic class, and tier of drugs identified from <i>in vitro</i> screens against <i>Y. pestis</i>	119
Table 1B: Tier 1 drugs and therapeutic class	119
Table 2B: Tier 2 drugs and therapeutic class.....	120
References.....	123
Vita	136

List of Tables

Table 1:	Bacterial strains and plasmids used in this study.....	36
Table 2:	Putative T6SS clusters, Hcp protein homologs, and PAAR motif- containing proteins identified in <i>Y. pestis</i> CO92 genome.....	43
Table 3:	List of drugs, doses, and routes of administration for treatment in murine model of pneuemonic plague	65
Table 4:	Different concentrations and doses of TFP, DXP, and AXPN tested in mouse model of pneumonic plague	76
Table 1A:	Sequences of primers used in this study	116
Table 1B:	Tier 1 drugs and therapeutic class.....	119
Table 2B:	Tier 2 drugs and therapeutic class.....	120

List of Figures

Figure 1:	Model of the T3SS injectisome structure	21
Figure 2:	Structure of the T6SS in comparison to T4 bacteriophage	23
Figure 3:	Survival of mice challenged with <i>vasK</i> deletion mutants of <i>Y. pestis</i> CO92 or their complemented strains	24
Figure 4:	Virulence of T6SS-associated genes in a pneumonic plague mouse model	44
Figure 5:	Vaccine potential for selected <i>Y. pestis</i> CO92 combinatorial mutants	46
Figure 6:	Growth of <i>Y. pestis</i> CO92 T6SS mutant strains <i>in vitro</i> at 28°C	48
Figure 7:	Growth of <i>Y. pestis</i> CO92 T6SS mutant strains <i>in vitro</i> at 37°C	49
Figure 8:	Production of the T6SS effector Hcp6 and the T3SS effector YopE ...	51
Figure 9:	Possible mechanisms of attenuation of <i>Y. pestis</i> CO92 mutants	54
Figure 10:	Phagocytosis of WT CO92, $\Delta vasK$, $\Delta hcp6$, and $\Delta vasK\Delta hcp6$ mutants in RAW264.7 murine macrophages with presence of exogenous recombinant Hcps.	55
Figure 11:	Schematic illustration of FDA-approved drug screening method	63
Figure 12:	Tier 1 post-treatment drugs identified using a host cell-based screen to evaluate macrophage viability	71

Figure 13:	Tier 2 post-treatment drugs identified using a host cell-based screen to evaluate macrophage viability	72
Figure 14:	Quantification of intracellular bacterial survival of <i>Y. pestis</i> CO92- <i>lux</i> in RAW 264.7 murine macrophages.....	74
Figure 15:	Chemical structures of TFP, AXP, and DXP.....	75
Figure 16:	Survival analysis of mice infected with <i>Y. pestis</i> CO92 and then drug treated at the time of infection	77
Figure 17:	Dose-response effects of 3 drugs	78
Figure 18:	Effects of drugs on <i>Y. pestis</i> CO92.....	81
Figure 19:	Survival analysis of mice infected with <i>Y. pestis</i> CO92 and treated with TFP, AXP, or DXP at delayed time points	84
Figure 20:	Survival analysis of pneumonic plague infected mice treated with TFP, AXP, DXP, and/or levofloxacin at 48 h p.i.	85
Figure 21:	Survival analysis of drug treated mice re-challenged with WT CO92.....	87
Figure 22:	Resistance of <i>Y. pestis</i> with drug treated sera.....	88
Figure 23:	<i>Y. pestis</i> proliferation in lungs following DXP treatment.....	89
Figure 24:	Effects of TFP on <i>S. Typhimurium</i>	104
Figure 25:	Effects of TFP, AXP, and DXP on autophagy pathway	105
Figure 26:	Efficacy of TFP and AXP in a murine <i>C. difficile</i> model.....	107

List of Abbreviations

UTMB	University of Texas Medical Branch
GSBS	Graduate School of Biomedical Science
CDC	Centers for Disease Control
WHO	World Health Organization
FDA	Food and Drug Administration
T3SS	Type III secretion system
Yops	Yersinia outer proteins
LcrV	Low calcium response V antigen
F1	Fraction 1 capsular antigen
Pla	Plasminogen activator protein
T6SS	Type VI secretion system
Hcp	Hemolysin co-regulated protein
VgrG	Valine-glycine repeat protein G
PAAR	Proline-alanine-alanine-arginine
STM	Signature tagged mutagenesis
WWII	World War II
BWC	Biological and Toxin Weapons Convention
WT CO92	Wild-type <i>Yersinia pestis</i> CO92 strain
TLR-2	Toll-like receptor 2
HIB	Heart infusion broth
SBA	Sheep blood agar
GNL	Galveston National Lab
ATCC	American Type Culture Collection
DMEM	Dulbecco's modified medium
FBS	Fetal bovine serum
FRT	Flippase recognition target
Km ^r	Kanamycin resistance
Ap ^r	Ampicillin resistance
PCR	Polymerase chain reaction
ABSL3	Animal biosafety level 3
IACUC	Institutional Animal Care and Use Committee
LD ₅₀	Minimum lethal dose that kills 50% of animals
CFU	Colony Forming Unit
I.N.	Intranasal
ORF	Open reading Frame
Tc ^r	Tetracycline resistance
PBS	Phosphate buffered saline
LPS	Lipopolysaccharide
TCA	Trichloroacetic acid
OD ₆₀₀	Optical density at 600nm
MOI	Multiplicity of infection
MTT	3-(4,5-Dimethylthiazol-2-yl)-2,5-Diphenyltetrazolium Bromide

ICS	Intracellular survival
ANOVA	Analysis of variance
SD	Standard deviation
TFP	Trifluoperazine
DXP	Doxapram
AXPN	Amoxapine
BEI	Biodefense and emerging infections
Lux	Luciferase gene
I.P.	Intraperitoneal
S.C.	Subcutaneous

Chapter 1: *Yersinia pestis*

INTRODUCTION

Yersinia pestis, a Gram-negative bacterium of the *Enterobacteriaceae* family, is a zoonotic pathogen and the causative agent of plague. Plague manifest itself in three forms in humans, namely bubonic, septicemic, and pneumonic (1). Most commonly spread by the bite of inflected fleas, plague can also be spread in humans and animals through aerosol exposure. This bacterium has caused three pandemics throughout history with mortality estimates as high as 200 million (1). Currently, there is no vaccine approved for use in the United States and the antibiotic therapy for plague must be administered within 20-24 h after the onset of symptoms to be 100% effective (2, 3). Due to plague being endemic in many regions around the world, its relative ease of aerosolization, and the acute nature of virulence in humans, this pathogen is currently classified as a Tier-1 select agent by the Centers for Disease Control and Prevention (CDC) and a re-emerging human pathogen by the World Health Organization (WHO) (2, 4). This pathogen's extreme virulence, coupled with a lack of a Food and Drug Administration (FDA)-approved vaccine as well as treatment limited to antibiotic therapy, highlights the need for the development of new prophylactics as well as therapeutics to combat this truly devastating pathogen. In addition, isolation of natural antibiotic-resistant strains of *Y. pestis* from plague patients and generation of strains resistant to antimicrobial agents used to treat plague by some countries to be used as a biological warfare agent further underscore the necessity to develop new countermeasures against deadly *Y. pestis* infections.

BACTERIOLOGY

The genus *Yersinia* contains 17 species with three being pathogenic in humans, namely *Y. enterocolitica*, *Y. pseudotuberculosis*, and *Y. pestis* (5). While *Y. enterocolitica* and *Y. pseudotuberculosis* are food-borne pathogens spread primarily through the fecal-oral route to cause enterocolitis, *Y. pestis* is the causative agent of bubonic, septicemic, or pneumonic plague and is spread through the bite of infected fleas or inhalation of respiratory droplets of pneumonic plague patients or animals (5). Both enteric pathogens, *Y. enterocolitica* and *Y. pseudotuberculosis*, are less closely related on a genomic level than *Y. pestis* and *Y. pseudotuberculosis* (6). In fact, *Y. pestis* is believed to have evolved from *Y. pseudotuberculosis* between 2,600 – 28,000 years ago (6). Interestingly, despite the obvious differences in the clinical presentation of infections caused by these pathogens, they all share a penchant for colonization of lymphatic tissues (7).

Recent genomic studies have determined ancient *Y. pestis* strains were infecting humans in the Bronze Age in Eurasia, about 2,000 years earlier than previously thought (6). The virulent pathogen we know today, with a genome of about 4.65 Mb that also contains the three plasmids pCD1, pPCP1, and pMT1, evolved from these ancient strains through the acquisition of several virulence genes (8). The acquisition of the *Yersinia* murine toxin gene, *ymt*, is believed to be key to this organism's prevalence and virulence, as Ymt allows for colonization of the flea vector (6). Able to survive in the soil, as well as arthropod and vertebrate hosts, *Y. pestis* has proven to have a diverse lifestyle with the ability to replicate at both 30 and 37°C (1, 2, 9). This pathogen maintains its existence through an enzootic cycle involving rodents and their fleas (10). *Y. pestis* has a wide

range of both susceptible hosts and vectors, which make eradication of this pathogen extremely difficult and ultimately unfeasible in the near future. While the classical vector for plague is the oriental rat flea, *Xenopsylla cheopsis*, 30 different flea species have been shown to be vectors of *Y. pestis* (1). Additionally, while a definitive host reservoir has yet to be identified, reportedly over 200 species, particularly small rodents, are susceptible to infection (11). When these susceptible species become infected, an epizootic outbreak occurs, which can result into spillover into humans through either direct contact with infected animals or fleas from such animals looking for alternative blood meals.

FACTORS CONTRIBUTING TO BACTERIAL VIRULENCE

With a genome of approximately 4.65 Mb and three plasmids that encode numerous pathogenicity islands, *Y. pestis* contains several virulence factor genes and mechanisms that make it one of the deadliest pathogens in human history.

Type III secretion system (T3SS)

Perhaps the most well characterized virulence mechanism of the bacterium, the type III secretion system (T3SS), encoded on the pCD1 (~70 kb) plasmid, provides *Y. pestis* with a diverse array of mechanisms to suppress host innate immune defenses (12–14). T3SS's are complex nanomachines that form needle-like complexes allowing for the direct injection of effector proteins in eukaryotic host cells (**Fig. 1**) (13). The T3SS of *Y. pestis* is tightly regulated in response to the environmental variables of temperature and calcium levels (13). While the T3SS is not expressed at flea temperature (28°C) and plays no role in flea colonization, expression of the T3SS genes are critical for successful infection of mammalian hosts (13–15). In the mammalian host, an environment with low calcium levels and a temperature of 37°C, transcription of the T3SS-associated genes is

activated (16). Once contact with a host cell is made, the pore-forming translocon complex is assembled to facilitate the translocation of *Yersinia* outer proteins (Yops) across the host cell membrane. The major injected Yops; YopE, YopH, YopJ, YopM, YopO, and YopT, function by interfering with host cell transduction pathways to thwart the host innate immune defenses (13). While YopE, YopH, YopO, and YopT have been shown to interfere with signaling pathways involved in host cytoskeleton maintenance, YopJ has been reported to inhibit the activation of host signaling pathways (14, 17), and YopM blocks inflammasome activation (18). In addition to these injected Yop proteins, some other notable T3SS effector proteins include the secreted YopB and YopD translocon proteins, which together form the pore in the host cell membrane (12, 13, 16). The polymer of YscF, which determines the length of the needle (19) connects the needle complex to the basal body of the T3SS formed by the Ysc (*Yersinia* secretion component) proteins; YscD, YscJ, YscU, YscI, YscC, YscNKL, and YscC. As part of the basal body, YscC forms the outer membrane ring spanning the bacterial outer membrane traversing the periplasmic space (16). The low calcium response antigen V (LcrV) forms the tip of the needle complex, is required for the secretion of Yop effector proteins (13, 16), and is an important immunogen of the subunit plague vaccines which are in clinical trials (9, 20, 21).

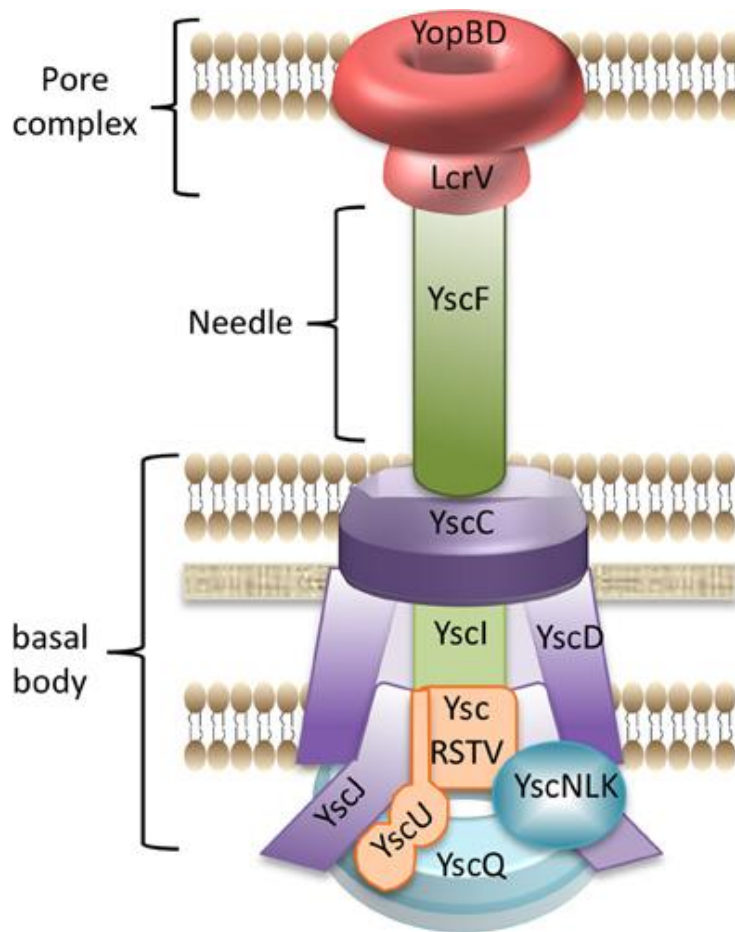


Figure 1. Model of the T3SS injectisome structure.

Cartoon model depicting the structural components of the *Yersinia* T3SS injectisome.

Figure adapted from Dewoody *et al.* with permission (16).

F1 capsule

Fraction 1 (F1) capsular antigen is encoded on the large (~100 kb) plasmid pMT1 by the gene referred to as *cafI*. F1 is a structural component that serves as both a primary immunogen, with passive transfer of F1 antibodies shown to be effective in protection against low dose inocula of *Y. pestis* in a mouse model of infection (22), and as a virulence factor of *Y. pestis* (23–25). Regulated by temperature, strong expression of F1 gene occurs only at 37°C, corresponding to the temperature of mammalian hosts (22, 26). As with other pathogens, the F1 capsule protects the bacterium from uptake by macrophages and other phagocytic cells (25). Interestingly, F1 negative strains of *Y.*

pestis have been identified in nature that are fully virulent. Additionally, deletion of F1 results in a highly variable phenotype that is route dependent and ranges from the bacterium being greatly attenuated to fully virulent depending upon the animal models used (23, 27).

Plasminogen-activator protease

The 9.5 kb pPCP-1 plasmid of *Y. pestis* encodes the plasminogen activator protease, Pla, which converts plasminogen to plasmin. This conversion allows for the degradation of the extracellular matrix and aids in the dissemination of the bacterium, particularly in bubonic plague (28). Pla also plays a role in pneumonic plague and is essential for the development of primary pneumonic plague through rapid replication of the bacterium in the airways (29). Pla has also been shown to play a role in the intracellular survival of *Y. pestis* in macrophages (30, 31).

Type VI secretion system (T6SS)

Unlike the T3SS, the T6SS has been mostly overlooked as a virulence mechanism of *Y. pestis*. In one study, while a T6SS locus deletion mutant was observed to be attenuated in macrophages *in vitro*, this attenuation was not translated in *in vivo* models of bubonic and pneumonic plague infection (32). *In silico* analysis revealed an additional five putative T6SS loci within the *Y. pestis* genome, for a total of six loci; however, the roles of these other loci in bacterial lifestyle and/or pathogenesis have not been characterized (33). Similar to the T3SS, the T6SS consists of a needle like complex to form an injectosome to translocate effector molecules into its target cells. Interestingly, the T6SS has significant homology and is functionally related to bacteriophage tails (**Fig. 2**) (34, 35). During the secretion process, hexameric rings of hemolysin coregulated

protein(s) (Hcp) form a tube complex capped with valine-glycine repeat protein G (VgrG) and proline-alanine-alanine-arginine (PAAR) repeat-containing protein (34–36). This intracellular tube is surrounded by a sheath of protein heterodimers and when an extracellular signal, such as contact, occurs, the sheath contracts. This leads to secretion of both the tube complex and effector molecules into the target cell (34).

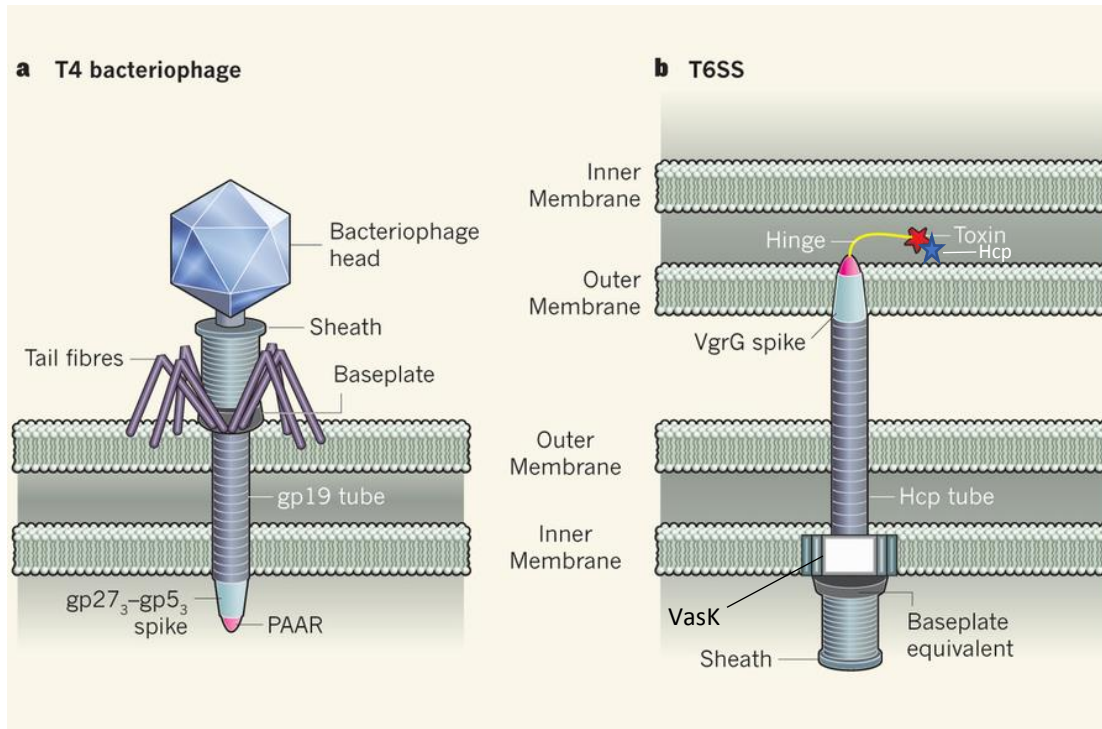


Figure 2. Structure of the T6SS in comparison to T4 bacteriophage

Cartoon model depicting the structural components of the T6SS and its similarities to T4 bacteriophage (A&B). Figure adapted from Filloux A, with permission (34).

Recently, utilizing a signature-tagged mutagenesis (STM) approach to identify potential novel virulence factors of *Y. pestis*, a total of three (*vasK*, *ypo498*, and *ypo1484*) T6SS component or effector-encoding genes were identified from our STM screen. Furthermore, through the generation of $\Delta vasK$ and $\Delta lpp\Delta vasK$ deletion mutant strains, the T6SS was confirmed, for the first time, to be an important virulence mechanism of *Y.*

pestis (**Fig. 3**) (37). Lpp encodes Braun lipoprotein and triggers Toll-like receptor (TLR-2) signaling to produce pro-inflammatory cytokines (38). Whether other T6SSs and

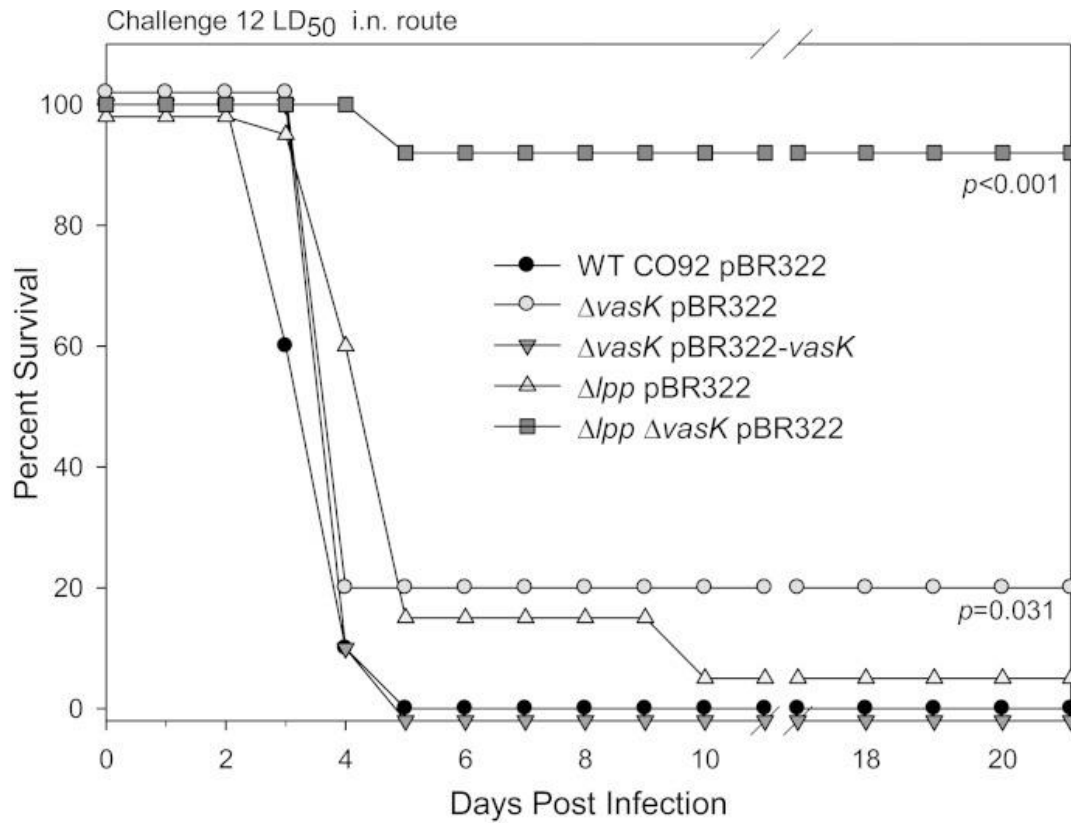


Figure 3. Survival of mice challenged with *vasK* deletion mutants of *Y. pestis* CO92 or complemented strains.

Adult Swiss-Webster mice were challenged by the intranasal (i.n.) route with 12 LD₅₀ of WT CO92 (pBR322) ($n = 10$) or the $\Delta vasK$ (pBR322) ($n = 10$), $\Delta vasK$ (pBR322-*vasK*; complemented strain) ($n = 10$), Δlpp (BR322) ($n = 20$), or $\Delta lpp \Delta vasK$ (pBR322) double mutant ($n = 10$). All of these strains contained pBR322 vector to serve as an appropriate control. Mice were followed for survival up to 21 days, and the data analyzed for significance by the Kaplan-Meier survival estimates with the Bonferroni *post hoc* test. The *P* values are for comparison of the results for each of the mutant strains to the results for wild-type (WT) CO92. Figure adapted from Ponnusamy, *et al.* with permission (37).

HISTORY

Pandemics

Y. pestis has been identified as the definitive causative agent for three plague pandemics spanning the course of human history. Although there are suggestions of plague occurring even earlier in history, such as the Plague of Athens in 430-427 BC and the Antonine Plague in 165-180 AD, there is a lack of consistent records and/or genomic data to provide conclusive evidence that *Y. pestis* was indeed the cause (6, 39). From the first great pandemic, referred to as the 6th century Justinian plague, human samples have provided genetic evidence linking *Y. pestis* as the causative agent of plague and this pandemic (6). The Justinian plague is believed to have originated in Central Africa in 541-544 AD and, from there, it spread north towards Egypt before finally making its way into Europe through Mediterranean countries (6, 39). The Justinian plague lasted for decades as disease continued to occur intermittently until about 750 AD, and estimates have predicted 100 million deaths to have occurred as a result of this pandemic (6, 39). The second, and probably most well-known and well-documented pandemic of plague, is what we refer to as the Black Death. This pandemic occurred primarily in Europe throughout the 14th century, with intermittent reemergence occurring several hundred years following the initial outbreak until the 18th century (6, 39). Estimates have indicated that through the course of the Black Death pandemic, 30-50% of Europe's population was killed (6). The final pandemic had its beginnings in China in the 1850s. In 1894, a major outbreak erupted and from that epidemic, plague rapidly spread worldwide in the late 19th century following trade routes (6, 39). Series of epidemics from this

spread continued until the middle of the 20th century. This third pandemic resulted in the global spread of the bacterium, including the introduction of *Y. pestis* to the western United States (6, 40). Although the number of casualties occurring during the third pandemic have been limited in comparison to those of the first two pandemics, recent reemergence of the disease in both Asian and African countries and the continued occurrence of small outbreaks worldwide make this a pathogen of global concern even to this day (1, 39).

Use as a biological warfare agent

In addition to its history of naturally occurring human pandemics, plague has also been utilized as a bioweapon throughout history. In 1346, during the siege of Caffa, a Crimean city on the coast of the Black Sea, corpses of plague victims were catapulted into the besieged city by the attacking Tatar army to facilitate the introduction of the disease (4, 41). During World War II (WWII), Unit 731, a secret branch of the Japanese army, was reported to have utilized *Y. pestis* as a bioweapon by dropping plague-infected fleas over areas of China to cause outbreaks (4, 41). In both the United States and the former Soviet Union, in order to subvert the use of the flea vector, biological weapon programs developed techniques to directly aerosolize plague bacilli (4, 42, 43). Although the United States was not successful in manufacturing large enough quantities of the organisms to be effective for weaponization, Soviet scientists were able to manufacture quantities large enough to be utilized for weaponization (4). In 1972, the Biological and Toxin Weapons Convention (BWC) was drafted, which called for the dismantling of all biological weapons programs. Despite the BWC, there has been evidence of these bioweapon programs continuing in the former Soviet Union and China (4, 42).

Additionally, while little information has been published regarding the threat of autonomous groups or individuals utilizing *Y. pestis* for weaponization, in 1995 a microbiologist from Ohio was arrested after acquiring *Y. pestis* by mail, which led to the introduction of new antiterrorism legislation (4). Since 2001 and the anthrax attacks in the United States, there has been a renewed interest in the development of diagnostics, prophylactics, and therapeutics for potential agents of bioterrorism, including *Y. pestis*.

PLAGUE EPIDEMIOLOGY AND THE CHALLENGES FACED TODAY

The global dissemination of *Y. pestis* in mammal, particularly rodent, reservoirs, and flea species make eradication of the pathogen unfeasible. Therefore, the need to understand the symptoms of disease, particularly in endemic areas, is of vital importance. Additionally, utilization and development of effective therapeutics and prophylactics can provide additional knowledge of the pathogenesis of this bacterium as well as provide tools to better combat this deadly pathogen.

Global epidemiology and plague in the United States

While it is true that plague is less common now than in centuries past, in the modern plague era of today, outbreaks have occurred on every continent with the exception of Antarctica. Per the WHO, the Democratic Republic of the Congo, Madagascar, and Peru are currently the most endemic countries (44). Between 2010-2015, over 3,000 cases of plague were reported worldwide, with 584 fatalities, indicating that this is still a disease of global concern (44).

In the United States, plague is a reportable disease, with all laboratory confirmed cases tracked by the CDC. Plague is endemic in the western half of the United States, with cases occurring annually, at a rate of about three per year (45, 46). However, more

recent years have shown an uptick in plague cases. In 2006, 13 cases, all occurring in the western United States, were reported with 2 fatalities (45, 47). Then in 2014, four cases of pneumonic plague were reported that were traced to an infected dog (48, 49). Alarming, there is evidence of human-to-human transmission, which would represent the first occurrence of this in the United States since 1924 (50, 51). Continuing with the increase in the number of cases, in the summer of 2015, there were 11 confirmed cases of plague in six different states that were ultimately linked to exposures at Yosemite park (52). This year, 3 cases of plague have been confirmed in New Mexico (53). While the cause for the recent increase in occurrence is unknown, all cases have resulted from exposure and outdoor activity in plague endemic areas, although some of these areas have not had reports of plague for decades.

Clinical disease, current treatments, and limitations

Most cases of plague today are bubonic, which has a distinctive clinical presentation that is often recognizable by both physicians and patients, particularly in endemic areas. During bubonic plague, the bacteria deposited from the bite of the infected flea migrate to regional lymph nodes, where they begin to multiply during an incubation period of 2-8 days (40, 54). Following the incubation period, patients report a sudden onset of fever and chills. These symptoms are accompanied by the formation of the characteristic and painful bubo, which results from the bacterial proliferation and subsequent inflammation of the lymph nodes (40, 54). While most cases involve bubo formation in the inguinal, femoral, or axillary regions from bites on extremities, flea bites on the head or neck can give rise to buboes in the cervical region. In addition to rapid enlargement, buboes are warm to the touch with erythema and sometimes associated with

edema in the surrounding area. Histological examination of buboes has shown massive influx of neutrophils, high numbers of bacteria, and necrosis with destruction of the lymph node architecture (40, 54). From the buboes, bacteria can disseminate into the blood stream and infect organs such as the liver, spleen, and lungs. In about 50% of untreated patients, bacterial dissemination can result in high-grade bacteremia, resulting in secondary septicemic plague and death 3-6 days after symptoms appear (47). In some cases, septicemic plague, the second most common form of plague, can occur without the formation of buboes as bacteria bypass the regional lymph nodes and grow directly in the blood. In some cases of septicemic plague, disseminated intravascular coagulation and vasculitis can lead to gangrene and the need for amputation (48).

For the third most common form of plague, pneumonic plague, infection can occur as secondary to bubonic or septicemic, when bacteria from the blood enter into the lungs, or primarily by the inhalation of infected aerosols of either another pneumonic plague patient or an infected animal (40, 54). Symptoms of pneumonic plague are nondescript and described as flu-like, with rapid onset of fever, chills and body-aches, accompanied by weakness, and nausea (55).

Pneumonic plague is the most virulent form of the disease, with the incubation period lasting 1-3 days post-exposure (55). While the case fatality rate for bubonic plague ranges from 30-60%, septicemic and pneumonic plague are almost always fatal without medical intervention (40, 54, 56). As a hallmark of plague infection is the rapid development of systemic infection, prompt intervention is critical for successful treatment of patients, particularly those with septicemic or pneumonic forms of the disease. Plague is currently treatable with antibiotics, with reports of gentamicin,

doxycycline, tetracyclines, and streptomycin being used in the successful treatment of patients (3, 54, 57, 58). Additionally, levofloxacin (Levaquin) and moxifloxacin (Avelox) were approved by the FDA in 2012 and 2015, respectively, for the treatment of all forms of plague (40, 57). However, a limitation is that antimicrobials must be administered within 20-24 h after the onset of symptoms to be effective, meaning that, in many cases, patients must be treated before there is a definitive diagnosis (2, 3). This is a critical issue, especially in areas where plague is not endemic and physicians are not familiar with symptoms. The value of antibiotic treatment is even further diminished because multiple-antibiotic-resistant *Y. pestis* strains have been isolated in nature, from both plague patients in Madagascar (59, 60) and rodents in Mongolia (61), as well as genetically engineered for use as a bioweapon (2, 4). These facts demonstrate the need for the development of alternative therapeutics that do not rely on antibiotic intervention alone.

Where do we stand with plague vaccines?

In addition to therapeutics, prophylactics, such as vaccines, have been fundamental for the control of several diseases. While there has been significant interest in the development of plague vaccines, today, there is no FDA-approved vaccine against plague. In the past, a heat-killed vaccine was utilized by the United States army, however, this vaccine was severely reactogenic. Recipients of this vaccine developed a high fever, and as such would not be approved for use in the general population (20, 21, 62). Also, while this vaccine was efficacious against bubonic plague, it failed to protect against pneumonic plague, which is the bigger threat in terms of bioterrorism (4, 21). A formalin inactivated whole-cell vaccine was licensed in the US in the mid-1900s, but required

booster doses and, like the heat-killed vaccine, it caused significant adverse events and failed to protect against pneumonic plague (63).

Recombinant subunit plague vaccines comprised of capsular antigen F1 and LcrV are currently in clinical trials and have shown promise in rodent models (20, 21). However, protection is inconsistent in different species of non-human primates (e.g., *Cynomolgus* macaques versus African green monkeys) with antibody titers not correlating with protection (62, 64). Further, the F1 and LcrV antibody titers generated by the subunit vaccine(s) in humans vary significantly and the F1-LcrV-based vaccines generate a poor T cell response (65). Recent studies, including ours, have indicated that cell-mediated immune responses are crucial in providing protection against *Y. pestis* infections, specifically pneumonic plague, and, as such, subunit vaccines are not likely to be highly effective as they primarily generate an antibody-mediated immune response (30, 66–68).

Other platforms for the development of a plague vaccine have been explored, with recent studies reporting the use of an adenovirus-based platform as well as a T4 bacteriophage platform to effectively protect animals from fatal infections (69, 70). While these platforms do help in generating cellular immune responses to plague, like subunit vaccines, these target the generation of antibodies to F1 and LcrV (21, 69, 70). Such vaccines will be relatively ineffective against infections caused by F1-minus strains of *Y. pestis*, which exist in nature and are equally virulent, or those harboring highly diverged variants of LcrV (23, 71).

Thus, live-attenuated vaccines offer a substantial advantage in triggering both protective humoral and cell-mediated immune responses. Indeed, a live-attenuated

vaccine strain, *Y. pestis* EV76, which lacks the pigmentation locus required for iron acquisition, provides protection against both bubonic and pneumonic plague in humans and is used in endemic regions of China and the former states of the Soviet Union (9, 62). However, this strain is highly reactogenic and can induce disease similar to that of wild-type (WT) bacteria in individuals with underlying diseases, such as hemochromatosis (72). Consequently, there is an urgent need for the development of alternative vaccine candidates, particularly live-attenuated ones, as they would trigger both arms of the immune responses in the host.

Chapter 2: Characterization of the Type VI Secretion System (T6SS) as a Virulence Mechanism of *Yersinia pestis* CO92

INTRODUCTION

With the continued absence of an FDA-approved vaccine for plague, identification and characterization of novel virulence factors/mechanisms of *Y. pestis* to rationally design a better live-attenuated vaccine candidate(s) is of significant importance to combat potential future outbreaks of plague (21, 62). Recently, we utilized a signature-tagged mutagenesis (STM) approach to identify novel virulence factors of *Y. pestis* (37). Through the generation of an in-frame single deletion mutant of *vasK* (identified through our STM screen), a known component of the T6SS, and a double deletion mutant of *lpp* and *vasK*, with the *lpp* gene encoding Braun lipoprotein which activates Toll-like receptor 2 (TLR-2) signaling (38), we reported for the first time the involvement of the T6SS in *Y. pestis* virulence. Thus, T6SS could be targeted for the development of novel live-attenuated vaccine candidates for plague (37).

The T6SS is a more recently identified protein secretion system first described in *Vibrio cholerae*, that is functionally related to the bacteriophage contractile tail (73). T6SSs are highly conserved amongst Gram-negative bacteria and are involved in the delivery of toxins and effector proteins to both prokaryotic and eukaryotic cells (34). In terms of virulence, the T6SS has been reported to play a “vital role in the virulence of several pathogens, including *Burkholderia mallei*, *B. pseudomallei*, *Francisella tularensis*, *Salmonella enterica* serovar Typhimurium, and *Aeromonas dhakensis* (previously *Aeromonas hydrophila*) (73–81). For *Y. pestis*, *in silico* analysis revealed 6

potential T6SS clusters, 6 putative Hcp-encoding genes, and 5 putative PAAR repeat-containing protein-encoding genes (33).”

To identify the role these various T6SS clusters and effectors play in *Y. pestis* virulence, in this study, we generated 5 T6SS cluster, 4 *hcp* homolog, and 3 PAAR motif repeat containing protein deletion mutants. One T6SS cluster had previously been characterized and revealed to play no role in *Y. pestis* virulence in either bubonic or pneumonic plague models, although attenuation was observed *in vitro* (32). Generation of the various T6SS deletion mutants, both whole clusters and single genes, resulted in varying levels of attenuation, with some being significantly attenuated in comparison to WT *Y. pestis* CO92. Furthermore, attenuation could be augmented through the generation of combinatorial deletion mutants as observed with $\Delta vasK\Delta hcp6$ and $\Delta ypo2720-2733\Delta hcp3$ double deletion mutants. Animals that survived challenge with the double deletion mutants were also observed to be significantly protected, 60-100%, from subsequent re-challenge with WT CO92. Consequently, *in vitro* studies were performed to further elucidate the mechanisms of attenuation of the generated T6SS deletion mutants. “We found that the attenuated mutant strains exhibited distinct phenotypes in terms of induction of host cell cytotoxicity, phagocytosis by murine macrophages, and intracellular survival in such macrophages. These results indicated that the T6SS effectors and clusters have distinct roles in *Y. pestis* virulence. Our data also provided further evidence of the utility of the STM screening approach for the identification of novel virulence factors to be targeted for deletion and rationally designing a potential new generation live-attenuated vaccine candidate(s).

MATERIALS AND METHODS

Bacterial strains and cell culture.

The bacterial strains used in this study are described in **Table 1**. *Y. pestis* strains were grown in heart infusion broth (HIB) (Difco; Voigt Global Distribution, Inc., Lawrence, KS) at 28 or 37°C with constant shaking at 180 rpm, or grown for 48 h on 5% sheep blood agar (SBA) (Teknova, Hollister, CA) or HIB agar plates. As appropriate, the organisms were cultivated in the presence of antibiotics ampicillin and kanamycin at concentrations of 100 and 50 µg/ml, respectively. All experiments with *Y. pestis* strains were performed in the CDC-approved select agent laboratory in the Galveston National Laboratory (GNL), University of Texas Medical Branch (UTMB).

The RAW 264.7 murine macrophage cell line (American Type Culture Collection [ATCC], Manassas, VA) were maintained in Dulbecco's modified eagle medium (DMEM) with 10% fetal bovine serum supplemented with 1% L-glutamine (Cellgro, Manassas, VA) and 1% penicillin-streptomycin (Invitrogen, Carlsbad, CA) at 37°C with 5% CO₂.

Construction of T6SS cluster, single gene, and combinatorial deletion mutants.

“To construct in-frame single gene deletion and cluster deletion mutants of CO92, the λ phage recombination system was used as previously described (37, 82). Briefly, the parent strains were transformed with plasmid pKD46 (**Table 1**) and grown in the presence of 1 mM L-arabinose to induce the expression of the λ phage recombinase gene on pKD46. The parent strains were processed for the preparation of electroporation-competent cells (37). The electrocompetent cells were then transformed with 0.5 to 1.0 µg of the linear ds DNA constructs carrying the kanamycin resistance (Km^r) gene

cassette, which was immediately flanked by the bacterial flippase recognition target (FRT) sequence, followed on either side by 50 bp of DNA sequences homologous to the 5' and 3' ends of the gene to be deleted from the parent strains. Plasmid pKD46 was cured from the mutants that had successful Km^r gene cassette integration at the correct location by growing the bacteria at 37°C. The latter mutants were transformed with plasmid pEF01 (**Table 1**) (83) to excise the Km^r gene cassette. Plasmid pEF01 was then cured from the Km^s clones by growing them at 37°C, followed by selection in a medium containing 5% sucrose. To confirm the in-frame deletion, mutants showing sensitivity to kanamycin and ampicillin were tested by polymerase chain reaction (PCR) using appropriate primer pairs (**Table 1A; Appendix A**) and sequencing of the PCR products.

Table 1. Bacterial strains and plasmids used in this study

Strain or plasmid	Description	Reference or source
<i>Y. pestis</i> CO92 strains		
WT CO92	Virulent <i>Y. pestis</i> biovar Orientalis strain isolated in 1992 from a fatal human pneumonic plague case and naturally resistant to polymyxin B	CDC
WT CO92:pBR322	WT <i>Y. pestis</i> CO92 transformed with pBR322 (Tc ^s)	(30)
WT CO92:pKD46	WT <i>Y. pestis</i> CO92 transformed with plasmid encoding phage λ recombination system	(37)
$\Delta vasK$	<i>vasK</i> deletion mutant of <i>Y. pestis</i> CO92	
$\Delta ypo0966-0984$	<i>ypo0966-0984</i> deletion mutant of <i>Y. pestis</i> CO92	This study
$\Delta ypo1458-1493$	<i>ypo1458-1493</i> deletion mutant of <i>Y. pestis</i> CO92	This study
$\Delta ypo2720-2733$	<i>ypo2720-2733</i> deletion mutant of <i>Y. pestis</i> CO92	This study
$\Delta ypo2927-2954$	<i>ypo2927-2954</i> deletion mutant of <i>Y. pestis</i> CO92	This study
$\Delta ypo3588-3615$	<i>ypo3588-3615</i> deletion mutant of <i>Y. pestis</i> CO92	This study
$\Delta ypo2793 (hcp3)$	<i>ypo2793(hcp3)</i> deletion mutant of <i>Y. pestis</i> CO92	This study
$\Delta ypo2793 (hcp3)$:pBR322-	$\Delta ypo2793(hcp3)$ strain	This study

<i>ypo2793</i>	complemented with pBR322- <i>ypo2793(hcp3)</i> (Tc ^s)	
$\Delta ypo2868(hcp4)$	<i>ypo2868(hcp4)</i> deletion mutant of <i>Y. pestis</i> CO92	This study
$\Delta ypo2868(hcp4)$:pBR322- <i>ypo2868</i>	$\Delta ypo2868(hcp4)$ strain complemented with pBR322- <i>ypo2868(hcp4)</i> (Tc ^s)	This study
$\Delta ypo2962(hcp5)$	<i>ypo2962(hcp5)</i> deletion mutant of <i>Y. pestis</i> CO92	This study
$\Delta ypo2969(hcp5)$:pBR322- <i>ypo2962</i>	$\Delta ypo2962(hcp5)$ strain complemented with pBR322- <i>ypo2962(hcp5)</i> (Tc ^s)	This study
$\Delta ypo3708(hcp6)$	<i>ypo3708(hcp6)</i> deletion mutant of <i>Y. pestis</i> CO92	This study
$\Delta ypo3708(hcp6)$:pBR322- <i>ypo3708</i>	$\Delta ypo3708(hcp6)$ strain complemented with pBR322- <i>ypo3708(hcp6)</i> (Tc ^s)	This study
$\Delta ypo0873$	<i>ypo0873</i> deletion mutant of <i>Y. pestis</i> CO92	This study
$\Delta ypo1484$	<i>ypo1484</i> deletion mutant of <i>Y. pestis</i> CO92	This study
$\Delta ypo3615$	<i>ypo3615</i> deletion mutant of <i>Y. pestis</i> CO92	This study
$\Delta vasK \Delta hcp6$	<i>vasK hcp6</i> double deletion mutant of <i>Y. pestis</i> CO92	This study
$\Delta ypo2720-2733 \Delta ypo2793(hcp3)$	<i>ypo2720-2733 ypo2793(hcp3)</i> double deletion mutant of <i>Y. pestis</i> CO92	This study
<hr/>		
Plasmids		
pKD46	Plasmid for phage λ recombination system under arabinose-inducible promoter	(82)
pKD13	Template plasmid for PCR amplification of the Km ^r gene cassette flanked by FRT sites	(82)
pEF01	Plasmid for FLP (flippase) enzyme under constitutively expressed <i>lac</i> promoter (Ap ^r)	(83)
pBR322	A variant of pBR322 (Tc ^s)	
pRB322- <i>ypo2793(hcp3)</i>	Plasmid containing the <i>ypo2793(hcp3)</i> coding region and its putative promoter inserted in the Tc ^r cassette of vector pBR322	This study
pRB322- <i>ypo2868(hcp4)</i>	Plasmid containing the <i>ypo2868(hcp4)</i> coding region and its putative promoter inserted in the Tc ^r cassette of vector pBR322	This study
pRB322- <i>ypo2962(hcp5)</i>	Plasmid containing the <i>ypo2962(hcp5)</i> coding region and its putative promoter inserted in the Tc ^r cassette of vector pBR322	This study

pRB322- <i>ypo3708(hcp6)</i>	Plasmid containing the <i>ypo3708(hcp6)</i> coding region and its putative promoter inserted in the Tc ^r cassette of vector pBR322	This study
pET30a	pBR322-derived expression vector with T7 <i>lac</i> promotor, up- and down- stream His tags; Ap ^r	Novagen

CDC=Centers for Disease Control and prevention; Tc^r=Tetracycline resistant; Tc^s=tetracycline sensitive; Km^r=Kanamycin resistant; Ap^r=Ampicillin resistance; FLP=flippase; FRT=flippase recognition target

Testing for attenuation of the *Y. pestis* CO92 mutant strains in a murine model of pneumonic plague infection.

All animal studies with *Y. pestis* were performed in an animal biosafety level 3 (ABSL-3) facility under an approved Institutional Animal Care and Use Committee (IACUC) protocol (UTMB). Six- to 8-week-old female Swiss Webster mice (17 to 20 g), purchased from Taconic Laboratories (Germantown, NY), were anesthetized by isoflurane inhalation and subsequently challenged intranasally (i.n.), to mimic pneumonic plague infection, with the indicated strains and LD₅₀ doses (1 LD₅₀ = 500 CFU by i.n. route) (30). Mice were assessed for clinical symptoms, morbidity and/or mortality for the duration of each experiment; up to 21 days post-infection (p.i.).

For re-challenge experiments, after 21 days p.i. with the selected mutant strains, WT CO92 was used to infect mice by the i.n. route as described previously at a dose of 10 LD₅₀. Mice were assessed for morbidity and mortality, as well as clinical symptoms, for the duration of each experiment.

Complementation of attenuated Hcp-encoding gene homolog deletion mutant strains.

Using primers 13, 16, 19, and 22 (Table 1A; Appendix A), the complete open reading frame (ORF) of the gene of interest, along with 200 bp of the upstream DNA

sequence corresponding to the promoter region of that gene, was PCR amplified with genomic DNA of WT CO92 as the template. Then, the amplified DNA constructs were cloned into plasmid pBR322 in place of the tetracycline resistance (Tc^r)-conferring gene (**Table 1**) (84). The recombinant pBR322 vector was electroporated in corresponding *Y. pestis* CO92 mutants to restore the functionality of the deleted genes.

Generation of recombinant Hcp6 protein.

The *hcp6* gene (*ypo3708*, residing relatively close to T6SS Cluster G) of *Y. pestis* CO92, (**Table 1**) with the highest homology to *hcp* of *A. dhakensis* (82%), was cloned in the pET-30a vector to produce recombinant protein from *E. coli* as previously described (85). The rHcp6 containing a 6× His tag was purified by nickel affinity chromatography, dialyzed against phosphate-buffered saline (PBS), and then passed through a polymyxin B column (Bio-Rad, Hercules, CA) to remove any residual lipopolysaccharide (LPS) (85). The pass-through fraction was filtered by using a 0.2 µm filter, and the protein concentration quantified by using the Bradford assay (Bio-Rad). The purity of rHcp6 was verified by Coomassie Blue and SYPRO-Ruby staining of the gels.

Western blot analysis for detecting the T6SS effector Hcp and type-III secretion system (T3SS) function of *Y. pestis* CO92 mutant strains.

Overnight cultures of CO92 strains, grown in HIB at 28°C, were diluted 1:20 in 5 mL HIB, supplemented with 5 mM EGTA to trigger the low-calcium response, and incubated at 28°C for 2 h before being shifted to 37°C for an additional 3 h of growth (to activate the T3SS). Bacterial cells and supernatants were separated by centrifugation. Cell pellets were dissolved in SDS-PAGE buffer and analyzed by immunoblotting using antibodies to YopE. For supernatants, 1 mL aliquots were precipitated with 20%

trichloroacetic acid (TCA, v/v) on ice for 2 h before being dissolved in SDS-PAGE buffer.

The rHcp6 of *Y. pestis* CO92 (as purified above) was used to raise polyclonal antibodies in mice for immunoblot analysis. Both cell pellets and supernatants from WT CO92 and its various mutant strains were then analyzed by immunoblotting using antibodies to Hcp6. The anti-DnaK monoclonal antibody (Enzo Life Sciences, Albany, NY) was employed for analysis of cell pellets as a loading control.

Assessing growth kinetics, cytotoxicity on host cells, phagocytosis, and intracellular survival of *Y. pestis* CO92 strains in RAW 264.7 murine macrophages.

For growth kinetics, overnight cultures of *Y. pestis* CO92 strains, grown in HIB at 28°C, were normalized to the same absorbance by measuring the optical density at 600 nm (OD₆₀₀). Subcultures were then inoculated into 20 mL of HIB contained in 125 mL polycarbonate Erlenmeyer flasks with HEPA-filtered tops. The cultures were incubated at 28 or 37°C with agitation, and samples for absorbance measurements were taken at the indicated time points.

Viability of murine RAW 264.7 macrophages following infection was used to assess cytotoxicity of *Y. pestis* strains. Briefly, RAW 264.7 cells were seeded in 96-well microtiter plates at a concentration of 2×10^4 cells/well to form confluent monolayers in a volume of 100 µL per well. *Y. pestis* strains were grown in HIB overnight as previously described. Plates were then infected with WT CO92 or the various mutant strains at a multiplicity of infection (MOI) of 100, centrifuged, and incubated at 37°C/5% CO₂ for 60 min. Infected macrophages were then washed with PBS, treated with gentamicin (50 µg/ml) for 60 min to kill extracellular bacteria, washed again with PBS, and maintained

in DMEM with a 10 µg/ml concentration of gentamicin for 12 h at 37°C/5% CO₂ (86). Reduction of MTT (3-(4, 5-dimethylthiazolyl-2)-2, 5-diphenyltetrazolium bromide) was used as an index of cell viability following the protocol outlined by ATCC. Briefly, MTT reagent was added to the microtiter plate wells (10 µL/well), and cells were incubated at 37°C/5% CO₂ for an additional 2 h. Then, 100 µL of the detergent reagent was added to the wells and incubated in the dark at ambient temperature for 2 h. Absorbance values were measured at 570 nm in an ELx800 absorbance reader (Biotek, Winooski, VT).

Phagocytosis and intracellular survival of *Y. pestis* strains were determined as previously described (38, 87). In brief, *Y. pestis* strains were grown in HIB overnight to saturation at 28°C. RAW 264.7 macrophages were seeded in 24-well plates at a concentration of 5×10^4 cells/well for confluency. Macrophages were then infected with WT CO92 or the various mutant strains at a MOI of 10 in DMEM, centrifuged, and incubated at 37°C/5% CO₂ for 60 min. Infected macrophages were then washed with PBS, treated with gentamicin (50 µg/ml) for 60 min, washed again with PBS, and maintained in DMEM with gentamicin at a concentration of 10 µg/mL until lysed for bacterial enumeration. For phagocytosis, macrophages were lysed immediately following gentamicin treatment, designated 0 h p.i., while macrophages were lysed 4 h p.i. (4 h post gentamicin treatment) for intracellular survival. The surviving bacteria inside the macrophages were assessed by serial dilution and plating on SBA plates (38, 87)."

Statistical analyses.

Kaplan-Meier survival estimates were used for statistical analysis of animal studies. Whenever appropriate, two-way or one-way analysis of variance (ANOVA) with

Tukey's *post-hoc* test or the student's t test was employed for data analysis. *P* values of ≤ 0.05 were considered significant for all statistical tests used.

RESULTS

“Deletion of T6SS clusters and effectors resulted in varying levels of attenuation in a pneumonic plague mouse model.

Using STM approach, we have previously reported the identification of three T6SS genes with virulence potential in *Y. pestis* CO92 (37). Indeed, the contribution of the T6SS to *Y. pestis* virulence was confirmed through generation of $\Delta vasK$ and $\Delta lpp\Delta vasK$ deletion mutants (37). Analysis of the CO92 genome revealed six T6SS clusters (32, 33), six Hcp protein-encoding gene homologs, and five PAAR motif-containing protein-encoding genes (**Table 2**). Hcp is a well-established structural component as well as an effector and marker of functional T6SS, while PAAR motif-containing proteins have been identified to form the spike complex along with valine glycine rich G family proteins (VgrG) to penetrate target host membranes to translocate/secrete effectors (34). One T6SS cluster (Cluster A, *ypo0498-0518*) was previously shown by our laboratory to have no effect on *Y. pestis* virulence *in vivo* (32), while the other five were previously uncharacterized. In this study, we have shown generation of these five T6SS cluster (B, C, E-G) deletion mutants (**Table 2**) resulted in varying levels of attenuation when evaluated in a mouse model of pneumonic plague (**Fig. 4A**). Deletion mutants for Cluster C (*ypo1458-1484*) and Cluster F (*ypo2927-2954*) exhibited limited, 14%, or no attenuation, respectively, while deletion mutants for Cluster

B (*ypo0966-0984*), E (*ypo2720-2733*), and G (*ypo3588-3615*), exhibited significant levels of attenuation, 30-42%, in comparison to WT CO92 (**Fig. 4A**).

Table 2. Putative T6SS clusters, Hcp protein homologs, and PAAR motif-containing proteins identified in *Y. pestis* CO92 genome.

Cluster name and location	Putative Hcp proteins (% identity to Hcp of <i>A. dhakensis</i>)	PAAR motif-containing proteins and their biologically-active domains
A: <i>ypo0498-ypo0518</i>	Hcp1: YPO0973 (31%)	YPO0762 tRNA nuclease (WapA)
B: <i>ypo0966-ypo0984</i>	Hcp2: YPO1470 (31%)	YPO0866
C: <i>ypo1458-ypo1493</i>	Hcp3: YPO2793 (32%)	YPO0873 pyocin S type
E: <i>ypo2715-ypo2733</i>	Hcp4: YPO2868 (34%)	YPO1484 Toxin 60 (RNase toxin)
F: <i>ypo2927-ypo2954</i>	Hcp5: YPO2962 (32%)	YPO3615 tRNA nuclease (WapA)
G: <i>ypo3588-ypo3615</i>	Hcp6: YPO3708 (82%)	

For the 6 *hcp* homologs, two (*ypo0973* and *ypo1470*; designated as *hcp1* and *hcp2*) were contained within the T6SS clusters B & C, respectively, while the other four were located outside of the identified T6SS clusters (**Table 2**). Consequently, only the four Hcp-encoding genes outside of these T6SS clusters had deletion mutants generated, as any effect resulting from *hcp1* or *hcp2* deletion would be observed through its corresponding whole T6SS cluster (B or C) deletion. All Hcp-encoding gene deletion mutants were observed to have statistically significant levels of attenuation, between 30-40%, compared to WT CO92 (**Fig. 4B**). To further confirm that attenuation was a direct result of deletion of the *hcp* homolog genes, mice were challenged with the

complemented strains, $\Delta hcp3$:pBR322-*hcp3*, $\Delta hcp4$:pBR322-*hcp4*, $\Delta hcp5$:pBR322-*hcp5*, and $\Delta hcp6$:pBR322-*hcp6*. Animals challenged with these strains all succumbed to infection in a pneumonic model. A delayed mean time to death was observed in some of the complemented strains, specifically the $\Delta hcp6$:pBR322-*hcp6* mutant (at a much lower challenge dose of 3 LD₅₀), this delayed death pattern did not reach statistical significance as compared to WT CO92. Thus, complementation of the *hcp* genes resulted in restoration of the WT phenotype (Fig. 4C).

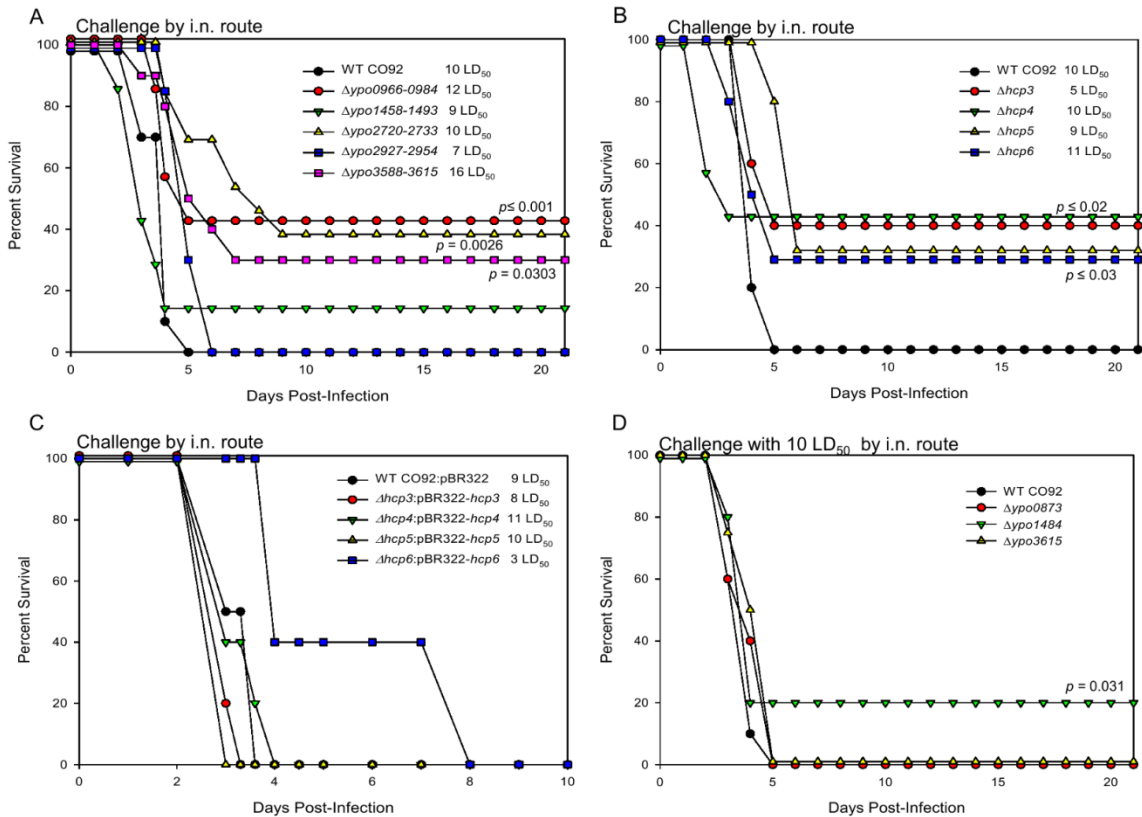


Figure 4: Virulence of T6SS-associated genes in a pneumonic plague mouse model.

Mice were infected with WT CO92 (n = 15; pooled from 3 independent experiments) or 1 of the 5 T6SS cluster deletion mutant strains, $\Delta ypo0966-0984$, $\Delta ypo1458-1484$, $\Delta ypo2720-2733$, $\Delta ypo2927-2954$, or $\Delta ypo3588-3615$ (n = 7-10) (A), 1 of the 4 Hcp-encoding gene deletion mutant strains, $\Delta hcp3$, $\Delta hcp4$, $\Delta hcp5$, or $\Delta hcp6$ (n = 5-7) (B), 1 of the 4 Hcp-encoding gene complemented deletion mutants strains, $\Delta hcp3$:pBR322-*hcp3*, $\Delta hcp4$:pBR322-*hcp4*, $\Delta hcp5$:pBR322-*hcp5*, or $\Delta hcp6$:pBR322-*hcp6* (n = 5) (C), or

1 of the PAAR motif-containing protein-encoding genes, $\Delta ypo0873$, $\Delta ypo1484$, or $\Delta ypo3615$ ($n = 5$) **(D)** with the indicated LD₅₀ doses by the i.n. route. Animals were observed for morbidity/mortality for 10-21 days. The data were analyzed for significance by using Kaplan-Meier survival estimates. The *P* values were determined based on comparison of animal survival for each mutant to the survival of WT CO92-infected control animals. Our target dose of the challenge was 10 LD₅₀; however, back titration of the inocula showed some variations. For the complemented *hcp6* strain, the target LD₅₀ dose was 5 **(C)**.

Of the identified PAAR motif-containing protein-encoding genes, 3 of the 5 had deletion mutants generated; $\Delta ypo0873$, $\Delta ypo1484$, and $\Delta ypo3615$. Of these mutants, only $\Delta ypo1484$ exhibited any level of attenuation, 20% survivability, in comparison to WT CO92 **(Table 2; Fig. 4D)**. This attenuation was similar to the level of attenuation, 14%, reported in the Cluster C ($\Delta ypo1458-1484$) deletion mutant, which contains $\Delta ypo1484$ **(Table 2; Fig. 4A)**.

Generation of combinatorial T6SS deletion mutants further augments attenuation in a murine model of pneumonic plague and provide some protection against re-challenge with WT CO92.

As single cluster and single *hcp* homolog deletion mutants exhibited significant attenuation *in vivo* **(Fig. 4A&B)**, we next wanted to evaluate whether this attenuation could be augmented through the generation of combinatorial deletion mutants. As we have previously reported $\Delta vasK$ to be attenuated and as *hcp6* has the highest homology to Hcp-encoding genes in other bacterial species such as *A. dhakensis* and *V. cholerae* (37, 73, 85), we generated a $\Delta vasK\Delta hcp6$ double deletion mutant. Additionally, we generated a $\Delta ypo2720-2733\Delta hcp3$ cluster and *hcp* homolog double deletion mutant. When evaluated for attenuation in a mouse model of pneumonic plague at a LD₅₀ dose equivalent to around 10 of WT CO92, both double deletion mutants exhibited

significantly high levels of attenuation, 60%, in comparison to WT CO92 (**Fig. 5**). It was also observed that in animals that did succumb to infection when challenged with the $\Delta ypo2720-2733\Delta hcp3$ mutant, there was an increased time to death (day 7-12 vs day 3-5).

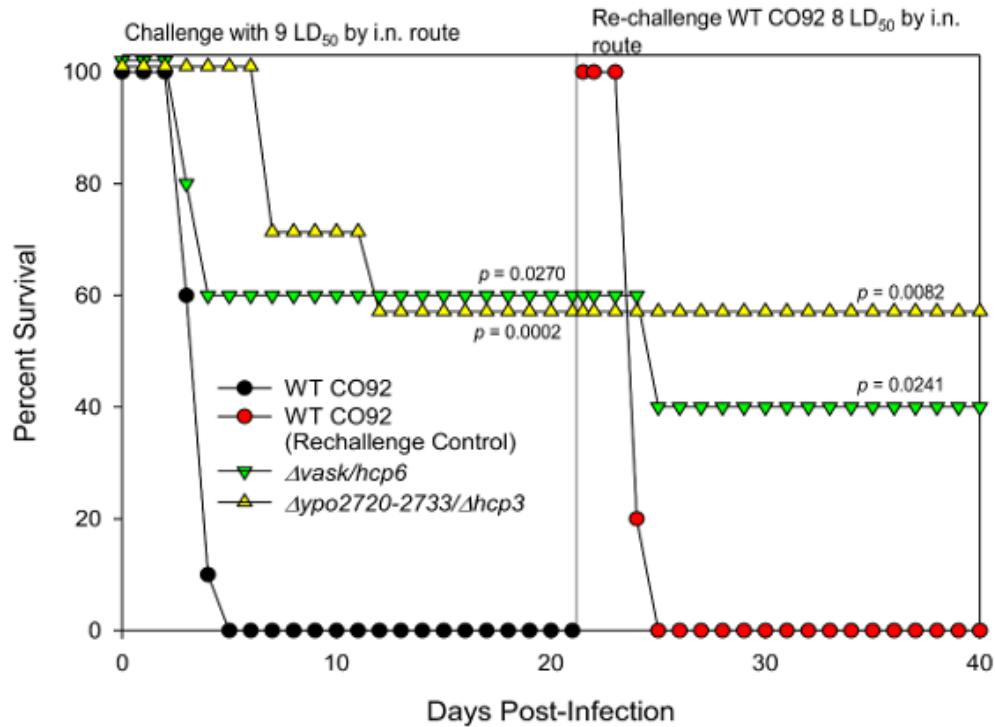


Figure 5: Vaccine potential for selected *Y. pestis* CO92 combinational mutants.

Animals were challenged by the i.n. route with the WT CO92 ($n = 10$ from 2 independent pooled experiments), $\Delta vasK\Delta hcp6$ ($n = 10$), or $\Delta 2720-2733 \Delta hcp3$ ($n = 7$) strain at 9 LD₅₀ and observed for mortality over a period of 21 days. Mice that survived the initial infection with the mutant strains and naive control animals ($n = 5$) were challenged with 8 LD₅₀ of the WT CO92 strain. Survival data were analyzed for significance by Kaplan-Meier survival estimates. The P values are for comparison of the results for the indicated strains to the corresponding result for WT CO92 (challenge experiment) or naive control infected with WT CO92 (re-challenge experiment).

As one of our long-term goals is to develop live-attenuated vaccine candidates, animals that survived initial infection with $\Delta vasK\Delta hcp6$ and $\Delta ypo2720-2733\Delta hcp3$ mutants were re-challenged with WT CO92 by the i.n. to mimic pneumonic infection. As shown in the results of **Fig. 5.**, 100% of the animals initially infected with $\Delta ypo2720-2733\Delta hcp3$ and re-challenged with WT CO92 at 10 LD₅₀ survived and were observed to be protected over a period of 18 days. For the $\Delta vasK\Delta hcp6$ mutant, one animal did succumb to infection, however, still exhibited significant, 60%, survivability in comparison to control WT CO92 challenged mice, which all succumbed to infection by day 4 (**Fig. 5**).

Characterization of growth kinetics and expression of effectors by attenuated T6SS mutant strains of *Y. pestis* CO92 *in vitro*.

Strains significantly attenuated in *in vivo* studies were further evaluated *in vitro* to begin to elucidate potential mechanisms of attenuation. We first evaluated growth kinetics of the attenuated mutant strains, $\Delta 0966-0984$, $\Delta ypo2720-2733$, $\Delta ypo3588-3615$, $\Delta hcp3$, $\Delta hcp4$, $\Delta hcp5$, $\Delta hcp6$, $\Delta vasK$, $\Delta vasK\Delta hcp6$, and $\Delta ypo2720-2733\Delta hcp3$, *in vitro* at both 28 and 37°C, to mimic both flea and eukaryotic host temperatures. At both 28 or 37°C, none of the mutants were observed to have any growth defects in comparison to WT CO92 (**Fig. 6&7**).

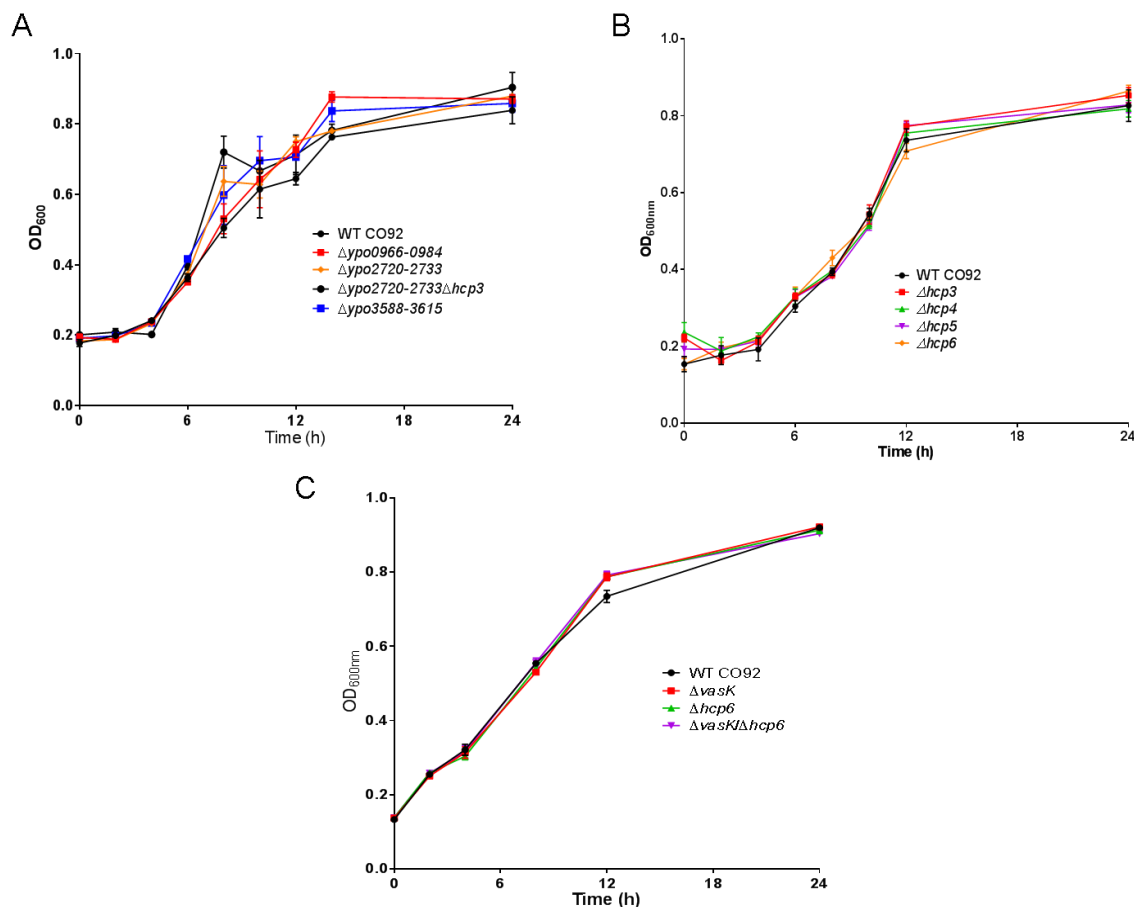


Figure 6: Growth of *Y. pestis* CO92 T6SS mutant strains *in vitro* at 28°C.

WT CO92 and the attenuated T6SS mutant strains were grown in HIB at 28°C. **(A)** Growth of the $\Delta ypo0966-0984$, $\Delta ypo2720-2733$, and $\Delta ypo3588-3615$ cluster deletion mutants and the double deletion mutant $\Delta ypo2720-2733\Delta hcp3$ in comparison to WT CO92. **(B)** Growth of *hcp* homolog deletion mutants $\Delta hcp3$, $\Delta hcp4$, $\Delta hcp5$, and $\Delta hcp6$. **(C)** Growth of $\Delta vasK$, $\Delta hcp6$, and $\Delta vasK\Delta hcp6$ in comparison to WT CO92. Samples were taken at the indicated time points for OD₆₀₀ measurements. Data shown are the mean values, while error bars represent standard deviations (SD) ($n = 4$). Statistical analysis was performed using Student's *t* test, with no mutant strains exhibiting any significant differences in growth in comparison to WT CO92.

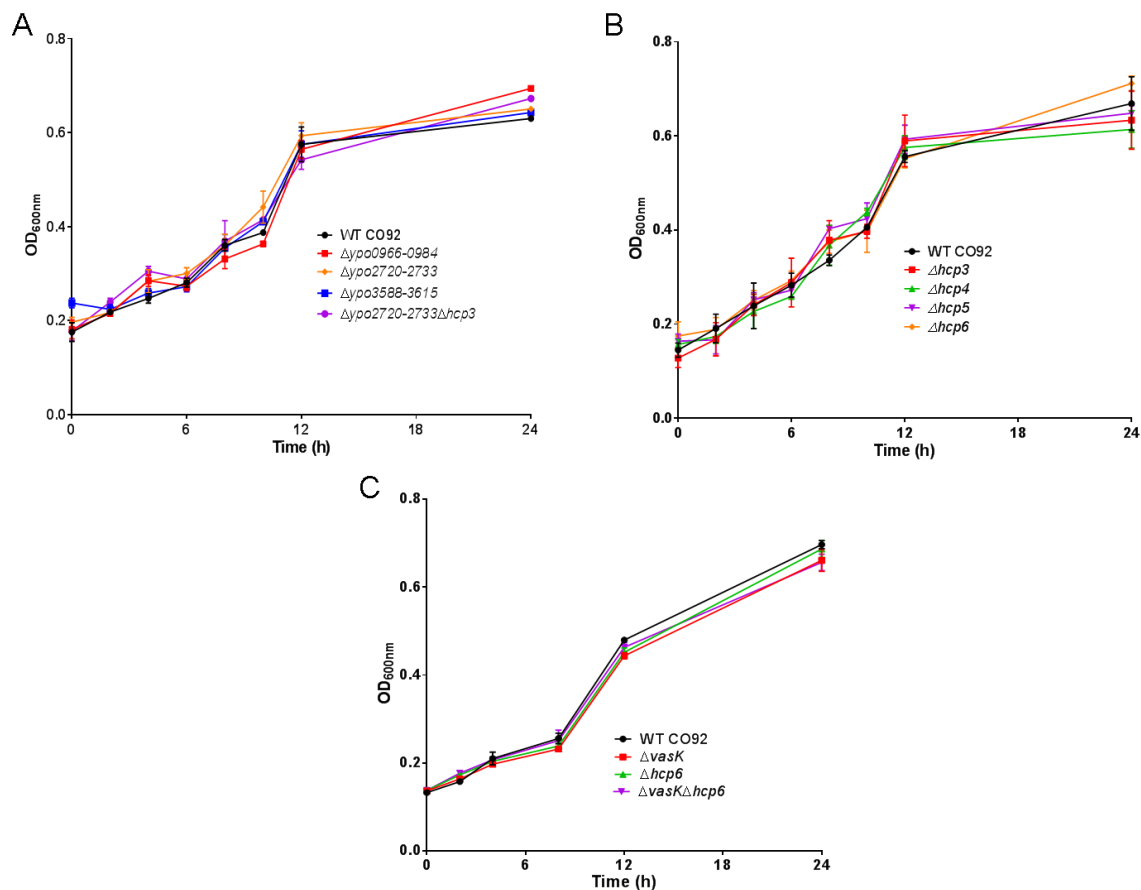


Figure 7: Growth of *Y. pestis* CO92 T6SS mutant strains *in vitro* at 37°C.

WT CO92 and the attenuated T6SS mutant strains were grown in HIB at 37°C. **(A)** Growth of the $\Delta ypo0966-0984$, $\Delta ypo2720-2733$, and $\Delta ypo3588-3615$ cluster deletion mutants and the double deletion mutant $\Delta ypo2720-2733\Delta hcp3$ in comparison to WT CO92. **(B)** Growth of *hcp* homolog deletion mutants $\Delta hcp3$, $\Delta hcp4$, $\Delta hcp5$, and $\Delta hcp6$. **(C)** Growth of $\Delta vasK$, $\Delta hcp6$, and $\Delta vasK\Delta hcp6$ in comparison to WT CO92. Samples were taken at the indicated time points for OD₆₀₀ measurements. Data shown are the mean values, while error bars represent standard deviations (SD) ($n = 4$). Statistical analysis was performed using Student's *t* test, with no mutant strains exhibiting any significant differences in growth in comparison to WT CO92.

Hcp secretion from bacteria is a well-established marker of a functional T6SS (73). In order to confirm that deletion of *hcp6* alone or in combination with *vasK*, as well as if any other deletion attenuated mutants had an effect on this effector, Hcp6 production and secretion was evaluated by Western blot analysis (**Fig. 8A**). Hcp6 was detected in both the supernatants and the pellets of all mutant strains with the exception of $\Delta hcp6$, $\Delta vasK/hcp6$, and $\Delta ypo3588-3615$, which served as negative controls. For the $\Delta ypo3588-3615$ mutant, production of Hcp6 was noted in the pellet fraction, but exhibited no secretion of Hcp6 in the supernatant fraction (**Fig. 8A**). These data indicated that Hcp6 is secreted through T6SS Cluster G. Anti-Hcp6 antibodies did not cross-react with other Hcp homologs because of low homologies (31-34%) (**Table 2**).

As the T3SS is an essential and well-studied virulence mechanism of *Y. pestis*, we wanted to determine if deletion of any T6SS components affected T3SS functionality. Production YopE, which destroys actin monofilaments, was evaluated by Western blot analysis in attenuated mutant strains and WT CO92. YopE production differed in several mutants in both pellet and bacterial supernatant fractions (**Fig. 8A-C**). While all mutants did produce YopE to some extent in pellet fractions, mutants $\Delta ypo3588-3615$, $\Delta hcp3$, and $\Delta hcp4$ exhibited increased production while mutants $\Delta vasK$, $\Delta hcp6$, and $\Delta ypo2720-2733/\Delta hcp3$ exhibited decreased production (**Fig. 8A-C**). In terms of YopE secretion, several mutants exhibited decreased production in supernatant fractions in comparison to WT CO92, apart from mutants $\Delta ypo0966-0984$ and $\Delta ypo3588-3615$, with expression levels comparable to WT CO92, and $\Delta hcp3$, with expression of YopE higher in comparison to WT CO92 (**Fig. 8A-C**).

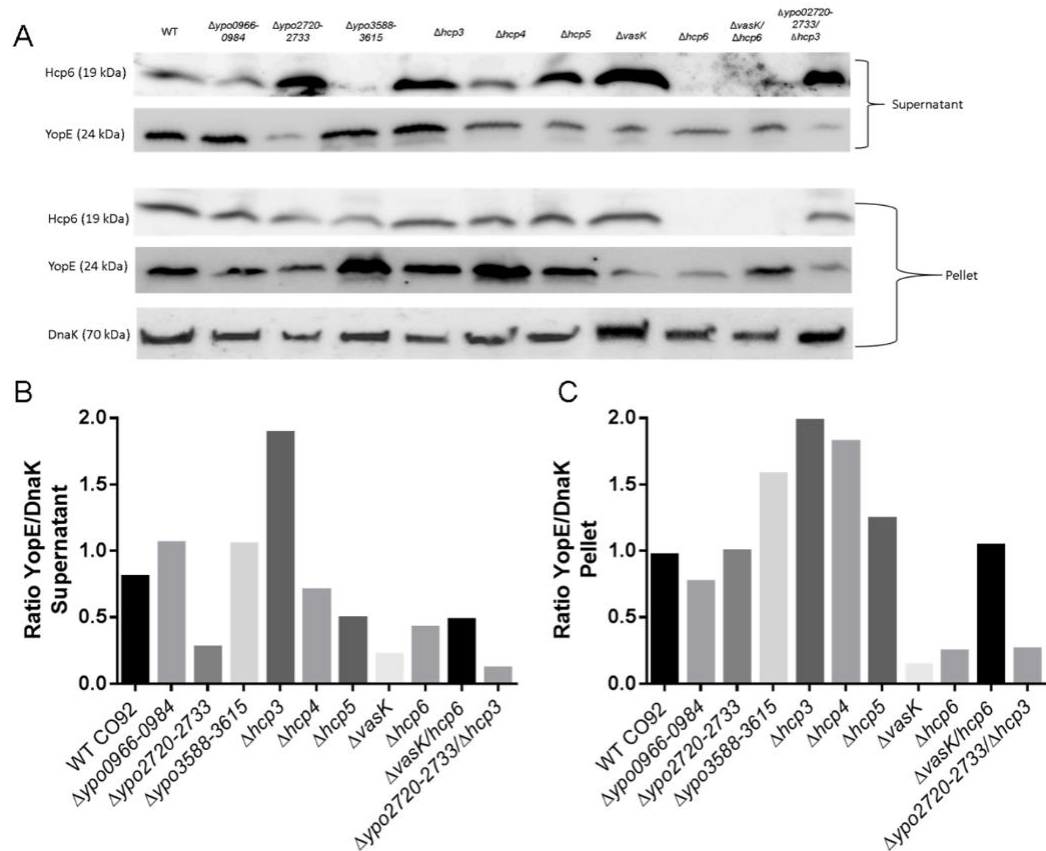


Figure 8: Production of the T6SS effector Hcp6 and the T3SS effector YopE.

WT *Y. pestis* CO92 and the indicated T6SS mutant strains were grown in HIB overnight and subsequently diluted 1:20 in fresh HIB supplemented with 5 mM EGTA. Growth was continued at 28°C for 2 h, followed by a temperature shift to 37°C for an additional 3 h of incubation. Supernatants, after TCA precipitation, and bacterial pellets were dissolved in SDS-PAGE buffer. Western blot analysis was then performed to detect Hcp6 and YopE in bacterial pellet and supernatant samples (A). Levels of DnaK in bacterial pellets were utilized as a loading control to ensure similar levels of bacteria were used across all samples examined. Sizes of the proteins are indicated in parentheses. Densitometry scanning was used to quantitate expression of YopE in ratio to DnaK in the supernatant (B) and pellet (C) samples. Densitometry scanning was performed using Image Studio™ Lite Software (Li-Cor Inc., Lincoln, NE).

Role of T6SS in host cell cytotoxicity following *Y. pestis* infection.

The T6SS delivers effector molecules into target cells using a needle like apparatus with high homology to the assembly, structure, and function of bacteriophage tails (35). It has been reported that T6SS can target both bacterial and eukaryotic cells and cause cytotoxicity (36). To evaluate any changes in cytotoxic effects of the attenuated T6SS deletion mutant strains on eukaryotic cells, we used the MTT assay to measure cell viability following infection. RAW 264.7 murine macrophages were infected with the various *Y. pestis* strains (WT CO92 or the $\Delta ypo0966-0984$, $\Delta ypo2720-2733$, or $\Delta ypo3588-3615$ clusters, $\Delta hcp3$, $\Delta hcp4$, $\Delta hcp5$, $\Delta hcp6$, $\Delta vasK$ single, or $\Delta vasK\Delta hcp6$ and $\Delta ypo2720-2733\Delta hcp3$ double deletion mutants) at a MOI of 100, and incubated for 12 h. Macrophages infected with two cluster deletion mutants ($\Delta ypo2720-2733$ and $\Delta ypo3588-3615$), three *hcp* homolog deletion mutants ($\Delta hcp3$, $\Delta hcp4$ and $\Delta hcp6$), and both combinatorial deletion mutants ($\Delta vasK\Delta hcp6$ and $\Delta ypo2720-2733\Delta hcp3$) exhibited significantly higher cell viabilities in comparison to WT CO92 (**Fig. 9A**). These results indicated that the above-mentioned mutant strains were significantly less cytotoxic to host cells during infection in comparison to WT CO92.

Quantification of phagocytosis and intracellular survival of T6SS deletion mutant strains.

The attenuated T6SS deletion mutants identified *in vivo* ($\Delta ypo0966-0984$, $\Delta ypo2720-2733$, $\Delta ypo3588-3615$, $\Delta hcp3$, $\Delta hcp4$, $\Delta hcp5$, $\Delta hcp6$, $\Delta vasK$, $\Delta vasK\Delta hcp6$, and $\Delta ypo2720-2733\Delta hcp3$), were evaluated for any significant changes in phagocytosis in comparison to WT CO92 in RAW 264.7 murine macrophages. For the cluster deletion mutants, including the double deletion mutant $\Delta ypo2720-2733\Delta hcp3$, only $\Delta ypo3588-$

3615, which includes *vasK* (*ypo3603*), exhibited any significant increase in phagocytosis (**Fig. 9B**). For the *hcp* homolog deletion mutants, $\Delta hcp4$ and $\Delta hcp6$ exhibited significant increases in phagocytosis in comparison to WT CO92, although it was noted that the increase observed for $\Delta hcp4$ was not to the extent of $\Delta hcp6$ ($p = 0.022$ for $\Delta hcp6$ vs. $\Delta hcp4$). Additionally, both the $\Delta vasK$ and $\Delta vasK\Delta hcp6$ double mutant exhibited significantly increased rates of phagocytosis.

We next evaluated the ability of the various attenuated T6SS deletion mutants to survive in RAW 264.7 murine macrophages to determine the role these genes may play in intracellular survival of *Y. pestis*. Macrophages were infected with WT CO92 or the $\Delta ypo0966-0984$, $\Delta ypo2720-2733$, and $\Delta ypo3588-3615$ clusters, $\Delta hcp3$, $\Delta hcp4$, $\Delta hcp5$, $\Delta hcp6$, $\Delta vasK$ single, or $\Delta vasK\Delta hcp6$ and $\Delta ypo2720-2733\Delta hcp3$ double deletion mutants at a MOI of 10. The evaluated strains all exhibited significantly lower intracellular survival at 4 h p.i. in comparison to WT CO92, with the exception of 2 strains; $\Delta ypo2720-2733$ and $\Delta ypo2720-2733\Delta hcp3$ (**Fig. 9C**).

As we have previously reported that Hcp inhibits phagocytosis of *A. dhakensis* (85), we further evaluated the phagocytic role of *hcp6*, which has high homology (82%) to *hcp* of *A. dhakensis*, in *Y. pestis*. RAW 264.7 murine macrophages were infected with WT CO92, $\Delta vasK$, $\Delta hcp6$, or $\Delta vasK\Delta hcp6$ mutant strains with or without the addition of recombinant(r)Hcp6 from CO92 (**Fig. 10A**) or rHcp from *A. dhakensis* (**Fig. 10B**), thus allowing for complementation of the mutants with exogenous Hcp6 protein. We noted that for all 3 mutant strains tested, the rate of phagocytosis was significantly increased in comparison to WT CO92 (**Fig. 10A&B**). Furthermore, the ability of these mutants to be phagocytosed was significantly reduced, to levels equivalent to that of WT CO92, with

the addition of rHcp6/rHcp at a physiologically relevant concentration of 10 μ g (85) (**Fig. 10A&B**).

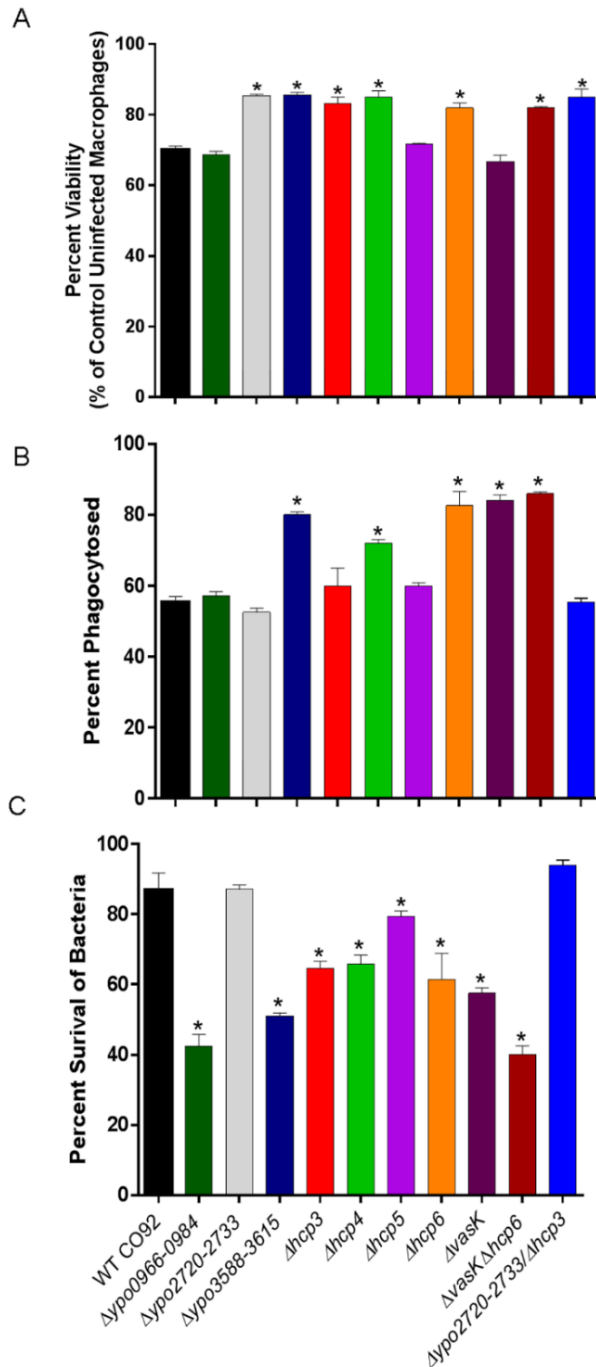


Figure 9: Mechanisms of attenuation of *Y. pestis* CO92 mutants.

(A) Determination of bacterial cytotoxicity to murine macrophages. RAW264.7 murine macrophages were infected with the indicated *Y. pestis* strains at an MOI of 100, treated with gentamicin, and then incubated for 12 h. Viability following infection was evaluated by MTT assay and data plotted as percentage of uninfected macrophages. (B) Percent phagocytosis of *Y. pestis* strains in RAW 264.7 murine macrophages. Macrophages were infected with the indicated *Y. pestis* strains at an MOI of 10 and, after gentamicin treatment, were lysed for bacterial enumeration as determined by serial dilution and plating on SBA plates. Percent of phagocytosed bacteria was calculated based on the number of bacteria used to infect the macrophages. (C) Quantification of intracellular survival of *Y. pestis* CO92 mutant strains in RAW 264.7 murine macrophages. RAW 264.7 macrophages were infected with *Y.*

pestis CO92 strains at an MOI of 10. At 4 h p.i., macrophages were lysed and CFUs determined as previously described. The data were analyzed by one-way ANOVA with Tukey's *post hoc* test. *, $P < 0.05$.

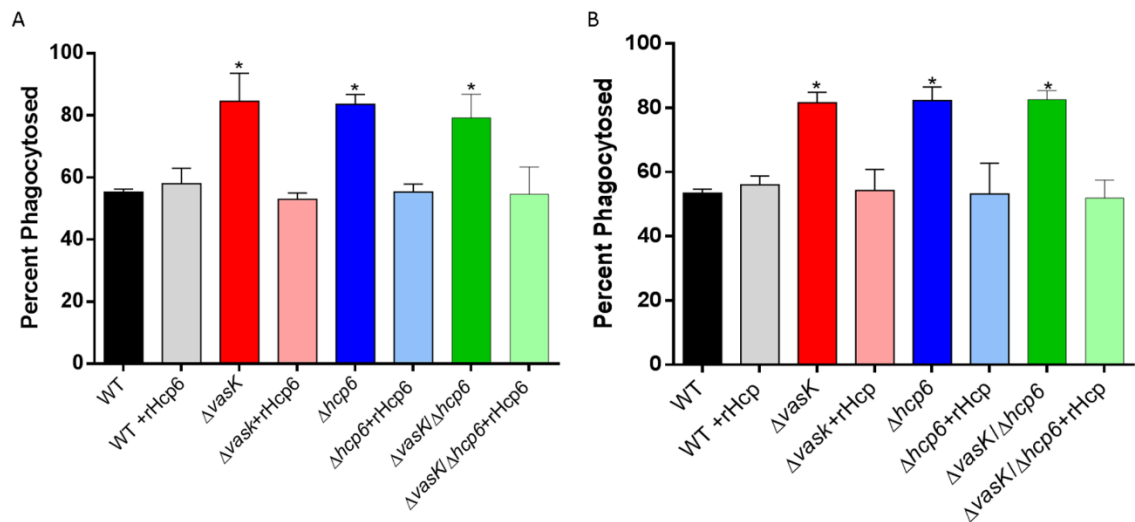


Figure 10: Phagocytosis of WT CO92, $\Delta vasK$, $\Delta hcp6$, and $\Delta vasK\Delta hcp6$ mutants in RAW264.7 murine macrophages in the presence of exogenous recombinant Hcps.

Macrophages were infected with WT and the indicated mutant strains at MOI of 10 and incubated for 1 h with or without 10 $\mu\text{g/ml}$ rHcp6 (*Y. pestis* (A)) or rHcp (*A. dhakensis* (B)). Cells were then washed and incubated for 1 h with gentamicin to kill extracellular bacteria before being lysed for intracellular bacterial enumeration (see legend for Fig. 9B). The data were analyzed by comparison of each strain with/out the addition of rHcp6/rHcp using one-way ANOVA with Tukey's *post hoc* test. *, $P < 0.01$.

DISCUSSION

The need to develop targeted live-attenuated vaccines for plague is evident given its status as a Tier 1 select agent, a re-emerging human pathogen, and potential for use as a biological weapon (2, 4). Although several virulence factors of *Y. pestis* have been identified and well characterized, they alone cannot account for the extremely virulent phenotype of the plague bacterium.”

“Three genes of the T6SS were identified in our STM screen, with the $\Delta vasK$ and $\Delta lpp\Delta vasK$ deletion mutants showing attenuation in both bubonic and pneumonic models

of plague providing the first evidence that T6SS is involved in *Y. pestis* virulence (37). Although the T6SS has been the target for potential vaccine development (88), its role in *Y. pestis* virulence remains mostly unknown. The *Y. pestis* genome contains several T6SS loci, which differ in both gene numbers and arrangements, and several T6SS effectors, which are contained both within and outside of these predicted T6SS clusters (32, 33). For this study, we generated five uncharacterized T6SS cluster deletion mutants, four *hcp* homolog deletion mutants, and three PAAR motif repeat-containing protein-encoding gene deletion mutants (Table 2). The T6SS locus *ypo2715-2733* contained the gene *lepA* (*ypo2716*), which has been shown to be an essential bacterial translation factor (89), so the deletion mutant Δ *ypo2720-2733* was generated to elucidate the role of this T6SS cluster on *Y. pestis* virulence. Additionally, only 4 of the 6 *hcp* genes were targeted for deletion as the other two were encoded within two of the T6SS loci, and, hence, any effects from these individual *hcp* homolog genes would be observed in the full T6SS cluster deletion mutants. For three cluster deletion mutants, Δ *ypo0966-0984*, Δ *ypo2720-2733*, and Δ *ypo3588-3615*, and all four *hcp* homolog deletion mutants generated, a significant attenuation of virulence (Fig. 4), was observed in a murine pneumonic plague model in comparison to WT CO92. Through the generation of two combinatorial deletion mutants, Δ *vasK* Δ *hcp6* and Δ *ypo2720-2733* Δ *hcp3*, attenuation could be further augmented (Fig. 5). Further, these two mutants generated protective immunity in mice (Fig. 5).

Attenuation of mutant strains *in vivo* may be the result of several factors including defects in growth or defects in ability to evade and survive the host's immune response. For all T6SS-associated attenuated strains identified *in vivo*, none had any growth defects

in comparison to WT CO92 when grown at both 28 and 37°C (Fig. 6&7). In evaluating T6SS functionality, specifically in terms of Hcp6 production and secretion, as expected, no Hcp6 production was noted in $\Delta hcp6$ or $\Delta vasK/\Delta hcp6$ mutant strains (Fig. 8). Interestingly, for $\Delta ypo3588-3615$ mutant, Hcp6 was not secreted in the supernatant fraction, but was found in the bacterial pellet fraction. These results indicated that Hcp6 could be secreted through the *ypo3588-3615* locus.

As T3SS is a well-established virulence factor of *Y. pestis* (12), we also evaluated this system's functionality in the attenuated mutant strains (Fig. 8). For YopE expression, several mutants showed varying production levels in comparison to WT CO92. In *P. aeruginosa*, studies have shown a link between regulation of the T3SS and T6SS, with evidence presented that c-di-GMP levels can modulate the switching of these secretion systems (90). While our results may suggest a similar link in *Y. pestis*, future studies looking more into this connection and mechanism are required.

To elucidate the fitness of the mutants against the host's immune defenses, we evaluated the intracellular survival of the attenuated mutant strains in RAW 264.7 murine macrophages. In comparison to WT CO92, all the mutant strains evaluated exhibited significantly decreased intracellular survival, with the exception of $\Delta ypo2720-2733$ and $\Delta ypo2720-2733\Delta hcp3$ (Fig. 9C), suggesting that decreased fitness of these two mutants in host macrophages is not involved in their attenuation in animals.

The T6SSs are involved in the delivery of effector proteins to both prokaryotic and eukaryotic cells and, hence, can cause toxicity to the target cells (36). Out of the 10 T6SS deletion mutant strains tested, 7 strains exhibited decreased host cell cytotoxicity in comparison to WT CO92 (Fig. 9A). For the $\Delta ypo2720-2733$ and $\Delta ypo2720-2733\Delta hcp3$

mutant strains, which exhibited no defects in intracellular survival in murine macrophages, this decrease in cytotoxicity may be responsible for not only the attenuation observed for both mutants *in vivo*, but also subsequent protection from re-challenge with WT CO92 (Fig. 5).

The Hcp protein is one of the most well characterized effectors of the T6SS (34, 36). In addition to its role as a structural component and secreted effector, in *A. dhakensis*, we have reported that Hcp is anti-phagocytic in nature (85). As Hcp6 of *Y. pestis* shares significant homology (82%) with the Hcp protein of *A. dhakensis*, we evaluated whether Hcp6 plays a similar role in *Y. pestis*. In macrophages infected with $\Delta vasK$, $\Delta hcp6$, or $\Delta vasK\Delta hcp6$ mutant strains, all exhibited similar and significantly higher rates of phagocytosis in comparison to WT CO92 (Fig. 9B).

Indeed, in this same model of infection, the addition of rHcp6 (*Y. pestis*) or rHcp (*A. dhakensis*) decreased the percentage of phagocytosed bacteria for all three strains ($\Delta vasK$, $\Delta hcp6$, and $\Delta vasK\Delta hcp6$) reverting the phenotype observed back to that of WT CO92 (Fig. 10A&B). These data indicated that Hcp6 of *Y. pestis* plays a similar role to that observed for Hcp in *A. dhakensis* and the rHcp/rHcp6 of these two pathogens can be interchangeably used (Fig. 10A&B). We previously reported no defect in secretion of *hcp6* in the $\Delta vasK$ deletion mutant of *Y. pestis* when grown in culture, as observed by immunoblot analysis (37). However, increased phagocytosis of this deletion mutant and subsequent reversion to the WT phenotype upon addition of rHcp6 (Fig. 10A) suggest a defect in either protein translocation or secretion in the host-pathogen co-culture model and warrants further investigation. For the other *hcp* homolog deletion mutants, only $\Delta hcp4$ exhibited any significant increase in phagocytosis in comparison to WT CO92

(Fig. 9B). For the cluster deletion mutants, only $\Delta ypo3588-3615$ (Cluster G; Table 2), which includes *vasK*, exhibited any significant increase in phagocytosed bacteria (Fig. 9B).”

These results indicate that these T6SS effectors and clusters have distinct roles in terms of *Y. pestis* virulence and represent novel targets for the further development of novel live-attenuated vaccine candidates for plague.

Chapter 3: Development and Testing of New Therapeutics Targeting Host Genes to Combat Plague Infection

INTRODUCTION

“Antibiotic resistance and the threat of a post antibiotic era continue to be a growing global problem. Further, the discovery and/or availability of novel classes of anti-microbial agents are in retreat (91, 92). Contributing to the latter, traditional drug discovery is a highly inefficient, costly, and challenging process. As a result, systematic screening of non-antibiotic FDA-approved drugs for other indications in humans offers a rapid alternative for novel antimicrobial drug discovery (93, 94). Such drugs could potentially have antibiotic-like activity, modulate bacterial virulence or regulate host genes necessary for bacterial replication, and, hence aid in pathogen clearance (93, 94). In recent years, increased focus has been placed on characterizing host mechanisms/pathways exploited by bacteria during pathogenesis. Drugs able to block these pathways represent novel therapeutic options and reduce the likelihood for the development of resistance, unlike antibiotics (95–97). Some recent studies have utilized such drug repurposing approaches to identify both novel bactericidal and host-directed drugs as potential therapeutics against pathogens such as, the Ebola virus, *Borrelia burgdorferi*, *Coxiella burnetii*, and *Legionella pneumophila* (95, 98–100).”

These studies focused on the highly virulent pathogen *Y. pestis* to identify novel therapeutics as it is still a prevalent public health threat and antibiotic resistant strains have been isolated in nature as well as bio-engineered (4, 56, 59, 101). “In order to

identify potential novel therapeutics, we conducted a screen of 780 FDA-approved drugs to assess macrophage viability following *Y. pestis* CO92 infection. Although not an exact clinical correlate, macrophages are an essential component in innate immunity and a first line of defense for numerous infections, including the facultative intracellular pathogen *Y. pestis* (1, 102, 103), making this approach a rapid and effective way to identify lead therapeutic compounds for further studies in *in vivo* models. From *in vitro* screening, we reproducibly, through two independent experiments performed in duplicate, identified 94 drugs significantly effective in preventing macrophage cytotoxicity during *Y. pestis* infection. From these 780 drugs, a total of 17 were prioritized, based on *in vitro* screening methods, and assessed in a murine model of pneumonic plague. Three drugs, trifluoperazine (TFP), an antipsychotic of the phenothiazine class, doxapram (DXP), a breathing stimulant, and amoxapine (AXPN), a tricyclic anti-depressant, increased animal survival. Interestingly, these three drugs were shown to have no impact on bacterial growth or expression/production of T3SS effectors or the T6SS effector Hcp6, and exhibited high minimum inhibitory concentration (MIC) values (≥ 100 $\mu\text{g/ml}$), which would be difficult to achieve in human plasma.

MATERIALS AND METHODS

Bacterial strains and cell culture.

A highly virulent *Y. pestis* CO92 strain was obtained from the Biodefense and Emerging Infections (BEI) Research Resources Repository, Manassas, VA. The *Y. pestis* CO92-*lux* strain was generated in our previous study, which harbors the luciferase gene (30). *Y. pestis* strains were grown as described in Chapter 2 and all experiments with *Y.*

pestis strains were performed in the CDC-approved select agent laboratory in the GNL, UTMB.”

RAW 264.7 murine macrophage cell lines (ATCC) were maintained as described in Chapter 2.

Reagents.

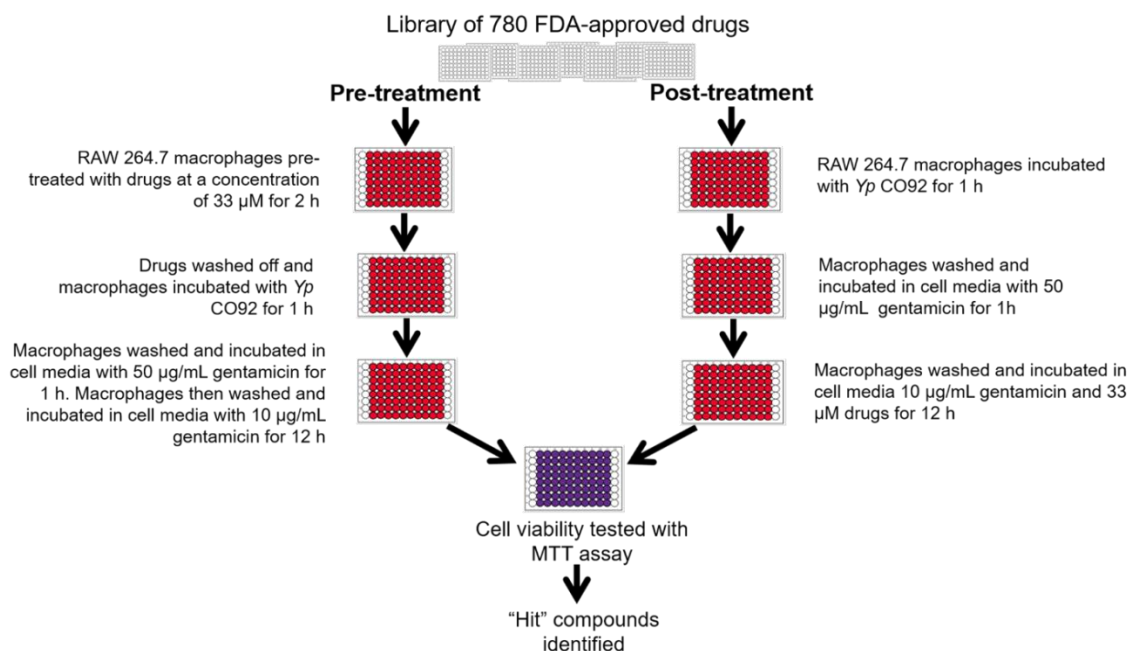
“The Screen-Well FDA-approved drug library V2, consisting of 780 compounds, was provided as 10 mM stock solutions in dimethyl sulfoxide (BML-2843-0100; Enzo Life Sciences, Albany, NY). Sterile, injectable formulations of levofloxacin, doxapram (DXP), haloperidol, carboplatin, dihydroergotamine mesylate, and promethazine were purchased from the UTMB Pharmacy. Tablet formulations of zarfirlukast, mesalamine, colchicine, and aspirin were also purchased from the UTMB Pharmacy. Amoxapine (AXPN), trifluoperazine (TFP), desogestrel, ethinyl estradiol, carglumic acid, apomorphine, and pantoprazole were purchased from Sigma-Aldrich (St. Louis, MO) in a dry powder form. Epinastine, also in dry powder form, was purchased from Abcam (Cambridge, MA). MTT [3-(4,5-dimethylthiazol-2-yl)-2,5-diphenyltetrazolium bromide] and detergent solution were purchased from ATCC.

Screening for macrophage cell viability.

Murine RAW 264.7 cells were seeded in 96-well microtiter plates at a concentration of 2×10^4 cells/well to form confluent monolayers in a volume of 100 μ L per well.

Pre-treatment screens:

Macrophages were incubated with 33 μM concentrations of drugs 2 h prior to infection (**Fig. 11**). Plates were then infected with *Y. pestis* CO92 at a MOI of 100, centrifuged at 1,250 rpm for 10 min to promote bacterial contact with the host-cells, and incubated at 37°C/5% CO_2 for 60 min. The wells were then washed with PBS, and



extracellular bacteria were killed with the addition of 50 $\mu\text{g/mL}$ of gentamicin to each well for 60 min at 37°C/5% CO_2 . The wells were then washed with PBS, and macrophages were maintained in medium containing a maintenance concentration (10 $\mu\text{g/mL}$) of gentamicin for 12 h before performing the MTT assay (see below).

Figure 11. Schematic illustration of FDA-approved drug screening method.

Using a modified gentamicin protection intracellular survival assay (33), we evaluated the efficacy of drugs (33 μM) on host cell viability as either a pre- or post- treatment option during *Y. pestis* (*Yp*) infection. Pre-treatment occurred 2 h prior to bacterial infection of macrophages, while post-treatment occurred immediately after gentamicin treatment (2 h post infection [p.i.]) to kill extracellular bacteria. Macrophages were incubated for 12 h and the MTT assay measured host cell viability.

Post-treatment screens:

Following infection and treatment with gentamicin (2 h p.i.), 33 μ M concentrations of drugs were added to macrophages (**Fig. 11**), and were incubated for 12 h at 37°C/5% CO₂. Reduction of MTT was used as an index of cell viability following the protocol outlined by ATCC. Briefly, MTT reagent was added to the microtiter plate wells (10 μ L/well), and cells were incubated at 37°C/5% CO₂ for an additional 2 h. Then, 100 μ L of the detergent reagent was added to the wells and incubated in the dark at ambient temperature for 2 h. Absorbance values were measured at 570 nm in a Spectramax M5e microplate reader (Molecular Devices, Sunnyvale, CA).

Screening for inhibition of *Y. pestis* CO92 intracellular survival.

The *Y. pestis* CO92-*lux* strain was grown in HIB overnight to saturation at 28°C. RAW 264.7 macrophages were seeded in 96-well plates at a concentration of 2×10^4 cells/well for confluency. Plates were then infected with *Y. pestis* CO92-*lux* at an MOI of 250 in DMEM medium, centrifuged, and incubated at 37°C/5% CO₂ for 60 min. Infected macrophages were then washed with PBS, treated with gentamicin, washed again with PBS, and maintained in DMEM as described above. Then, 33 μ M concentrations of drugs were added to each well of the microtiter plates and incubated at 37°C/5% CO₂. At 0, 4, 8 and 12 h p.i., luminescence was measured in a Spectramax M5e microplate reader.

Testing lead drugs in *Y. pestis* CO92 pneumonic plague model.

All animal studies with *Y. pestis* were performed as described in Chapter 2 in an ABSL-3 facility under an approved IACUC protocol (UTMB). Briefly, mice were anesthetized by the intraperitoneal (i.p.) route with a mixture of ketamine and xylazine

and subsequently challenged i.n. with 10 LD₅₀ *Y. pestis* CO92. Immediately following infection, mice were dosed through either the i.p. or the oral route with one of 17 lead drugs (identified through *in vitro* screens described above) at concentrations ranging from 0.025-150 mg/kg (**Table 3**). Dosing occurred once at the time of challenge or once every 24 h for up to 6 days. Beginning at 24 h p.i., an additional group of mice were dosed with 5 mg/kg levofloxacin administered i.p. at 24-h intervals for 3 or 6 days to serve as a positive control for therapeutic treatment. Mice were assessed for morbidity and/or mortality as well as clinical symptoms for the duration of each experiment (up to 21 days p.i.).

For a combinational study with TFP and levofloxacin, mice were dosed with TFP through the i.p. route at a concentration of 1.5 mg/kg at the time of infection, while levofloxacin (0.25 mg/kg; sub-inhibitory dose) was administered i.p. at 24 h p.i. and subsequently at 24-h intervals for 3 days. Saline, TFP (1.5 mg/kg)-only, and levofloxacin (0.25 mg/kg and 5 mg/kg)-only groups of mice were used as controls and dosed as described above.

Screening for dose response effects on macrophage viability following drug treatment and infection with *Y. pestis* CO92.

Following the post-treatment protocol outlined above, murine RAW 264.7 cells were seeded in 96-well microtiter plates at a concentration of 2×10^4 cells/well to form confluent monolayers in a volume of 100 μ L per well. Macrophages were then infected with *Y. pestis* CO92 at an MOI of 100 and subsequently incubated with gentamicin (2 h p.i.). TFP, DXP, and AXPN were then added at 1, 10, 20, 33, and 50 μ M concentrations to macrophages and incubated for 12 h at 37°C/5% CO₂. Reduction of MTT was used as

an index of cell viability, and absorbance values were measured at 570 nm in a Spectramax M5e microplate reader.

Table 3: List of drugs, doses, and routes of administration for treatment in murine model of pneumonic plague.

Drug name	Drug concentration	Route of administration	LD ₅₀ based on route of administration in mice ¹
Trifluoperazine	5mg/kg	i.p.	133 mg/kg
Mesalamine	100mg/kg	oral	> 2800 mg/kg
Haloperidol	5mg/kg	i.p.	30 mg/kg
Promethazine	20mg/kg	i.p.	160 mg/kg
Aspirin	100mg/kg	oral	250 mg/kg
Colchicine	2mg/kg	i.p.	> 2 mg/kg
Carboplatin	30mg/kg	i.p.	> 100 mg/kg
Doxapram	50mg/kg	i.p.	175 mg/kg
Zarfirlukast	10mg/kg	i.p.	> 100 mg/kg
Desogestrel	0.125mg/kg	oral	300 mg/kg
Ethinyl Estradiol	0.025mg/kg	oral	> 1000 mg/kg
Amoxapine	5mg/kg	i.p.	112 mg/kg
Apomorphine	5mg/kg	i.p.	128 mg/kg
Carglumic acid	150mg/kg	oral	> 1000 mg/kg
Pantoprazole	5mg/kg	i.p.	> 10 mg/kg
Dihydroergotamine mesylate	0.5mg/kg	i.p.	> 200 mg/kg
Epinastine	3mg/kg	oral	300 mg/kg

LD₅₀ based on literature¹

Growth kinetics and sensitivity of *Y. pestis* CO92 to TFP, DXP, and AXPN.

Overnight cultures of *Y. pestis* CO92, grown in HIB at 28°C, were normalized to the same absorbance by measuring the optical density at 600 nm (OD₆₀₀). Subcultures were then inoculated into 20 mL of HIB contained in 125 mL polycarbonate Erlenmeyer flasks with HEPA-filtered tops containing 33 µM concentrations of TFP, DXP, AXPN, levofloxacin (positive control), or PBS (negative control). The cultures were incubated at 37°C with agitation, and samples for absorbance measurements were taken at the indicated time points. For MIC determinations, the broth macro-dilution method was utilized (33). Briefly, *Y. pestis* CO92 was grown to saturation at 28°C and adjusted to a 0.5 McFarland standard before addition of the same volume of the culture to serial dilutions of each drug (highest concentration tested was 100 µg/mL) in 5mL of HIB. Cultures were grown for 24 h with agitation at 37°C. Bacterial growth with PBS or with levofloxacin served as negative or positive controls, respectively.

Evaluation of *Y. pestis* CO92 virulence factor expression and plasminogen activator (Pla) protease activity in response to TFP, DXP, and AXPN.

For Western blot analysis of T3SS effectors, overnight cultures of *Y. pestis* CO92, grown in HIB at 28°C, were diluted 1:20 in 5 mL HIB, supplemented with 5 mM EGTA to trigger the low-calcium response. Then, 33 µM concentrations of TFP, DXP or AXPN were added and the culture incubated at 28°C for 2 h before being shifted to 37°C (to activate the T3SS) for an additional 3 h of growth. After centrifugation, the cell pellets were dissolved in SDS-PAGE buffer and analyzed by immunoblotting using antibodies to YopE,” Hcp6, “and LcrV (Santa Cruz Biotechnology, Santa Cruz, CA). Aliquots (1mL) of supernatants were precipitated with 20% (v/v) trichloroacetic acid (TCA) on ice for 2

h. The TCA precipitates were then dissolved in SDS-PAGE buffer and analyzed by immunoblotting using antibodies to YopE” and Hcp6. “The anti-DnaK monoclonal antibody (Enzo) was employed for analysis of cell pellets to ensure similar numbers of bacteria were used across testing conditions.

For Pla protease activity, WT CO92 was plated on a HIB agar plate from -80°C glycerol stock and incubated at 28°C for 36 h. A single colony was re-plated on a fresh HIB agar plate and incubated at 28°C for 20-22 h. Bacteria was then suspended in HIB and incubated with a 33 μ M concentration of either TFP, AXPN, DXP, or PBS, as a control, and grown overnight. Cultures were centrifuged, washed twice, and re-suspended in PBS with 33 μ M of each respective drug to obtain a final optical density (OD₆₀₀) value of 0.25 in a spectrophotometer (SmartSpec[™] 300, Bio-Rad). For each sample, 50 μ l suspensions (3.1×10^6 CFU/well) were added to wells of a black microtiter plate (Costar Corning Inc., Corning, NY) in triplicate. Samples containing only PBS and each drug were also analyzed for any drug auto-fluorescence. The hexapeptide substrate DABCYL-Arg-Arg-Ile-Asn-Arg-Glu (EDANS)-NH₂, synthesized on Sieber amide resin (34), was added to the wells at a final concentration of 2.5 μ g/50 μ l. The kinetics of substrate cleavage by Pla was measured every 10 min for 3 h by fluorometric assay (Excitation/Emission 360/460nm) at 37°C on BioTek Synergy HT spectrophotometer (BioTek Instruments Inc., Winooski, VT).”

Testing TFP, AXPN, and DXP as therapeutics in a murine model of pneumonic plague infection alone or in combination with levofloxacin.

Mice were anesthetized by isoflurane inhalation and subsequently challenged i.n. with the indicated LD₅₀ dose of *Y. pestis* CO92. At 0, 6, 12, or 24 p.i. mice were dosed

through the i.p. route with TFP (1.5mg/kg), AXPB (3mg/kg), DXP (20mg/kg), or levofloxacin (5mg/kg). For levofloxacin combinatorial studies, at 48 p.i. mice were dosed through the i.p. route with TFP (1.5mg/kg), AXPB (3mg/kg), DXP (20mg/kg), and/or levofloxacin (0.25mg/kg or 5mg/kg). Dosing for TFP occurred once at the indicated time point, while AXPB, DXP, and levofloxacin were dosed a total of 3 times at 24 h intervals. Mice were assessed for morbidity and/or mortality as well as clinical symptoms for the duration of each experiment (up to 21 days p.i.).

For re-challenge experiments, after 21 days p.i., surviving animals were infected with WT CO92 by the i.n. route as described previously in Chapter 2 at a dose of 8-10 LD₅₀. Mice were again assessed for morbidity and mortality, as well as clinical symptoms, for the duration of each experiment.

Resistance of *Y. pestis* CO92 to DXP- and AXPB-treated serum.

Mouse serum was collected from naïve, DXP, or AXPB treated animals. Animals were dosed with 20 mg/kg DXP or 3 mg/kg AXPB for a total of 3 times and sera was collected 6 h post each dose. WT CO92 was grown overnight, harvested, and then diluted in PBS to an optical density at 600 nm (OD₆₀₀) of 0.8 (10⁸ CFU/mL). A 50 µl volume of the diluted bacteria was mixed with 200 µl of sera or PBS as a control. The samples were incubated at 37°C for 2 h with shaking at 180 rpm. The number of surviving bacteria (CFU) in each sample was determined by serial dilution and plating on SBA plates. Percent bacterial survival was calculated by dividing the average number of CFU in PBS by the average number of CFU in each sera sample.

Bacterial proliferation in murine lungs following infection and treatment with DXP.

Mice were divided into 2 groups infected with 10 LD₅₀ of WT CO92 by the i.n. route and one group was treated with DXP beginning 24 h p.i. At 30 h, 54 h, 78 h, and 10 days p.i., 3 animals from each group were humanely euthanized and lungs were immediately collected. The tissues were homogenized in 1 ml of PBS, and serial dilutions of the homogenates were spread onto SBA plates to assess proliferation of the bacteria in the lungs.

Statistical analyses.

Statistical analyses were performed as described in Chapter 2.

RESULTS

“A high-throughput *in vitro* screen identifies FDA-approved drugs that are effective in inhibiting host-cell cytotoxicity during a *Y. pestis* infection.

Using a modified gentamicin protection assay (38) in conjunction with the MTT assay, we developed a high-throughput screening method to evaluate a library of 780 FDA-approved drugs, with known molecular targets, for their ability to inhibit macrophage (murine RAW 264.7) death normally associated with *Y. pestis* infections (**Fig. 11**) (17, 104). Of the 780 compounds, we identified a total of 94 drugs that inhibited host-cell cytotoxicity when infected with WT CO92, with 36 drugs identified using a pre-treatment method and 58 drugs identified using a post-treatment method (**Tables 1B&2B; Appendix B**). Drugs were then grouped into either a Tier 1 or Tier 2 classification, with Tier 1 drugs significantly reducing infected macrophages' cytotoxicity (based on the MTT assay) to levels seen in uninfected (no bacteria) control macrophages (**Table 1B; Appendix B**). Tier 2 drugs also significantly reduced infected

macrophages' cytotoxicity, but not to uninfected control macrophage levels, as was observed for Tier 1 drugs (**Table 2B; Appendix B**).

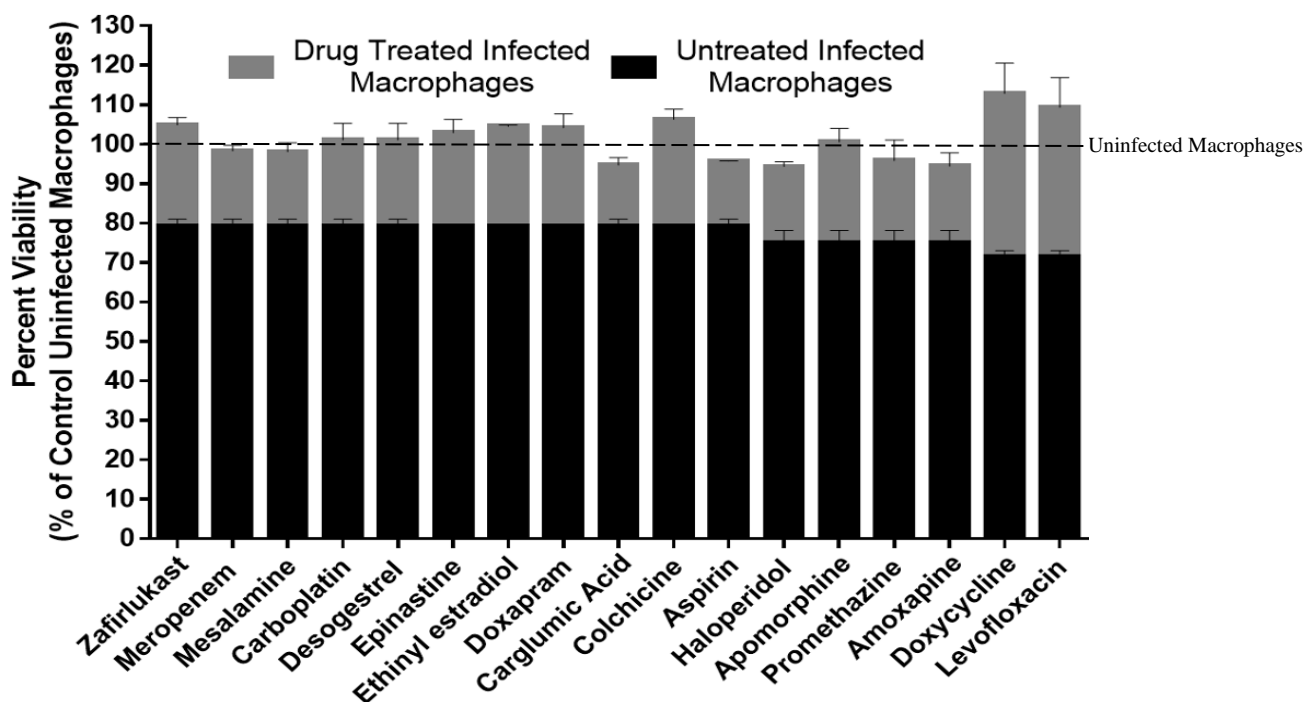


Figure 12. Tier 1 posttreatment drugs identified using a host cell-based screen to evaluate macrophage viability.

The drug-treated (33 μ M) and infected macrophages (gray) exhibited viability equivalent to that of uninfected macrophages (no bacteria) and significantly higher viability than that of drug-untreated and infected macrophages (black). The data were plotted as percentages of uninfected macrophages (dashed line) and were analyzed by 2-way ANOVA with Tukey's *post hoc* test.

Using a post-drug treatment method, 15 drugs were identified as being Tier 1 (**Fig. 12**) while the other 43 were classified as Tier 2 (**Fig. 13**). Overall, the drugs identified from the pre- and post-treatment screens included antineoplastics, antihistamines, antihypertensives, antivirals, antipsychotics, antidepressants, and

hormone receptor modulators, which regulate several molecular pathways in the host cells (Tables 1B&2B; Appendix B).

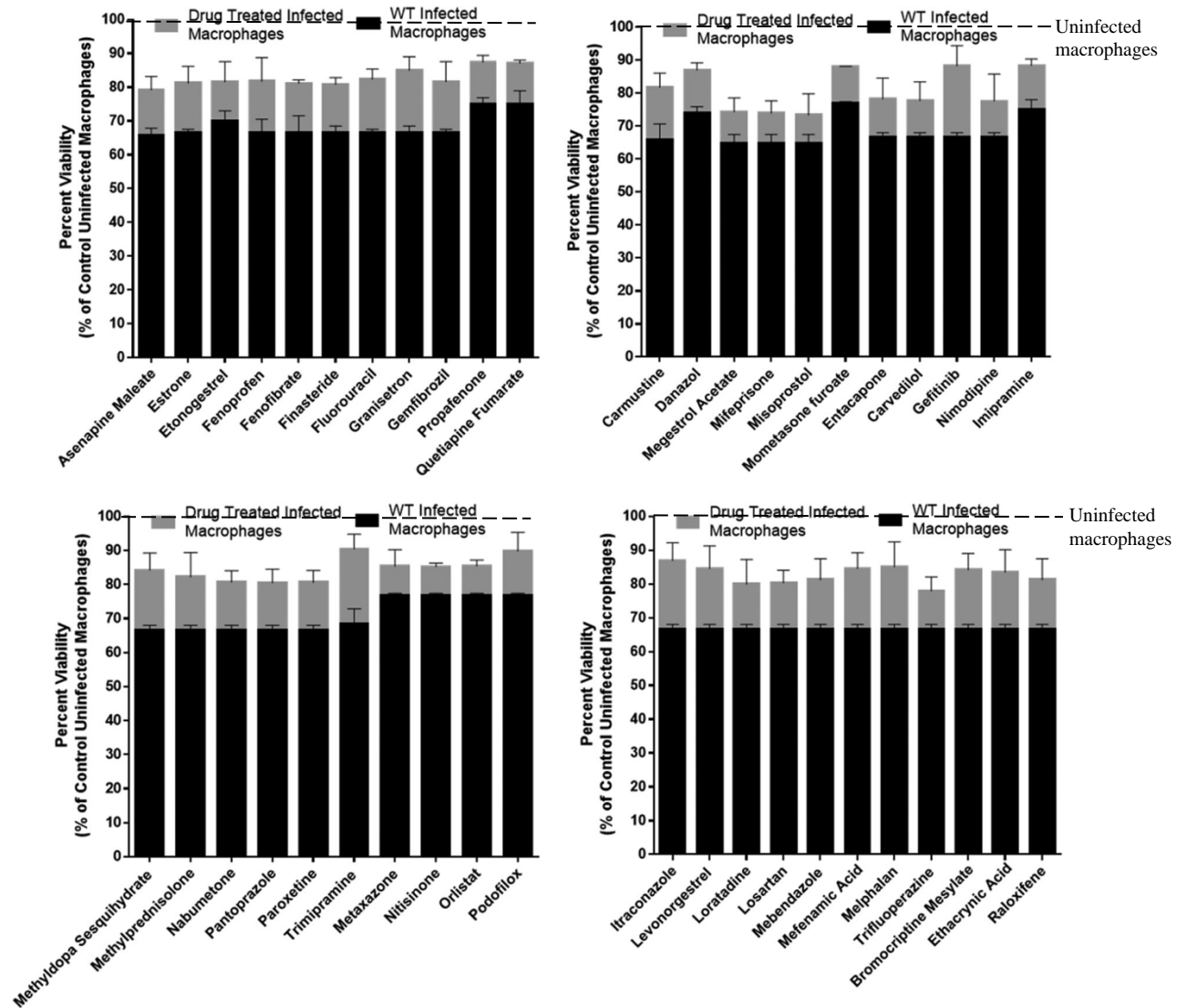


Figure 13. Tier 2 posttreatment drugs identified using a host cell-based screen to evaluate macrophage viability.

The drug-treated (33 μ M) and infected macrophages (gray) exhibited viability values that were significantly higher than those of *Y. pestis* CO92 infected and drug-untreated macrophages (referred to as WT) (black) but were not equivalent to those of uninfected macrophages (dashed line). The data were plotted as percentages of uninfected macrophages and analyzed by 2-way ANOVA with Tukey's *post hoc* test.

Quantification of bacterial survival *in vitro* identifies 3 drugs capable of limiting host-cell death and decreasing intracellular *Y. pestis* survival.

Continuing analysis was limited to Tier 1 and Tier 2 drugs identified in our post-treatment screen, since these were considered to be the most clinically relevant. Using a bioluminescent *Y. pestis* CO92 strain that was created with the Tn7- luciferase gene (*lux*)-based system (68, 105, 106), bacterial survival was quantitated in real time. Focusing on the 58 drugs identified from the post-treatment screens and using a gentamicin protection assay in RAW 264.7 macrophages, the effects of the drugs at a concentration of 33 μ M were tested on intracellular bacterial survival. From these experiments, 3 of the 58 drugs were shown to affect intracellular bacterial survival: haloperidol, TFP, and pantoprazole (**Fig. 14**). Haloperidol, an antipsychotic, was classified as a Tier 1 drug in our viability screens while TFP, an anti-depressant, and pantoprazole, a treatment for gastroesophageal reflux disease (GERD), were classified as Tier 2 drugs (**Tables 1B&2B; Appendix B**). To eliminate any false positive results due to host-cell cytotoxicity for the 58 drugs, cell viability was assessed by using the MTT assay with the drugs alone (no bacterial challenge) at a concentration of 33 μ M for 12 h. Of the 58 drugs tested, none induced any cytotoxicity in RAW 264.7 macrophages.

Three drugs exhibited protection in the murine pneumonic plague infection model.

Based on efficacy from *in vitro* screens, the 15 drugs classified as Tier 1 from our post-treatment viability screens (**Fig. 12**), as well as the Tier 2 drugs TFP and pantoprazole, which both disrupted bacterial intracellular survival (**Fig. 13 & 14**), were chosen for further analysis in order to determine if the results seen *in vitro* could be

replicated *in vivo*. Mice were challenged through the i.n. route with WT CO92 (10 LD₅₀) and immediately

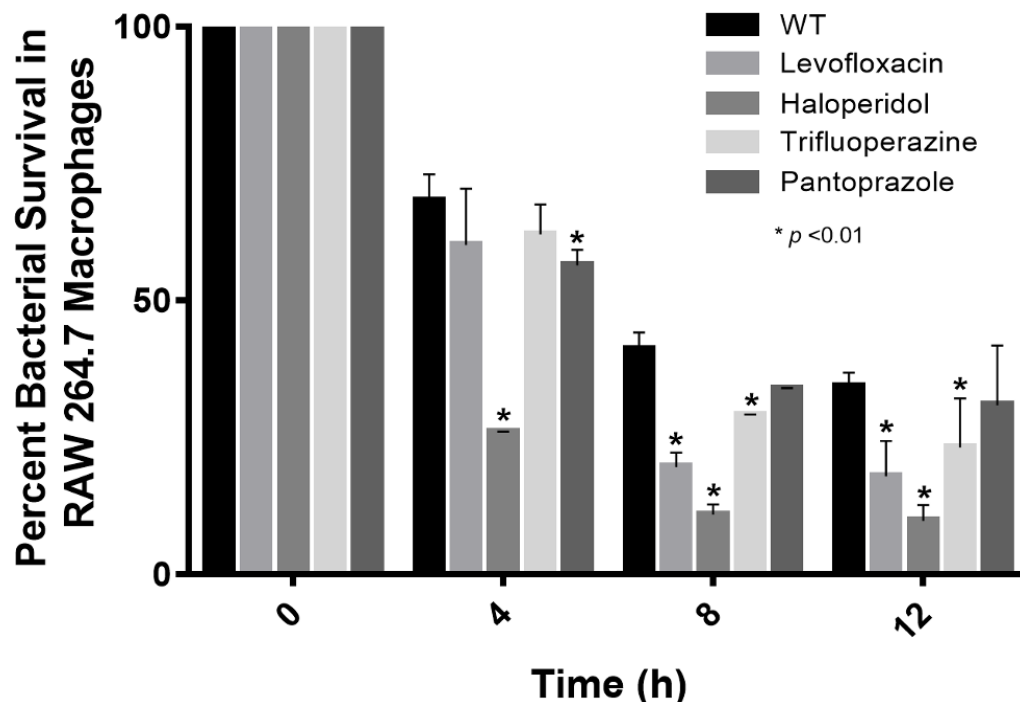


Figure 14. Quantification of intracellular survival of *Y. pestis* CO92-*lux* in RAW 264.7 murine macrophages.

RAW 264.7 macrophages were infected with *Y. pestis* CO92-*lux* for 1 h at an MOI of 250. Monolayers were then treated with gentamicin at a concentration of 50 µg/ml for 1 h, washed twice with PBS, and incubated with a maintenance dose of 10 µg/ml gentamicin. At this time, 33 µM drug, or PBS as a control, was added to the monolayers. Following drug treatment, intracellular bacterial survival was measured at 4, 8, and 12 h post-infection through bioluminescence measurement. The data were analyzed by comparison of drug-untreated and infected controls (WT) to treatment groups at each time point by using 2-way ANOVA with Tukey's *post hoc* test. *, $P < 0.01$.

following infection, were dosed with one of the 17 lead drugs through either the oral or the i.p. routes (**Table 3**). Dose concentrations were determined either based on the literature (107–115) or empirically (**Table 3**). Initially, mice were dosed for up to 6 days at 24 h intervals to mimic the dosing regimen of levofloxacin (57) and monitored daily

for morbidity and mortality. Three drugs, TFP (5 mg/kg), DXP (50 mg/kg) and AXPN (5 mg/kg) (**Fig. 15 A-C**), were identified to alleviate the early clinical manifestations in mice such as ruffled fur, lethargy, and inability to groom, although animals did eventually expire, possibly due to drug toxicity from prolonged treatment, specifically after 4 doses, rather than the infection. Since the aforementioned three drugs alleviated some symptoms of disease, we sought to optimize the number of doses and drug concentrations to increase animal survival rates (**Table 4**).’’

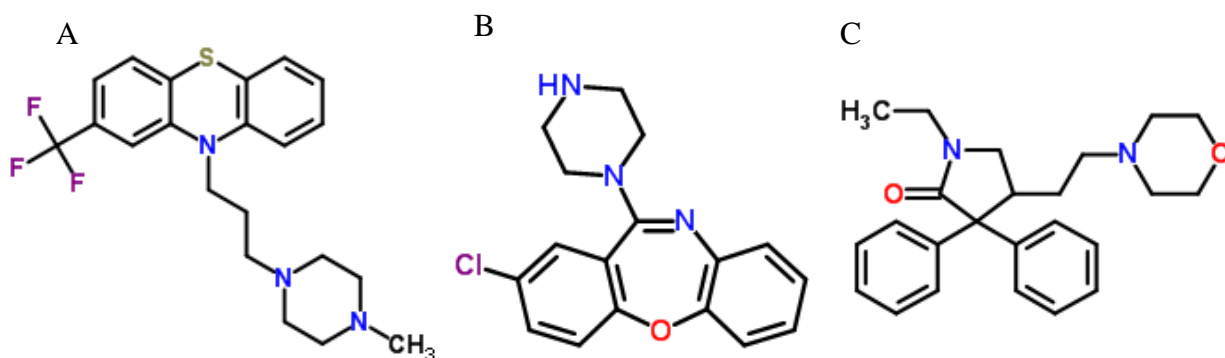


Figure 15: Chemical structures of TFP (A), AXPN (B), and DXP (C) from the Royal Society of Chemistry.

“Through optimization studies, TFP was observed to be equally or even more effective at one dose compared to three, and, therefore, in subsequent mouse pneumonic plague experiment, animals were administered TFP (1.5 mg/kg once), AXPN (3 mg/kg, 3 doses 24 h apart) and DXP (20 mg/kg, 3 doses 24 h apart) by the i.p. route at the time of WT CO92 infection. To maximize the effectiveness of the chosen drugs, we preferred to deliver the drugs at the time of infection in these initial studies (10 LD₅₀ of WT CO92). As noted in **Fig. 16A**, although the untreated control animals succumbed to infection, 40-60% of mice treated with any of these three drugs were protected from developing pneumonic plague, with no clinical signs of the disease or drug toxicity. The remaining

14 drugs evaluated in this model exhibited no survival benefits to animals when administered individually. Although all drugs were given well below LD₅₀ values (**Table 3**), additional optimization of dosing regimens may be required to observe beneficial effects in mice.

Table 4. Different concentrations and doses of doxapram (DXP), trifluoperazine (TFP), and amoxapine (AXPN) tested in mouse pneumonic plague model with 10 LD₅₀ of WT *Y. pestis* CO92. Percent survival rates are also listed.

Drug	Drug Concentration	# of Doses	Percent Survival
Doxapram	10mg/kg	3	40%
Doxapram	20mg/kg	3	50%
Doxapram	30mg/kg	3	40%
Doxapram	50mg/kg	5	0%
Amoxapine	1mg/kg	3	20%
Amoxapine	3mg/kg	3	40%
Amoxapine	5mg/kg	3	0%
Trifluoperazine	1.5mg/kg	3	40%
Trifluoperazine	10mg/kg	3	30%
Trifluoperazine	1.5mg/kg	1	50%
Trifluoperazine	10mg/kg	1	40%

As TFP was the most efficacious drug in terms of animal survival after WT CO92 infection when administered at the time of infection, we chose to perform a combinatorial study with levofloxacin to discern if any additive or synergistic effects could be observed. TFP was administered as described above (1.5 mg/kg dose i.p. once at the time of

infection) while a sub-inhibitory dose of levofloxacin (0.25 mg/kg) was injected by the i.p. route 24 h p.i. and subsequently at 24 h intervals for three days. While only 20% of mice dosed with 0.25 mg/kg levofloxacin alone were protected from infection, 70% of dually treated mice were protected from developing pneumonic plague (**Fig. 16B**), indicating there was possible additive effect.

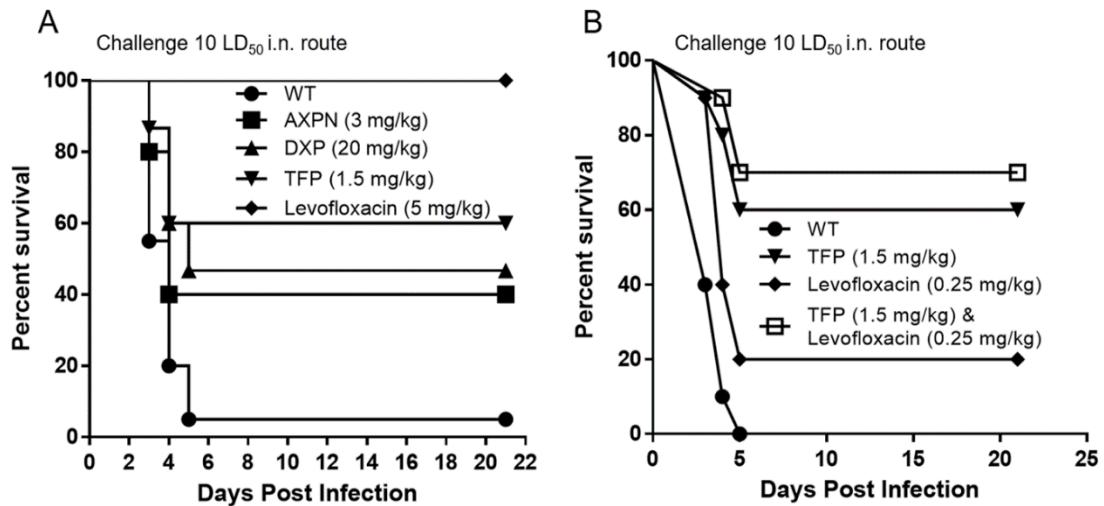


Figure 16. Survival analysis of mice infected with *Y. pestis* CO92 and then drug treated at the time of infection.

(A) Mice were challenged by the i.n. route with 10 LD₅₀ of WT *Y. pestis* CO92 and administered TFP ($n = 15$; pooled from three independent experiments) at a dose of 1.5 mg/kg, AXPN ($n = 10$; pooled from 2 independent experiments) at a dose of 3 mg/kg, DXP ($n = 15$; pooled from 3 independent experiments) at a dose of 20 mg/kg, or saline ($n = 20$; pooled from 4 independent experiments) as a control by the i.p. route at the time of infection. Levofloxacin was administered at a dose of 5 mg/kg at 24 h p.i. ($n = 10$; pooled from two independent experiments). Animals were dosed for 3 days (at 24-h intervals) for levofloxacin, DXP, and AXPN or given only 1 dose of TFP ($P = 0.0374$; AXPN, $P = 0.0044$; DXP, $P = 0.0007$; TFP, and $P = 0.0003$; levofloxacin). (B) Mice were challenged by the i.n. route with 10 LD₅₀ of WT *Y. pestis* CO92, and two groups were administered TFP at a dose of 1.5 mg/kg by the i.p. route at the time of infection. A control group of animals was given saline at the time of infection. At 24 h p.i.,

levofloxacin at a dose of 0.25 mg/kg was administered i.p. to animals. Groups receiving TFP, levofloxacin, or saline alone served as controls. The data were analyzed for significance by use of Kaplan-Meier survival estimates. The P values were determined based on comparison of the results for each of the drug treatment groups to the results for saline-treated and infected controls (WT). $P = 0.0006$ for TFP, $P = 0.0190$ for levofloxacin, and $P < 0.0001$ for TFP and levofloxacin.

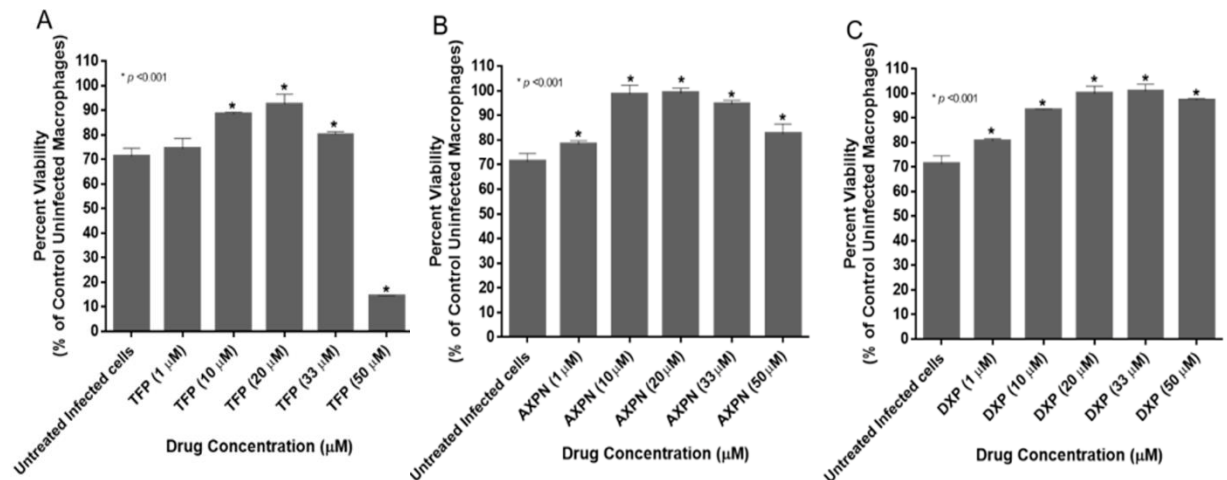


Figure 17. Dose-response effects of 3 drugs.

Dose-response effects of TFP (A), AXPN (B), and DXP (C) identified using a host cell-based, high-throughput screen to evaluate macrophage viability by the MTT assay following infection with WT CO92 and subsequent drug treatment for 12 h. Macrophages were treated with drug concentrations of 1, 10, 20, 33, and 50 μ M. The data were analyzed by comparison of drug-untreated and infected macrophages to drug treatment groups at each concentration by using 2-way ANOVA with Tukey's *post hoc* test. *, $P < 0.001$.

TFP, DXP, and AXPN exhibited a dose response effect on macrophage viability after *Y. pestis* CO92 infection.

To determine the dose response effects of these three drugs on macrophage viability following infection, RAW 264.7 macrophages were grown to confluency, infected with *Y. pestis* at an MOI of 100 and subsequently incubated with TFP, DXP and

AXPN at concentrations of 1, 10, 20, 33 and 50 μM . For all three drugs, the 10, 20, and 33 μM concentrations resulted in statistically significant increases in macrophage viability after WT CO92 infection compared to infected, untreated control macrophages (**Fig. 17**). TFP (**Fig. 17A**) and AXPN (**Fig. 17B**) showed highest macrophage viability between 10-20 μM concentrations while DXP (**Fig. 17C**) demonstrated highest viability between 20 -33 μM concentrations. For all three drugs, at a 50 μM concentration, macrophage viability began to decrease, with TFP exhibiting the most cytotoxic effect (**Fig. 17A**).

TFP, DXP, and AXPN exhibited no bactericidal or bacteriostatic effects on *Y. pestis* CO92.

To determine if these three drugs had any bactericidal or bacteriostatic effects, *Y. pestis* CO92 was grown in the presence of each drug for 24 h at 37 °C at a concentration of 33 μM , as this was the concentration used in the *in vitro* screening assay and was the highest concentration to exhibit no cytotoxic effects. None of the tested drugs, except for levofloxacin (positive control), negatively influenced the growth of *Y. pestis* CO92 (**Fig. 18A**). To confirm that there were no bacteriostatic effects, samples from each drug containing culture grown for 24 h were re-inoculated in fresh HIB and grown for another 24 h. Once again, growth was only influenced by levofloxacin (data not shown). Additionally, for all three drugs, the MICs were determined to be >100 $\mu\text{g/ml}$ (data not shown), indicating that even at a high concentration, no direct antimicrobial effects could be observed for these drugs against *Y. pestis* in an *in vitro* culture.

TFP, DXP, and AXPN exhibited no effects on *Y. pestis* CO92 virulence.

Since no bactericidal or bacteriostatic effects of the abovementioned drugs were observed on *Y. pestis* CO92, we sought to determine whether any of these drugs could impact bacterial virulence in some way, possibly accounting for the increased mouse survival. We first examined whether the production of T3SS effectors by *Y. pestis* CO92 was affected by treatment with all three drugs (individually) at 33 μ M. After mimicking the conditions of the *in vitro* screening assay, cell pellets were evaluated for the expression/production of LcrV and YopE, specifically, by immunoblot analysis. To probe whether Yops secretion was affected, supernatants were also evaluated for the presence of YopE by immunoblot analysis. None of the tested drugs impacted the expression/production of LcrV and YopE in cell pellets or secretion of YopE in culture supernatants (**Fig. 18B**).” We also assessed whether the T6SS was affected by examining the production of Hcp6 by *Y. pestis* CO92 in the presence of the 3 drugs by immunoblot analysis. As observed with the effectors of the T3SS, Hcp6 expression was not affected by any of the drugs when observed in cell pellets or supernatants (**Fig. 18C**). “We also assessed whether Pla protease activity of *Y. pestis* CO92 was affected by the presence of the three drugs individually. As with evaluation of T3SS components, conditions of the *in vitro* assay were mimicked, with bacteria grown in the presence of all three drugs (individually) at 33 μ M. Protease activity was then measured using a fluorometric assay with the Pla substrate (116). As with the T3SS and T6SS effectors probed, we observed no drug inhibition or impact on Pla protease activity (**Fig. 18D**). Taken together, the three anti-*Y. pestis* candidate drugs, identified through *in vitro* and *in vivo* screens, reduced

bacterial pathogenesis by seemingly targeting host cell pathways rather than the bacterial pathogen directly.”

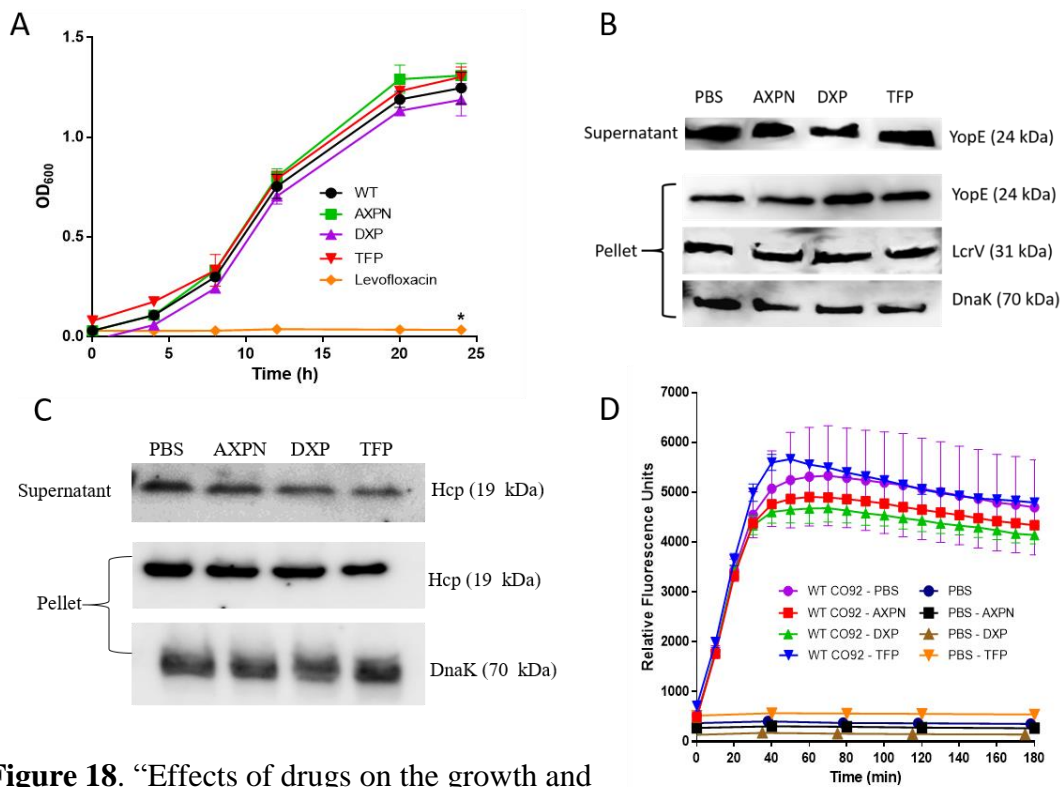


Figure 18. “Effects of drugs on the growth and virulence factors of *Y. pestis* CO92.

(A) Growth of *Y. pestis* CO92 in HIB in the presence of TFP, AXP, DXP, or levofloxacin (at 33 μ M) or with PBS (control). Samples were taken at the indicated time points for OD₆₀₀ measurement. Data shown are the mean values, while error bars represent standard deviations (SD) ($n = 4$). Statistical analysis was performed using Student's *t* test, with only levofloxacin showing significantly lower OD values than those obtained with PBS during growth of *Y. pestis* (*Yp*) CO92 (WT) ($P < 0.001$). (B&C) Production of the T3SS effectors LcrV and YopE (B) and T6SS effector Hcp6 (C). *Y. pestis* CO92 was grown in HIB overnight and subsequently diluted 1:20 in fresh HIB supplemented with 5 mM EGTA, for chelation of calcium, in the presence of 33 μ M TFP, AXP, or DXP or with PBS (control). Growth was continued at 28°C for 2 h, followed by a temperature shift to 37°C for an additional 3 h of incubation. Cell pellets and supernatants were separated by centrifugation, and following TCA precipitation of proteins in the supernatants, cell pellet and supernatant samples were dissolved in SDS-PAGE buffer. Western blot analysis was then employed to detect LcrV and YopE in bacterial pellets and YopE in supernatants (B) as

well as Hcp6 in bacterial pellets and supernatants (C). Levels of DnaK in bacterial pellets were utilized as a loading control to ensure similar levels of bacteria across all samples examined. (D) Pla protease activity assay. *Y. pestis* CO92 was grown on HIB agar plates at 28°C for 20 to 22 h, and bacteria were then suspended in HIB, incubated with 33 μ M TFP, AXPN, or DXP or with PBS (control), and grown overnight. Cultures were resuspended in PBS with a 33 μ M concentration of the respective drug to obtain a final OD₆₀₀ of 0.25. Samples containing only PBS and each drug were also analyzed for any drug auto-fluorescence. Pla protease activity was then measured in a fluorometric assay. The kinetics of substrate cleavage (increase in relative fluorescence units [RFUs] versus time) by Pla was plotted for each treatment group. Statistical analysis was performed by one-way ANOVA with the Bonferroni *post hoc* test with drug only (no bacteria) samples showing significantly lower RFUs compared to *Yp* CO92-PBS and *Yp* CO92-drug groups, $P < 0.001$.”

TFP, AXPN, and DXP exhibited therapeutic efficacy in a murine model of pneumonic plague infection.

Based on the effects of these three drugs against *Y. pestis* infection when given at the time of infection, we chose to evaluate the therapeutic efficacies of TFP, AXPN, and DXP following delayed treatment in a murine pneumonic plague model. Mice were challenged by the i.n. route with WT CO92 (8 LD₅₀) and were dosed with either TFP, AXPN or DXP at 0, 6, 12, or 24 h p.i. TFP dosing was limited to only 1 dose while AXPN and DXP were dosed at 24 h intervals for 3 days. For TFP, treatment at all time points significantly protected animals from fatal pneumonic plague infection, with 40-60% of animals surviving, however, it was noted that efficacy diminished as dosing time was delayed (**Fig. 19A**). As with TFP, delayed treatment with AXPN and DXP provided significant protection to animals across all time points (40-90%) (**Fig. 19B&C**). Interestingly, for both AXPN and DXP, delayed treatment resulted in an increase of drug

efficacy, with survival of animals treated with either of these drugs at 24 h p.i. ranged from 70-100% (**Fig. 19B&C**).

As significant efficacy was observed for all three drugs when administered at 24 h p.i., we chose to further evaluate their efficacies when administered at 48 h p.i. It is noted that efficacy of antibiotics is limited when administered past 42 h p.i. (57), and, therefore, we also evaluated the potential for additive or synergistic effects of these drugs when administered in combination with levofloxacin. Mice were administered TFP (1.5mg/kg), AXPN (3 mg/kg), DXP (20mg/kg) and/or levofloxacin (0.25mg/kg or 5mg/kg) beginning at 48 h p.i. TFP was administered once while AXPN, DXP and levofloxacin were administered at 24 h intervals for 3 days.

For TFP, when administered alone at 48 h p.i., there was no significant difference between the WT CO92 control group (14% vs. 0%, respectively). However, when TFP was administered in combination with levofloxacin (Levo), a synergistic effect was observed with both low dose (0.25mg/kg) and high dose (5mg/kg) levofloxacin treatment, as both combination groups exhibited significantly higher survival rates in comparison to WT CO92 control group (57-100%) (**Fig. 20A**). Additionally, the TFP/Levo (5mg/kg) group exhibited statistically significant higher survival rates in comparison to the TFP alone group (**Fig. 20A**).

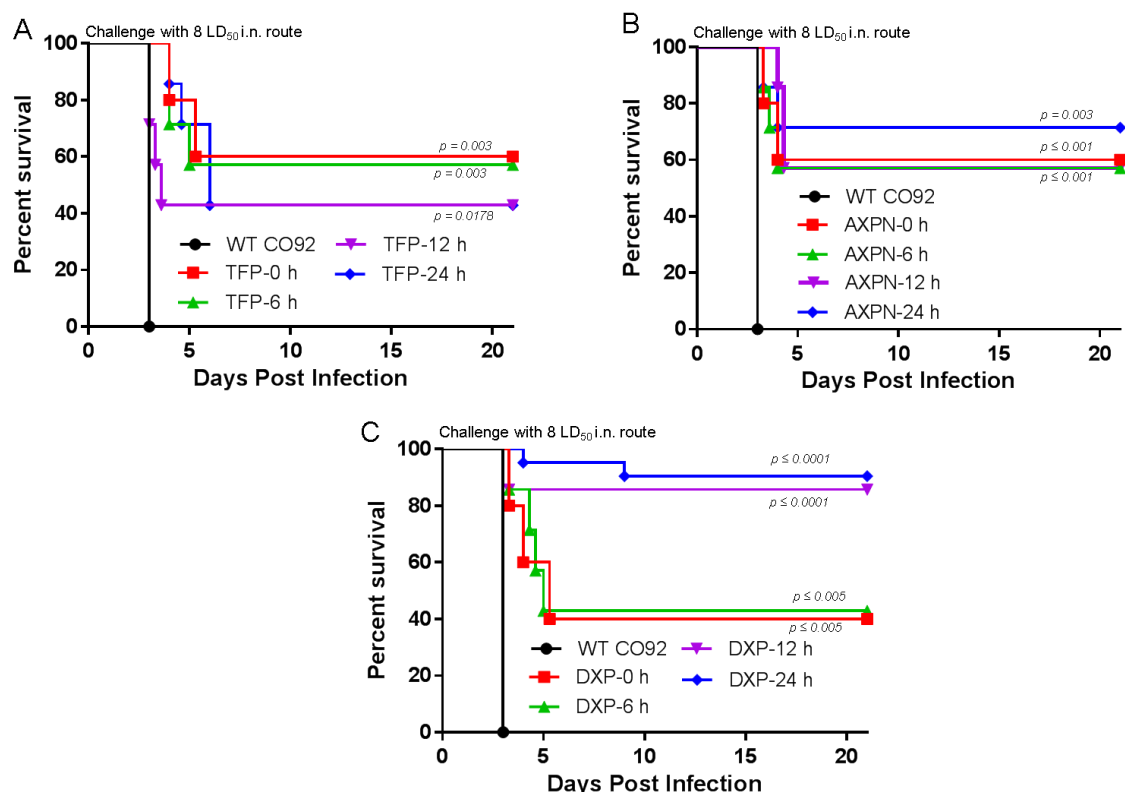


Figure 19. Survival analysis of mice infected with *Y. pestis* CO92 and treated with TFP, AXP, or DXP at delayed time points.

Mice were challenged by the i.n. route with 8 LD₅₀ of WT CO92 and administered TFP (n = 7; 1.5mg/kg) (**A**), AXP (n = 7; 3mg/kg) (**B**), or DXP (n = 7; 20mg/kg) (**C**) by the i.p. route at the indicated time points p.i. Animals were dosed for 3 days (24 h intervals) for DXP and AXP or only 1 dose of TFP at the indicated time. Mice were monitored for signs of morbidity and mortality for 21 days. The data were analyzed for significance by Kaplan-Meier survival estimates. The *P* values were determined based on comparison of the results for each of the drug treatment groups to the results of WT CO92 infected controls.

When administered at 48 h p.i., AXP treatment resulted in significantly higher survival rates (72%) in comparison to WT CO92 controls, which all succumbed to infection by day 4 (**Fig. 20B**). However, an interaction between AXP and levofloxacin was observed when administered together, and results were therefore not reported here as

continued optimization of the dosing regimen of these drugs when administered together were needed.

Groups treated with DXP alone as well as in combination with levofloxacin all exhibited significantly higher survival rates (50-100%) in comparison to WT CO92 controls (**Fig. 20C**). It was also noted that the DXP/Levo (5mg/kg) group had a statistically higher survival rate in comparison to the DXP alone treated group, further indicating an additive effect with dual drug treatment of DXP and levofloxacin (**Fig. 20C**).

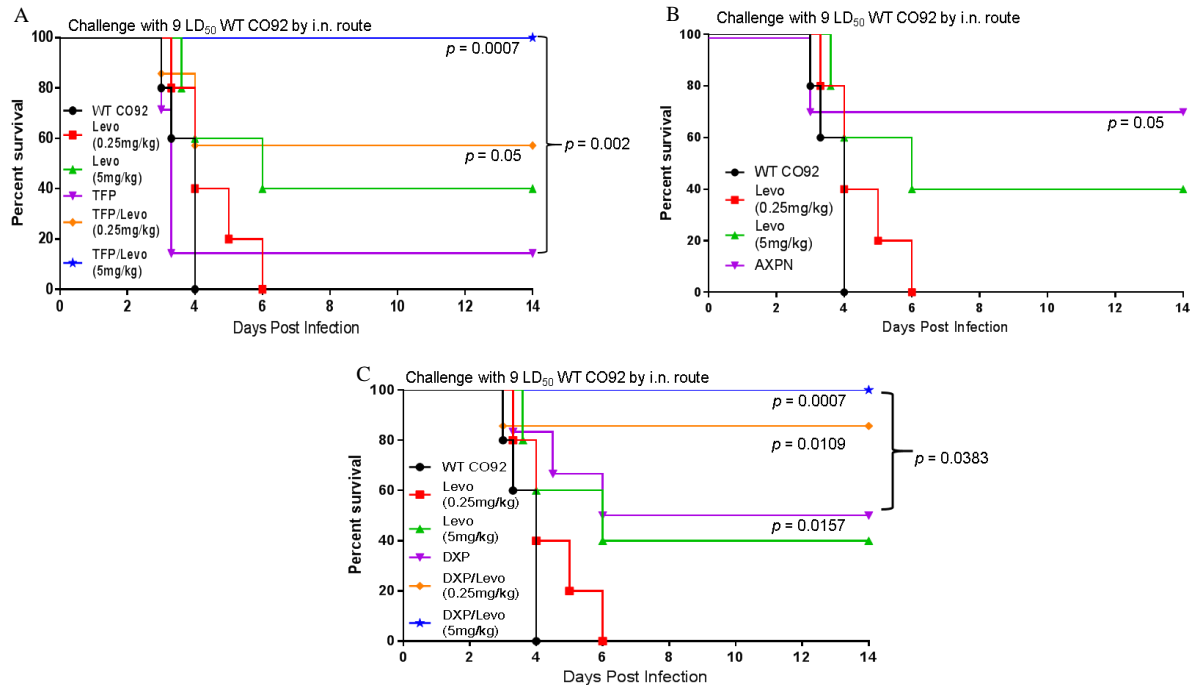


Figure 20. Survival analysis of pneumonic plague infected mice treated with TFP, AXPN, DXP and/or levofloxacin at 48 h p.i.

Mice were challenged by the i.n. route with 9 LD₅₀ of WT CO92 (n = 5-7 per group) and administered TFP (**A**), AXPN (**B**), DXP (**C**), and/or levofloxacin (5 mg/kg or 0.25mg/kg) by the i.p. route at the indicated time points p.i. Animals were dosed for up to 3 days (24 h intervals) beginning at 48 h p.i.

Mice were monitored for signs of morbidity and mortality for 14 days. The data were analyzed for significance by the Kaplan-Meier survival estimates. The *P* values were determined based on comparison of the results for each of the drug treatment groups to the results of WT CO92-infected controls or indicated groups.

Animals treated with TFP, AXP, and DXP during initial infection exhibited some protection upon re-challenge with *Y. pestis* CO92.

In order to evaluate whether a protective immune response was generated in treated animals that survived initial infection, at 21 p.i. surviving animals in the indicated groups were re-challenged (**Fig. 19**) by the i.n. route with WT CO92 (8 LD₅₀) to monitor morbidity and mortality. For all groups of treated animals, some protection, ranging from 25-100%, from subsequent challenge was observed, while all naïve control animals did succumb to infection by day 5 (**Fig. 21**).

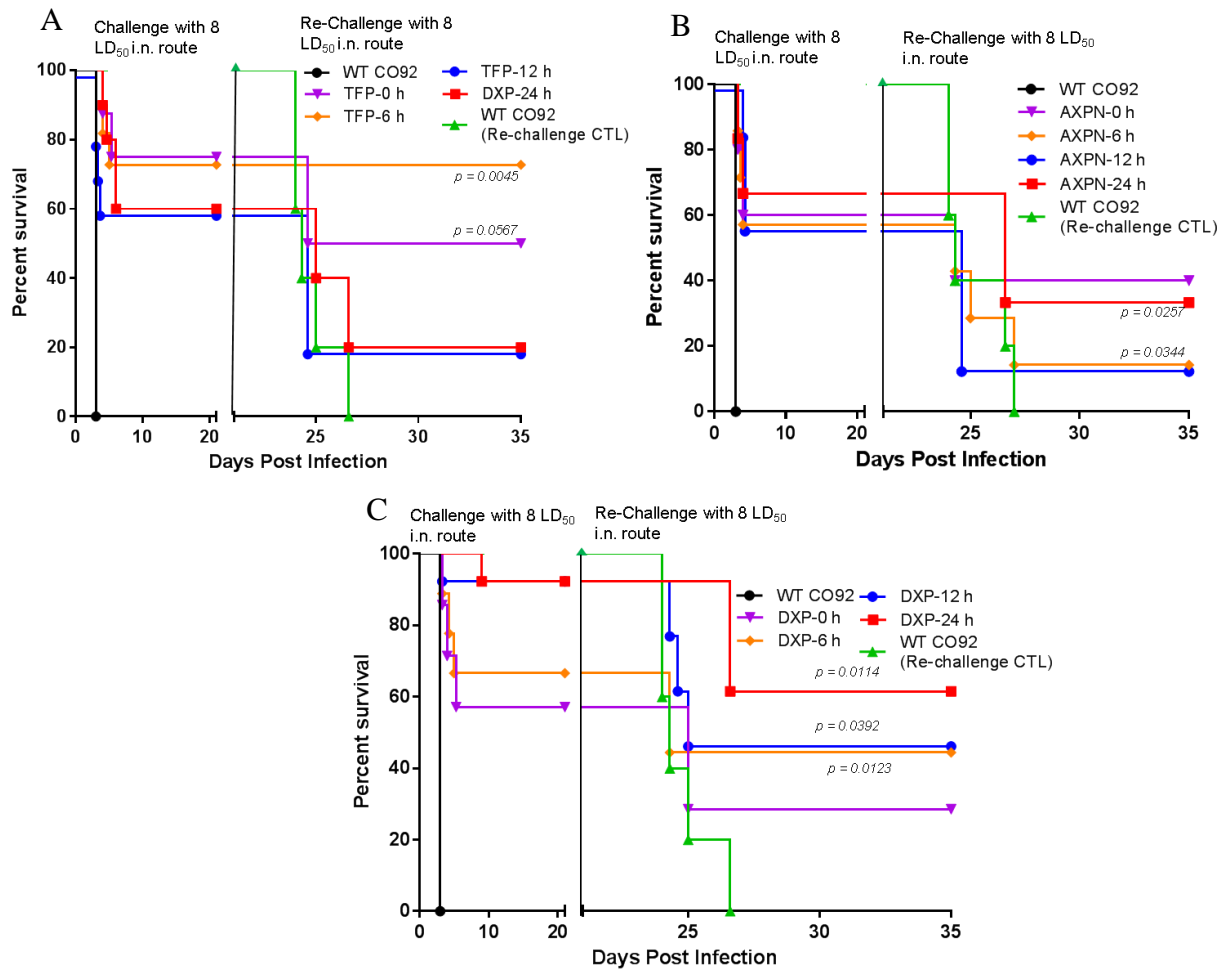


Figure 21. Survival analysis of drug treated mice re-challenged with WT CO92.

Mice initially treated with TFP (A), AXPN (B), or DXP (C) that survived a pneumonic plague challenge were re-challenged on day 21 by the i.n. route with 8 LD₅₀ of WT CO92. Naïve infected animals (WT CO92 re-challenge CTL) served as controls. Mice were monitored for signs of morbidity and mortality for an additional 14 days. The data were analyzed for significance by Kaplan-Meier survival estimates. The *P* values were determined based on comparison of the results for each of the drug treatment groups to the results of WT CO92 infected controls.

Treatment with AXPB or DXP did not alter serum resistance of *Y. pestis* CO92.

To evaluate if the efficacies of these drugs were linked to the activation of complement, which would lead to increased bacterial killing *in vivo*, we administered AXPB and DXP to uninfected mice and collected sera 6 h post drug treatment, with a total of 3 doses of each drug administered to animals. We limited these studies to AXPB and DXP as an increase in the efficacy was observed for both drugs as treatment time was delayed up to 24 h p.i. in mice (**Fig.19**). As observed in **Fig. 22**, no differences in drug treated versus naïve sera in bacterial killing was observed, with all samples exhibiting

≥100% survival.

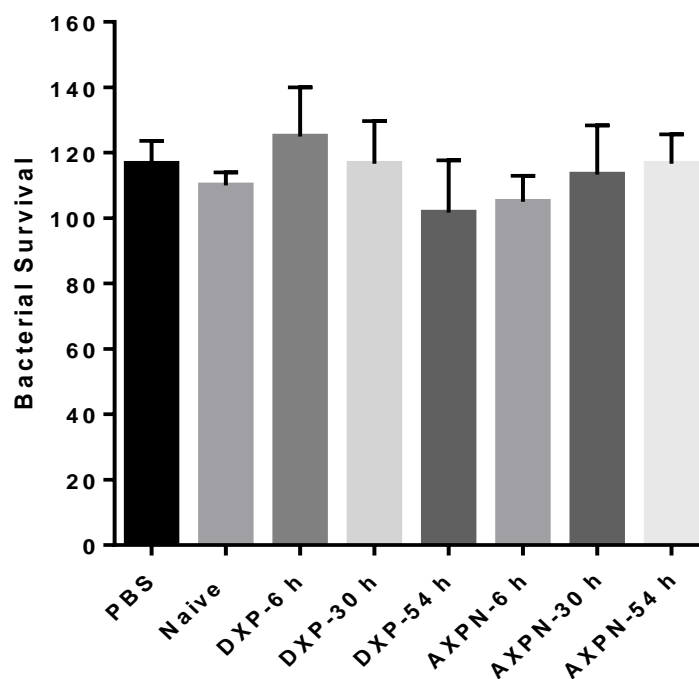


Figure 22. Resistance of *Y. pestis* with drug-treated sera.

Overnight grown culture of *Y. pestis* CO92 was harvested and diluted in PBS to OD₆₀₀ of 0.2. An aliquot (50 µl) of diluted bacteria was inoculated in 200 µl drug- treated or untreated sera or PBS and incubated at 37°C for 2 h. CFUs were determined by serial dilution and plating on SBA plates.

Treatment with DXP inhibited *Y. pestis* proliferation in the lungs of infected animals.

As DXP was the most efficacious drug when administered alone at 24 h p.i., we evaluated the proliferation of WT CO92 in the lungs of infected and treated

animals. At 30, 54, 78 h or 10 days p.i., we noted that the CFUs in DXP-treated animals were reduced in comparison to those of untreated animals, although statistical significance was only observed at 30 and 78 h p.i (Fig. 23). It was also observed that by day 10, no detectable number of bacteria could be observed in the lungs of DXP treated animals (Fig. 23).

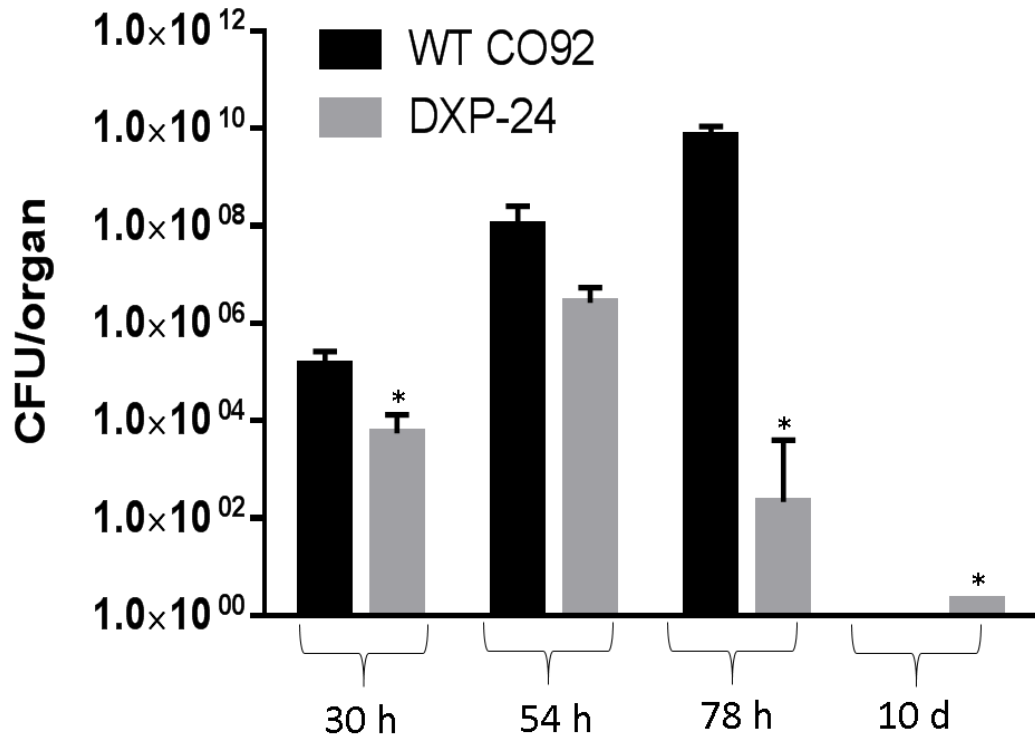


Figure 23. *Y. pestis* proliferation in lungs following DXP treatment.

At each indicated time point, 3 animals per group infected with 8 LD₅₀ of WT CO92 and treated or untreated with DXP 24 h p.i. were euthanized and lungs harvested 6 h after the administration of each dose. CFUs were determined by homogenization of the lungs followed by serial dilution and plating on SBA plates. Statistical analyses were performed by student's t test with $P < 0.05$ was considered statistically significant.

DISCUSSION

“In efforts to identify novel anti-bacterial chemotherapeutics from a library of 780 FDA-approved drugs, we employed a high-throughput screening method based on evaluation of *Y. pestis*-induced macrophage cytotoxicity. During infection, *Y. pestis* preferentially targets host macrophages as the organism is protected from contact with other immune components and acquires the ability to evade subsequent phagocytosis (102, 103). Macrophages are key effectors of the host innate immune response to infection and intracellular survival and growth of *Y. pestis*, and since macrophages play a pivotal role in the pathogenesis of the plague (102, 103, 117), 51), this *in vitro* model was well suited for our screening purposes. In total, 94 FDA-approved drugs were identified in our screen as being able to inhibit *Y. pestis*-induced macrophage cytotoxicity. Candidate drugs were placed into Tier 1 and Tier 2 categories based on the degree to which treatment reduced *Y. pestis*-induced macrophage cytotoxicity (Fig. 12&12; Tables 1B&2B).

Decreased host-cell cytotoxicity associated with *Y. pestis* infection by the drugs could have been a result of a reduction in intracellular survival of the invading pathogen or the stabilization of infected macrophages (e.g., a disruption of apoptotic pathway). Some drugs identified in *in vitro* screens have previously been shown to have some antimicrobial activity, such as TFP and proton pump inhibitors, such as pantoprazole, being known to have anti-*M. tuberculosis* effects (118, 119). After validating that none of the 58 drugs from the more clinically relevant post-treatment screens (Tables 1B&2B) had any cytotoxic effects on macrophages alone (data not shown), three identified drugs that inhibited host-cell death were also shown to decrease bacterial intracellular survival

(Fig. 14). One drug, haloperidol, was classified as Tier 1, while TFP and pantoprazole were classified as Tier 2 drugs. As the remaining 55 compounds did not decrease intracellular bacterial survival, but did exhibit increases in macrophage viability, we speculated that these drugs were stabilizing macrophages to prevent their death associated with infection. This, in turn, may aid in altering subsequent immune responses to the infection to better allow for bacterial clearance at a later time point in the whole animal. Indeed, it has been shown that early inhibition of macrophage apoptosis following *Y. pestis* infection aids in reducing inflammation and allowing for better bacterial clearance (117).

From *in vitro* studies, a set of 17 drugs, 15 Tier 1 and two Tier 2 drugs, TFP and pantoprazole (Figs. 12 & 13), were prioritized for evaluation to determine if efficacy *in vitro* could be translated *in vivo*. Our results indicated that three drugs, AXPB and DXP (Tier 1), and TFP (Tier 2), significantly increased the survival of mice in a pneumonic plague model (Fig. 16A). Additional studies with TFP indicated that combinatorial treatment with TFP and a sub-inhibitory dose of levofloxacin showed an additive effect on animal survival rate (Fig. 16B). Poor efficacy for the other 14 drugs, particularly haloperidol or pantoprazole, which were both able to inhibit intracellular survival of *Y. pestis* CO92, may indicate the need for additional optimization of *in vivo* dosing regimens, as was needed for our three reported lead drugs (Tables 3&4).

In order to evaluate if there was a dose response effect on macrophage viability from TFP, AXPB or DXP treatment following infection with *Y. pestis* CO92, we employed the same procedure used for the initial high throughput screen. Using drug concentrations of 1, 10, 20, 33 and 50 μ M, it was observed that there was a dose response

effect for each drug (Fig. 17) and at the highest concentration of 50 μ M, signs of cytotoxicity could be observed, particularly for TFP (Fig. 17A). These results validated the use of 33 μ M concentration in initial screening procedures, as high efficacy was observed at this concentration for all three drugs while also remaining non-cytotoxic to macrophages.

In order to elucidate whether *Y. pestis* was being affected directly, AXPN, DXP and TFP were evaluated for possessing either bactericidal or bacteriostatic activity. Our results indicated that none of the drugs had a direct bactericidal/bacteriostatic effect (Fig. 18A), suggesting that these drugs may be inhibiting bacterial virulence factors (not associated with bacterial growth) or may be modulating pathogenicity signaling pathways. To assess if these drugs were acting through bacterial or host targets, we evaluated the expression of two T3SS effector proteins, LcrV and YopE, of which the latter destroys actin monofilaments. No measurable differences in the production levels of these antigens were observed following drug treatments in cell pellets, and, likewise, no differences in the secretion levels of YopE were observed in culture supernatants (Fig. 18B).” We also evaluated expression of the T6SS effector Hcp6, which is an established marker to T6SS function, and observed no measurable differences in Hcp6 expression or secretion (Fig 18C). “Furthermore, no measurable differences in Pla protease activity, another key *Y. pestis* virulence factor, were observed when WT CO92 was grown in the presence of each drug individually (Fig. 18D). These data provided further evidence that these drugs were likely operating through host-directed targets to alleviate disease pathogenesis.”

To determine the actual therapeutic potential of these drugs, their efficacies when administered at delayed time points p.i. were evaluated. For all three drugs, animal survival was significantly increased when administered up to 24 h p.i. (Fig. 19). Surprisingly, for both AXP and DXP, delayed treatment resulted in an increase in efficacy, with 70-100% survivability observed in groups administered treatment beginning 24 h p.i. (Fig. 19).

Since all three drugs exhibited efficacy when administered at 24 h p.i. (Fig. 19), their protective effects were evaluated when the treatment was further delayed. As it has been well established that the efficacy of antibiotics begins to wane when administration is delayed past 42 h in a pneumonic plague murine model (57), treatment for all three lead drugs was delayed until 48 h p.i. Additionally, to determine if combination therapy could result in an extended therapeutic window, the effect of these drugs in combination with levofloxacin, at both a suboptimal (0.25mg/kg) and efficacious (5mg/kg) dose, were also evaluated in a pneumonic plague infection model. For TFP, a synergistic effect was observed with levofloxacin while DXP exhibited an additive effect with levofloxacin (Fig. 20A&C). Interestingly, TFP and DXP groups treated in combination with levofloxacin at 5mg/kg resulted in 100% survival of animals (Fig. 20A&C). For AXP, however, there seemed to be an interaction between AXP and levofloxacin when these two drugs were administered simultaneously, resulting in rapid deaths of animals, and, therefore, these results were not reported (Fig. 20B). Future studies will focus on whether dosing AXP and levofloxacin by different routes or by staggering administration times of these drugs will alleviate the adverse effects observed in these studies. Overall, our

results indicated that the therapeutic intervention window could be extended by combinatorial drug treatment.

Although we hypothesize these drugs are activating host defenses to aid in the clearance of the bacteria, the true mechanism(s) of action of these drugs is unknown. To begin to delineate potential host defense mechanisms these drugs could be activating, we first evaluated the potential effect of these drugs on complement activation. It is well known that *Y. pestis* can resist the host mediated defense of complement bacteriolysis (120). Therefore, if these drugs did work by activating complement, enhanced killing of the bacteria would be observed in the serum of treated animals. As DXP and AXPN had increased efficacy in clearing WT CO92 when administered 24 h p.i. (Fig. 19), this study was limited to just these two drugs. Using serum from DXP- and AXPN-treated animals, no increase in bacterial killing was observed, indicating that activation of complement was not the mechanism through which these drugs were operating (Fig. 22). However, the protection from pneumonic plague in some re-challenged mice (Fig. 21) indicated that the adaptive immune response was being activated, at least to some extent.

With up to 100% of animals surviving pneumonic plague challenge following administration of DXP at 24 h p.i. (Fig. 19C), a rapid clearance of bacteria from these animals was expected. In order to test this hypothesis, lungs of infected- and DXP-treated and infected animals were collected for bacterial enumeration. Throughout all time points tested, DXP-treated animals had lower bacterial counts in the lungs, with complete bacterial clearance observed by day 10, while all untreated and infected animals succumbed to infection by day 3 (Fig. 23). This clearance of bacteria further indicated activation of host defense mechanisms to better combat bacterial assault.

The use of pharmaceutical agents capable of modifying host signaling pathways “for the treatment of antibiotic-resistant bacteria has recently garnered much attention (95, 121, 122). Additionally, the repurposing of FDA-approved drugs offers the advantage of readily moving *in vitro* candidates to *in vivo* models since the LD₅₀ and ED₅₀ values are readily available and considerable information about their molecular targets and host pathway interactions is known.

“TFP belongs to a class of phenothiazine drugs and is a dopamine antagonist historically used as an antipsychotic for patients with psychiatric disorders, such as schizophrenia, and can also be used to treat nausea caused by chemotherapy (123). The current therapeutic dose for TFP varies based on the condition it is being used to treat, but is generally recommended to be no more than 40 mg a day for schizophrenia or no more than 6 mg for non-psychotic anxiety (123). However, although TFP can be prescribed for human use for long-term use, we administered this drug (1.5 mg/kg) only once in mice. In addition to its known therapeutic uses, TFP has been reported to protect human lung fibroblasts from intoxication caused by *C. difficile* toxin B (124), and to reduce *S. Typhimurium* virulence in both *in vitro* and *in vivo* models. TFP is a known anti-mycobacterial agent, has been shown to have bactericidal properties against several pathogens including *Staphylococcus*, *Vibrio*, *Salmonella*, and *Pseudomonas* spp. (118, 125, 126), and is known to accumulate in macrophages, enhancing its activity against intracellular pathogens. However, the bactericidal activity of TFP varies based on bacterial strains for various pathogens (118, 125, 127), which may account for why we observed no bactericidal effects for *Y. pestis* (Fig 18B). Besides having direct bactericidal effects, a decrease in intracellular survival of *S. Typhimurium* strain SL1344 in epithelial

cells treated with TFP at 10 µg/mL has been described to be the result of host autophagy modulation activities of TFP (128). As no direct bactericidal effects were observed in *in vitro* models of *Y. pestis* infection, TFP may be targeting the autophagy pathway in macrophages to promote bacterial clearance.

AXPN is a tricyclic anti-depressant drug which inhibits the uptake of norepinephrine and serotonin and blocks dopamine's effect on dopamine receptors. The current therapeutic dosage of AXPN is recommended not to exceed 600 mg daily, with the average dosage being around 300 mg daily, placing the dosage of 3 mg/kg used in this study well below that of the therapeutic window (129). In addition to its use as an antidepressant, AXPN and its metabolites have shown efficacy for alleviating cancer drug toxicity and resistance through potent bacterial β -glucuronidase and p-glycoprotein transporter inhibitor activity (130–132). In regards to host responses to infection, AXPN has been shown to have membrane-stabilizing activity, which causes inhibition of fast inward passive Na⁺ current, resulting in membrane hyperpolarization and up-regulation of immune cell activity (133–135). Though AXPN was not observed to decrease bacterial intracellular survival in macrophages, its described membrane stabilizing activity may be responsible for the increase in host-cell and animal survival seen in *Y. pestis* infection models (Figs. 12 & 16A). A reduction in immune cell cytotoxicity caused by AXPN may aid in overall clearance of the pathogen through an altered host inflammatory response and promotion of phagocytosis normally inhibited during later stages of *Y. pestis* infection (104, 117).

Unlike TFP and AXPN, which are both used for psychiatric conditions, DXP is a breathing stimulant that causes an increase in tidal volume and respiratory rate through

stimulation of chemoreceptors in the carotid bodies independent of oxygen levels (136, 137). Similar to TFP and AXPB, the therapeutic dose of DXP depends on the condition for which it is being used in humans, but can be administered at a rate of 1-2 mg/min by intravenous (IV) infusion for up to 2 h (123). Based on this, our dose for *in vivo* studies were well below this limit. DXP has been shown to work through inhibition of TASK-1/TASK-3 heterodimeric potassium channels (138), which, in general, provide a background “leak” potassium conductance important in determining resting membrane potential and excitability of host-cells (138–140). This inhibition of potassium channels is predicted to stimulate catecholamine release, which in turn, results in the stimulation of peripheral carotid chemoreceptors. It has been demonstrated that inhibition of K⁺ influx enhanced macrophage intracellular killing of bacteria (141, 142). Therefore, as both DXP and AXPB have been shown to inhibit the K⁺ channel(s) in various types of cells, these drugs may promote bacterial killing in macrophages through inhibition of the Na⁺/K⁺ channels. Although not detected in *in vitro* models with DXP or AXPB treatment, decreased intracellular survival may be occurring at a later time point not observed here, or may only be occurring in the more immunologically complex *in vivo* environment.” Since DXP is a breathing stimulant, enhanced breathing as well as potential activation of host immune defenses in the lung may be the key to this drug’s efficacy in a pneumonic model. Future studies evaluating DXP’s efficacy against other pneumonias, both bacterial and viral, may provide greater insight into this drug’s mechanism of action against infections and warrants further investigation.

For the first time, we have demonstrated “increased animal survival following treatment with the drugs TFP, AXPB, and DXP,” none of which has antimicrobial

activity against *Y. pestis*, in a murine model of pneumonic plague both alone and in combination with levofloxacin at increasingly delayed time points of administration after infection. “These three drugs represent promising lead compounds for continued evaluation and optimization in treatment to gauge their true therapeutic potential.” Whether these drugs have applicability as therapeutics against other pathogens, specifically multiple-antibiotic resistant ones, remains to be elucidated.

Chapter 4: Broad Applicability of Identified Drugs

INTRODUCTION

“To demonstrate the potential for broad applicability of the novel drugs, the therapeutic potential of TFP”, which has been noted to have anti-mycobacterial as well as bactericidal properties to several other pathogens, “was tested in murine models of *Salmonella enterica* serovar Typhimurium and *Clostridium difficile* infections. Multidrug-resistant *Salmonella* strains represent an inevitable consequence of the use of antibiotics in food-producing animals or for human treatment (91, 143–145). *C. difficile* is an emerging worldwide public health problem and the leading cause of nosocomial antibiotic-associated diarrhea in the United States (146). Patients experience repeated episodes of recurrent diarrhea and require antibiotic treatment for prolonged periods (147). The emergence of hyper-virulent and antibiotic-resistant strains has increased the risk of developing pseudomembranous colitis worldwide (147). As such, both *S. Typhimurium* and *C. difficile* represent emerging public health problems on account of their multiple-drug resistance (148–150), underscoring the need for the rapid development of alternative therapeutics.”

“For both the *S. Typhimurium* and *C. difficile* infection models, TFP significantly increased the survival of infected mice when administered as a prophylactic.” Additionally, for the *C. difficile* infection model, AXPB increased animal survival when administered at the time of infection. “Thus, the drugs identified through the high-throughput screen may have broad applicability, as numerous pathogens may rely on similar mechanisms to modulate bacterial virulence or host pathways. Such new drugs

may be highly effective against multiple-antibiotic-resistant pathogens, thus countering the current and growing problem of antimicrobial ineffectiveness.”

MATERIALS AND METHODS

Bacterial strains.

“The *S. Typhimurium* 14028 strain was obtained from ATCC. The organism was grown in Luria-Bertani (LB) broth at 37°C with constant shaking at 180 rpm.

The *C. difficile* VPI 10463 strain was also obtained from ATCC. The organism was grown anaerobically in a cooked meat medium (Fluka, St. Louis, MO) as previously described (151, 152).”

Testing TFP as a therapeutic in models of *S. Typhimurium* and *C. difficile* infections and AXP as a therapeutic in model of *C. difficile* infection.

“All of the animal studies with *S. Typhimurium* and *C. difficile* were performed in an ABSL-2 facility under approved IACUC protocols (UTMB). For *S. Typhimurium*, 6- to 8-week-old female Swiss Webster or BALB/c mice were dosed with 1.5 mg/kg TFP or saline by the i.p. route 3 h prior to infection. TFP has previously been reported to increase animal survival in a septicemic model of *Salmonella* infection when dosed prior to infection (125). Following drug treatment, mice were challenged i.p. with WT *S. Typhimurium* (1.0×10^6 CFU [1,000 LD₅₀]) (153). Following infection, an additional group of mice was dosed at 24-h intervals with either 5 mg/kg or 0.25 mg/kg levofloxacin for up to 3 days to serve as a therapeutic control. Mice were assessed for morbidity and/or mortality as well as clinical symptoms over the duration of the experiment (14 days p.i.).

For the *C. difficile* infection model, female C57BL/6 mice were purchased from the Jackson Laboratory (Bar Harbor, ME) and housed under specific-pathogen-free conditions. At 8 weeks of age, mice were administered an antibiotic cocktail in the drinking water (colistin, 850 U/ml; gentamicin, 0.035 mg/ml; kanamycin, 0.4 mg/ml; metronidazole, 0.215 mg/ml; and vancomycin, 0.045 mg/ml) for 3 days to sensitize animals to infection and then were switched to regular water. Two days later, mice received a single dose of clindamycin (32 mg/kg) via i.p. injection to disrupt the normal intestinal microbiota, allowing *C. difficile* colonization. The next day, 3 h prior to infection, mice were dosed with 1.5 mg/kg TFP or saline by the i.p. route and were infected, with 10^5 spores of *C. difficile* (strain VPI 10463) by oral gavage. The group of animals receiving AXPN treatment were administered AXPN by the i.p. route at the time of infection and then at 24 h intervals for 3 days. Following infection, an additional group of mice were dosed with 20 mg/kg vancomycin at 24-h intervals for 5 days p.i. to serve as a therapeutic control.”

For the infection, “briefly, *C. difficile* was grown under anaerobic conditions in cooked meat medium for ~7 days at 20 to 26°C to allow for sporulation. Spores were then separated from vegetative cells via density gradient centrifugation (152), heat shocked at 56°C for 20 min to kill any remaining vegetative cells, and then centrifuged. Resultant pellets were resuspended at 1×10^6 cells/ml in sterile saline and enumerated on *C. difficile* selective agar plates containing 7% horse blood, D-cycloserine, and cefoxitin. Spore suspensions with a purity of >99% were stored at 20°C. All mice were monitored daily for signs of infection, including weight loss, presence of diarrhea, hunched posture, and prolonged lethargy. At necropsy, ceca and colons were removed

and processed for histological analysis to assess the degree of inflammation and damage to the mucosa.”

Growth kinetics and sensitivity of *S. Typhimurium* to TFP.

“Overnight cultures of *S. Typhimurium*, grown in LB broth at 37°C, were sub-cultured to an OD₆₀₀ of 0.1. Cultures were then inoculated with 33 µM TFP or levofloxacin (positive control) or with PBS (negative control) and incubated at 37°C with shaking. Samples for OD₆₀₀ measurements were taken at the indicated time points. For MIC determinations, the broth macro-dilution method was utilized as described” in Chapter 3.

Evaluation of TFP, AXP, and DXP effect on autophagy in RAW 264.7 macrophages.

RAW 264.7 murine macrophages were seeded in a 96-well microtiter plate as previously described in Chapter 2 and 3. Following overnight incubation, macrophages were infected with *S. Typhimurium* and subsequently incubated with TFP, AXP or DXP, at a concentration of 33 µM. Following incubation for 4 h, the medium was removed and macrophages were lysed and collected in SDS-PAGE buffer. Cell pellets were analyzed by immunoblotting using antibodies to LC3.

Statistical analyses.

Statistical analysis was performed as described in Chapter 2 with the exception that. Kaplan-Meier survival estimates or chi-square analyses were used for animal studies, with *P* values of ≤0.05 considered significant for all the statistical tests used.

RESULTS

“TFP exhibited protection in a murine model of *S. Typhimurium* infection, with no direct bactericidal or bacteriostatic effects.

Since TFP exhibited the most promising results in our *Y. pestis* infection model when administered at the time of bacterial challenge, we decided to examine if protection could be afforded to other bacterial infection models. As TFP has previously been shown to increase survival in a septicemic mouse model of *Salmonella* infection (125), we attempted to corroborate these findings by using a different strain of *S. Typhimurium* and at a higher bacterial challenge dose. Mice were dosed once with 1.5 mg/kg TFP i.p. 3 h before infection, as this was the most successful dosing regimen reported (125), and then subsequently challenged by the i.p. route with 1.0×10^6 CFU (1,000 LD₅₀) of bacteria. Through this model, a statistically significant increase in animal survival was observed for TFP-treated animals (60% survival) compared to untreated controls (0% survival) or levofloxacin-treated controls (0% survival for 5-mg/kg and 0.25-mg/kg dosing)” (**Fig 24A**).

“To evaluate if TFP had any bactericidal or bacteriostatic effect on this pathogen, *S. Typhimurium* 14028 was grown in the presence of 33 μ M TFP in order to mimic the concentration used for *Y. pestis* CO92. At this concentration, TFP was observed to have no effect on bacterial growth (**Fig. 24B**). In order to determine if there were any bacteriostatic effects, samples grown for 24 h in drug-containing medium were re-inoculated into fresh LB broth and grown for another 24 h. As observed with *Y. pestis*, the growth of *S. Typhimurium* was not affected by TFP treatment. While an MIC of 80 μ g/ml has been reported for *S. Typhimurium* strains NCTC 11 and NCTC 74 for TFP

(125), we determined the MIC of TFP for *S. Typhimurium* 14028 to be above 100 $\mu\text{g/ml}$ (data not shown), indicating that TFP was not bactericidal to *S. Typhimurium* 14028 at clinically relevant concentrations.”

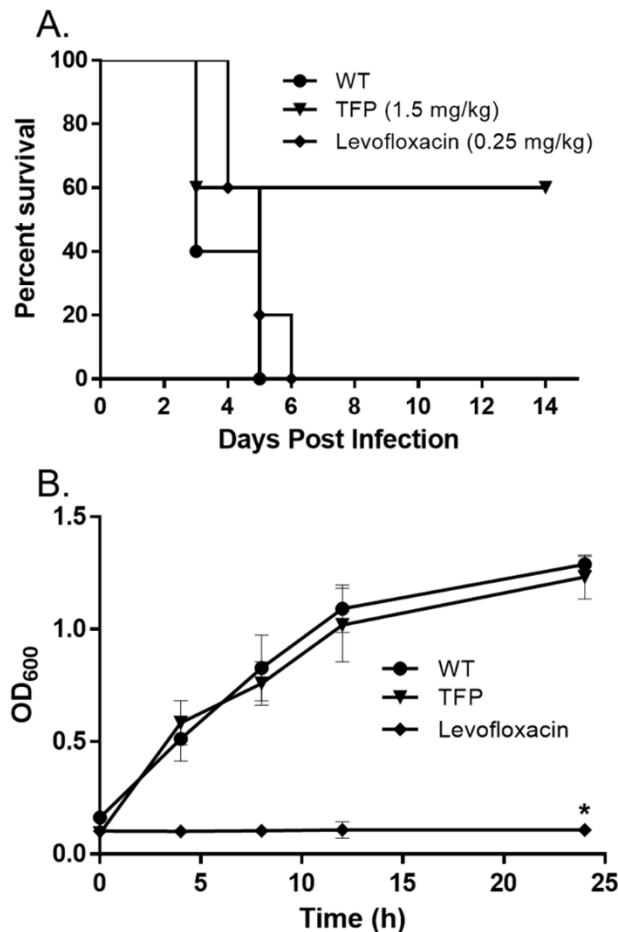


Figure 24. Effects of TFP on *S. Typhimurium*.

(A) Mice ($n = 5$ per group) were dosed with either TFP or saline as a control by the i.p. route 3 h before challenge by the i.p. route with 1000 LD_{50} of *S. Typhimurium*. Twenty-four hours p.i., another group of infected animals were dosed with 0.25 mg/kg levofloxacin as a therapeutic control. Animals were then observed for mortality over a period of 14 days post infection. The data were analyzed for significance by the chi square test based on comparison of the results for the TFP treatment group to the results of saline treated and infected controls (WT) and levofloxacin treated animals, $p = 0.0384$ for both. (B) Growth of *S. Typhimurium* in LB broth in the presence of TFP and levofloxacin at a concentration of 33 μM or PBS as a control. Samples were taken at the indicated time points for OD_{600} measurements. Data shown are the mean values while error bars represent the SD ($n = 4$). Statistical analysis was performed by using one-way ANOVA with only levofloxacin showing a significantly lower OD_{600} value when compared to WT ($p < 0.001$).

TFP, but not AXPB or DXP, treatment with and without infection resulted in an increase in autophagy in murine macrophages.

TFP is a known inducer of autophagy (128, 154), and, therefore, to determine perturbations of the autophagy pathway in our *in vitro* infection model with TFP, AXPB, or DXP, macrophages were infected with *S. Typhimurium* and subsequently incubated with each drug for 4 h before being lysed for Western blot analysis. LC3 conversion from LC3-I to LC3-II has proven to be a useful biomarker to detect autophagy (155), and was therefore chosen as a marker for this study. As observed in **Fig. 25**, while TFP treatment resulted in an increase in LC3 conversion for both uninfected and infected macrophages, AXPB and DXP treatment resulted in no noticeable changes.

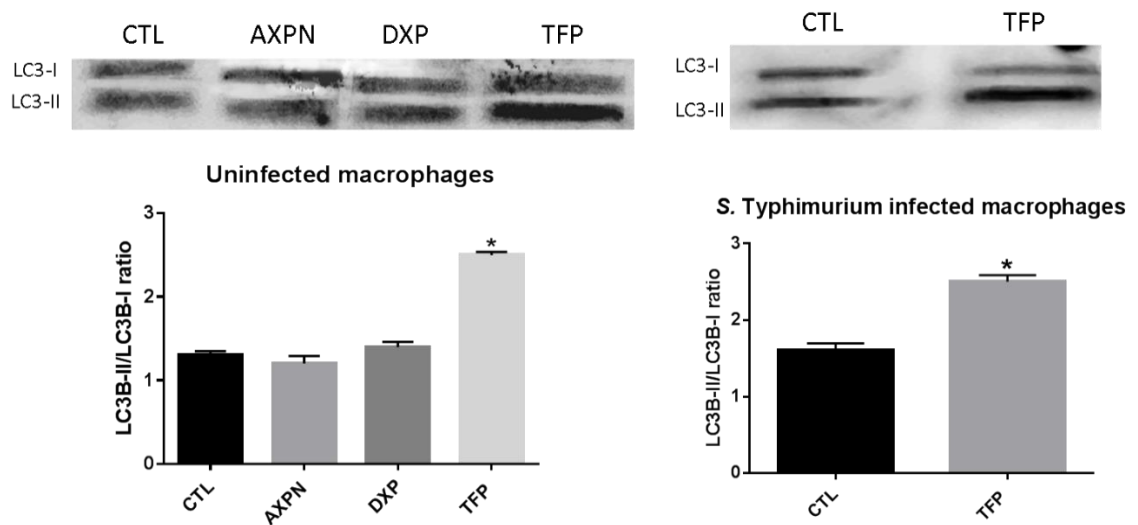


Figure 25: Effects of TFP, AXPB, and DXP on autophagy pathway. **(A)** RAW 264.7 murine macrophages were incubated with TFP, AXPB, or DXP at 33 μ M concentration, or PBS as control (CTL), for 4 h and subsequently lysed in SDS-PAGE buffer for immunoblot analysis. **(B)** RAW 264.7 murine macrophages were infected with *S. Typhimurium* and subsequently incubated with a 33 μ M concentration of TFP for 4 h. Cell pellet samples were then analyzed for LC3 levels through Western blot analysis. Data were analyzed by using one-way ANOVA with comparison between CTL and treatment groups * $P < 0.05$.

TFP and AXPN exhibited protection in a murine model of *C. difficile* infection.

“To determine whether any drug possessed antibacterial properties beyond *Y. pestis* and *S. Typhimurium* 14028, we chose to test the efficacy of TFP and AXPN in a *C. difficile* infection model. Following the parameters of our *S. Typhimurium* infection model, mice were dosed with 1.5 mg/kg TFP by the i.p. route 3 h before infection and subsequently challenged by oral gavage with 10^5 *C. difficile* (VPI 10463) spores.” For AXPN, animals received this drug at the time of infection and then at 24-h intervals for 3 days to mimic our *Y. pestis* infection model. “Although the difference was not statistically significant, we did observe an increase in survival of TFP-treated animals compared to vancomycin-treated animals. We did, however, observe a significant increase in survival (60%) for TFP-treated animals compared to the untreated controls, which all succumbed to infection” (**Fig. 26A**). For the AXPN group, although not statistically significant, we did observe an increase in animal survival (40%) compared to untreated controls. This level of protection was slightly better than that of vancomycin (28%). “Following an initial decrease in body weight, TFP and AXPN treatment resulted in recovery of animal body weights that were significantly higher than those of vancomycin-treated animals (**Fig. 26B**). Furthermore, histological examination of tissues at necropsy revealed significant differences between untreated and TFP-treated animals. Untreated animals demonstrated abundant inflammatory infiltrate, edema, and formation of pseudo-membranes that were not apparent, or were greatly decreased, in TFP-treated mice” (**Fig. 26C**). Further detailed studies with AXPN and DXP are warranted and constitute future goals.

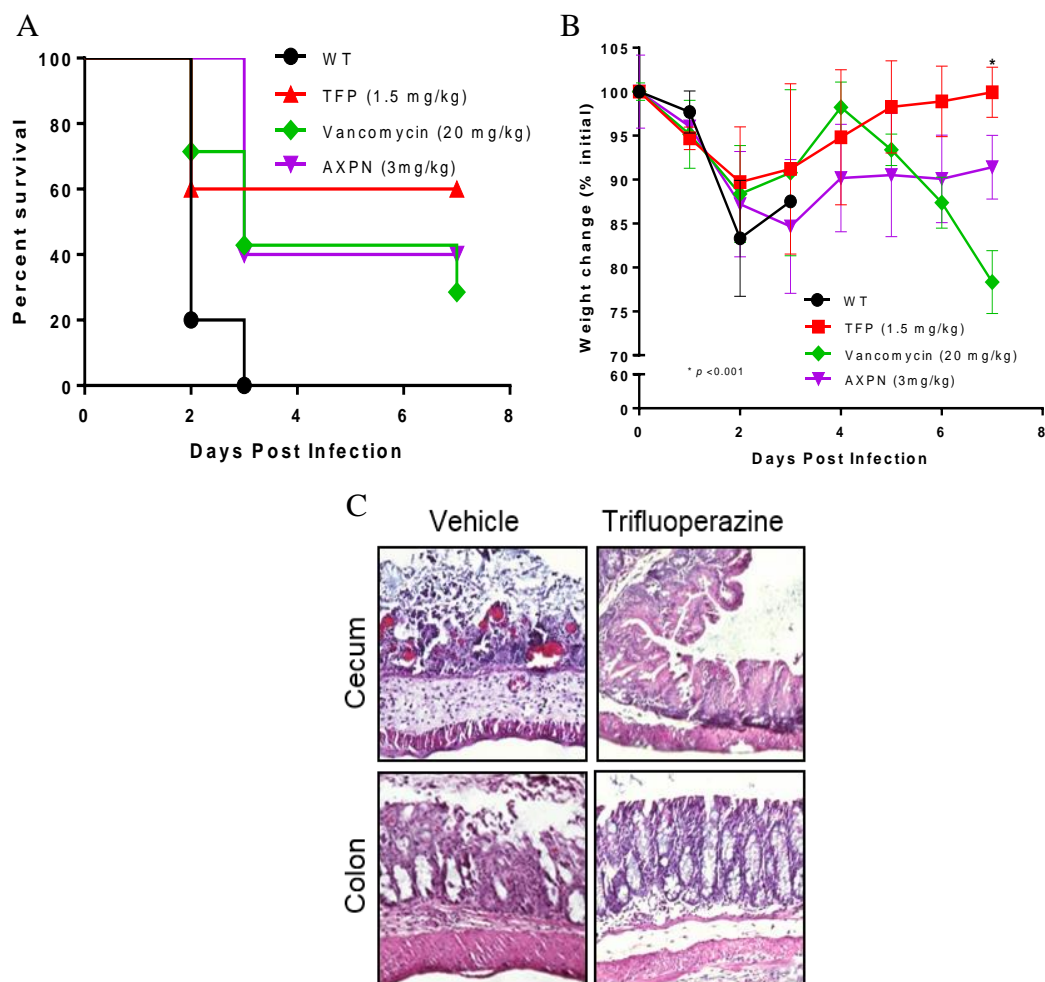


Figure 26: Efficacy of TFP and AXPN in murine *C. difficile* infection model.

C57BL/6 mice were infected by oral gavage with 10^5 *C. difficile* (VPI10463) spores. Three hours prior to infection, mice were treated with a single dose of TFP (1.5 mg/kg) or vehicle alone by the i.p. route. AXPN was administered at the time of infection at 24 h intervals for 3 days. Animals were monitored for 7 days. TFP- and AXPN-treated mice showed increased survival (**A**) and were able to restore body weights (**B**). Results are mean \pm SD ($n = 5$ mice/treatment for vehicle, AXPN, and TFP; $n = 7$ for vancomycin). (**C**) Representative intestinal tissue H&E sections collected at the time of necropsy (Day 7 from TFP-treated mice, and Day 3 from a vehicle control). The survival data was analyzed for significance by the chi square test based on comparison of the results for the TFP treatment group to the results of saline treated controls (Vehicle). $p = 0.0384$. Weight change data was analyzed by using one-way ANOVA with comparison between TFP and vancomycin treatment groups ($p \leq 0.001$).

DISCUSSION

As we have shown the potential utility of TFP, AXP, and DXP against *Y. pestis* infection, we wanted to further evaluate if these drugs had broader applicability against other pathogens. With the increasing isolation of multiple-drug resistant strains of both *S. Typhimurium* and *C. difficile* (144, 145, 150, 156–158), the need for the rapid development of alternative therapeutics against these pathogens is clear. Therefore, we chose to evaluate the efficacy of TFP against both *S. Typhimurium* and *C. difficile*, as it has been reported to have some effect on *S. Typhimurium* infection in both *in vitro* and *in vivo* infection models as well as have an effect on limiting *C. difficile* toxin B associated toxicity on human lung fibroblasts *in vitro* (124, 125, 128). Through the studies reported here, TFP significantly increased survival in both *S. Typhimurium* (Fig. 24A) and *C. difficile* (Fig. 26A) infection models. Interestingly, similar to the results observed with *Y. pestis* in Chapter 3, “TFP exhibited no direct bactericidal or bacteriostatic effects on *S. Typhimurium* (Fig. 24B), further indicating that the broadly acting drug TFP likely targets common host cell signaling pathways exploited by multiple bacterial pathogens during infection.”

TFP has been shown to induce autophagy (128, 159), a highly conserved process involved in cellular homeostasis to recycle proteins and remove damaged organelles (160). In addition to these processes, autophagy has been described to play a crucial role in the innate immune defense against several pathogens (128, 159–161). Regarding *S. Typhimurium* specifically, TFP has been reported to aid in the inhibition of bacterial replication due to its effects as an autophagy modulator (128, 159). Here, we confirmed TFP’s role in inducing autophagy in murine macrophages using Western blot analysis

(Fig. 25). This increase was specific to TFP, as AXPB and DXP exhibited no differences in conversion of LC3-I to LC3-II in comparison to untreated controls (Fig. 26). Whether TFP's modulation of the autophagy pathway is the mechanism behind its observed efficacy *in vivo* against *Y. pestis*, *S. Typhimurium*, and *C. difficile* requires further investigation.

In addition to observing efficacy with TFP against *C. difficile* infection in mice, we also observed efficacy with AXPB treatment when administered at the time of infection. Although the survival of the AXPB treated group of mice (40%) was not statistically significant to the control group, this survival rate was somewhat better to that of vancomycin -treated animals (Fig. 26A). Also noted, animals treated with AXPB regained weight loss during infection more robustly than those treated with vancomycin.

Through these studies, we have confirmed TFP's role as an autophagy modulator and also as an effective prophylactic against *S. Typhimurium* infection. We have also demonstrated, for the first time, the effective use of TFP and AXPB in a *C. difficile* infection model. Further studies to optimize dosing regimens, evaluating therapeutic efficacy against not only these but other multi-drug resistant pathogens, as well as determining whether combinatorial therapy (e.g., with vancomycin) would result in better efficacy of these drugs is warranted.

Chapter 5: Conclusions and Future Directions

CONCLUSIONS

Yersinia pestis, a pathogen with a devastating history causing hundreds of millions of deaths, continues to be a problem of global concern. The endemic nature of this bacterium coupled with its ability to circulate in numerous rodent populations makes eradication unlikely and impractical. Therefore, our best defenses lie in the development of effective prophylactics, particularly for use in endemic areas, and effective therapeutics. Currently, there are no FDA-approved vaccines against plague and our therapies are limited to antibiotic intervention.

The goal of these studies was to tackle these gaps in knowledge and contribute to the development of both novel plague vaccines and therapeutic drugs. Focusing on the development of novel vaccines through the course of the studies presented in Chapter 2, we have provided the following conclusions:

- Determined that out of six T6SS loci in the *Y. pestis* genome, three (Cluster B; *ypo0966-9084*, Cluster E; *ypo2720-2733*, and Cluster G; *ypo3588-3615*) contributed to bacterial virulence in a mouse model of pneumonic plague infection, with attenuation of these cluster deletion mutants ranging from 30-40%.
- Generated and characterized four out of six Hcp protein encoding gene homolog (one of the effectors of the T6SS) deletion mutants for attenuation in a mouse model of pneumonic plague infection. All four deletion mutants generated exhibited attenuation in this model, with 30-40% animal survival observed when challenged with these mutant strains.
- Generated and characterized three out of five PAAR-motif containing protein (another effector of the T6SS) encoding gene deletion mutants for attenuation in a mouse model of pneumonic plague infection and observed

no significant attenuation for any of these mutants in comparison to WT CO92.

- Determined, through combinatorial deletion of *vasK* and *hcp6* or *ypo2720-2733* (T6SS cluster E) and *hcp3*, attenuation could be further augmented, with 60% animal survival observed when challenged with either of these double deletion mutant strains. Furthermore, animals surviving initial infection with the double deletion mutant strains were protected (60-100% survival) from subsequent re-challenge with WT CO92 by the i.n. route, mimicking pneumonic plague.
- Observed no overt growth defects for any of the attenuated T6SS-associated mutant strains when grown at either 28 or 37°C *in vitro*.
- Determined Hcp6 is secreted through the T6SS cluster G (*ypo3588-3615*).
- Determined YopE (an effector of the T3SS) production differed in several mutant strains deleted for components/effectors of the T6SS in both pellet and bacterial supernatant fractions, indicating a potential link between the T3SS and the T6SS.
- Observed significantly decreased intracellular survival in all attenuated mutant strains in comparison to WT CO92, with the exception of *Δypo2720-2733* and *Δypo2720-2733Δhcp3* mutants.
- Observed that out of the ten attenuated mutant strains, seven exhibited decreased host cell cytotoxicity to RAW 264.7 murine macrophages in comparison to WT CO92. For the *Δypo2720-2733* and *Δypo2720-2733Δhcp3* mutant strains, which exhibited no defects in intracellular survival in murine macrophages, this decrease in cytotoxicity may be responsible for not only the attenuation observed for both mutants *in vivo*, but also subsequent protection from re-challenge with WT CO92.

- Observed, in macrophages infected with $\Delta vasK$, $\Delta hcp6$, or $\Delta vasK\Delta hcp6$ mutant strains, significantly higher rates of phagocytosis in comparison to WT CO92.
- Determined the addition of rHcp6 (from *Y. pestis*) or rHcp (from *A. dhakensis*) decreased the percentage of phagocytosed bacteria for $\Delta vasK$, $\Delta hcp6$, or $\Delta vasK\Delta hcp6$ mutant strains to levels observed for WT CO92, further indicating Hcp6's phagocytic role in *Y. pestis* infection.

In terms of therapeutics, development of antibiotic resistance in bacteria is alarming, and therefore, new therapeutics that target host genes rather than bacteria should be sought with much reduced chances of bacteria to develop resistance against them. With this in mind, the studies presented in Chapter 3 provided following conclusions:

- Provided initial evidence of the utilization of host-directed screening techniques to identify novel therapeutics against microbes.
- Identified 94 drugs that inhibited host-cell cytotoxicity when infected with WT CO92. Of these, 58 drugs were identified in a post-treatment model.
- Identified 3 drugs (TFP, AXP, and DXP), from a total of 17 tested *in vivo*, which exhibited efficacy (40-60% survival) against a murine model of pneumonic plague when administered at the time of infection.
- Determined TFP, AXP, and DXP were efficacious against a pneumonic plague infection model even when administered 24 h p.i., with 40-100% survival observed. Additionally, for AXP and DXP treatment groups, significantly higher survival rates in comparison to WT CO92 control infected animals were observed even when these drugs were administered at 48 h p.i. (50-72% survival).

- Determined animals treated with TFP, AXP, and DXP during an initial infection exhibited some protection (25-100%) from subsequent re-challenge with WT CO92.
- Observed an additive effect with DXP treatment in combination with levofloxacin and a synergistic effect with TFP treatment in combination with levofloxacin, with 57-100% survival rates observed, when drugs were administered 48 h p.i. in a pneumonic plague model.
- Determined TFP, AXP, and DXP exhibited no bactericidal or bacteriostatic effects on WT CO92 *in vitro*, as well as determined the MIC of all three drugs to be > 100 µg/ml.
- Determined TFP, AXP, and DXP exhibited no effects on *Y. pestis* virulence in terms of expression/production of the T3SS effectors LcrV or YopE, expression/production of the T6SS effector Hcp6, or Pla protease activity.
- Showed that treatment with AXP or DXP did not alter serum resistance of *Y. pestis* CO92.
- Showed that treatment with DXP inhibited bacterial proliferation and led to the rapid clearance of bacteria from the lungs of infected animals.

To determine the potential for broad applicability of these drugs, the studies in Chapter 4 provided following conclusions:

- Provided evidence of the utility of TFP against *S. Typhimurium* infection in a mouse model of septicemic infection, with 60% survival of animals treated 3 h before infection.
- Showed TFP is not bactericidal or bacteriostatic against *S. Typhimurium* strain 14028.

- Confirmed TFP as a modulator of autophagy and its ability to increase expression of autophagy associated proteins in macrophages infected with *S. Typhimurium*.
- Provided evidence of the utility of TFP and AXPB against *C. difficile* infection in a mouse model, with 40-60% survival of animals.
- Showed pre-treatment with TFP resulted in decreased formation of pseudo-membranes, edema, and inflammatory infiltrate in comparison to untreated and infected controls, as shown by histological examination.

Overall, these results indicate a distinct role for T6SS effectors and clusters in *Y. pestis* virulence and represent novel targets for the continued development of live-attenuated vaccine candidates for plague. Furthermore, these results show the utility of host-directed screening approaches to identify novel therapeutics for infections. From these studies, three drugs were identified and represent promising lead compounds for the continued evaluation and optimization in treatment not only against plague, but also other infectious agents, particularly those that are multi-drug resistant.

FUTURE DIRECTIONS

Through the course of these studies, we have accomplished the goals of furthering the development and testing of both novel live-attenuated vaccine candidates and potential therapeutics. Moving forward, future studies on the vaccine development aspect will focus on the mechanistic characterization of these newly described, T6SS-associated virulence factors, including the potential link between the T6SS and the T3SS. In addition to mechanistic studies, the development of combinatorial deletion mutants inclusive of the T6SS-associated effectors/components identified to alter virulence in these studies as the background strain, will be continued. The ultimate goal of these

studies will be the development of live-attenuated vaccine candidate strains, that exhibit a successful balance between efficacy and safety.

Future studies on the therapeutic aspect will focus on determining the mechanism(s) of action of TFP, DXP, and AXP. Although we have shown that these drugs do not seem to directly affect the bacteria, how they modulate the host immune response remains unknown. Some preliminary data from RNA-seq on *in vitro* infection samples (data not shown) indicated perturbations in several host genes related to functions including cell cycle, apoptosis, and specifically for TFP, autophagy. These preliminary results confirm the role of TFP in promoting autophagy, as also observed in Western blot analysis, and hence may be part of the mechanism of the observed attenuation for TFP. In the same arm, as TFP has shown efficacy against bacterial pathogens such as *S. enterica* serovar Typhimurium and *C. difficile* as a prophylactic, and AXP has shown efficacy against *C. difficile* when administered at the time of infection, the utilization of all three drugs against other, particularly multi-drug resistant pathogens such as *Klebsiella pneumoniae*, *Acinetobacter baumannii*, and *Pseudomonas aeruginosa* will be further explored. As antibiotics are well known to perturb the microbiome and can cause significant side effects, another direction of inquiry would include determining the effects of these drugs on the host microbiome. Lastly, the pharmaco-kinetics of these drugs without and with infection will be evaluated.

Appendix A: Primers used in this study

Table 1A. Sequences of primers used in this study

Primer or primer pair	Primer sequences (5' – 3'; forward, reverse)	Purpose
1 Kmypo0966-0984	CTGAAGACCCCATTAACGTTGGCTATTCTCTT AACAGGACGTTAAAAATGTGTAGGCTGGAGCT <u>GCTTC</u> (FRT sequence), TGTAATTAACGCAAAACAGGCAATCGGGCTTG GTGTTGAACTGGAAATTA <u>ATTCCGGGGATCCGT</u> <u>CGACC</u> (FRT sequence)	Construction of a DNA fragment with Km ^r gene cassette and FRT sequence for the <i>ypo0966-0984</i> mutation
2 <i>ypo0966-0984V</i>	ACTCCCCCTTCCTTGCAATTAATCACTTCA, ATGATAGGGACAGGCTACAAATGCT	PCR verification of <i>ypo0966-0984</i> deletion
3 Kmypo1458-1493	TGGGCTCCTTATTCTTGAGCGTATCGATAACCA CTTACGGCGTTATCGCT <u>GTGTAGGCTGGAGCTG</u> <u>CTTC</u> (FRT sequence), TAATTGCCTGTTTTTGATATCTTCACTCCAACAA CGGAGACAGGCAAATT <u>ATTCCGGGGATCCGTC</u> <u>GACC</u> (FRT sequence)	Construction of a DNA fragment with Km ^r gene cassette and FRT sequence for the <i>ypo1458-1493</i> mutation
4 <i>ypo1458-1493V</i>	GAATAGGGGTCTACTCTTATGGTTC, AATTTACAGGCAATGGAAGCCATAAAGCTG	PCR verification of <i>ypo1458-1493</i> deletion
5 Kmypo2720-2733	AAGTGAAATCAGGCTGGGCAGATGACGAACGT GCATTGCGCAGCTTAGGCTATACCGACGATTG AAATAAGGCTTGCCGGTGTAGGCTGGAGCTGCT <u>TC</u> (FRT sequence), ATTACACTGCGACGGCGGTTTTTCAGTTGCTGAA GATTATTGATGATATAACCTCCCCCTAATCGCT CTCACTAATTATTT <u>ATTCCGGGGATCCGTCGAC</u> <u>C</u> (FRT sequence)	Construction of a DNA fragment with Km ^r gene cassette and FRT sequence for the <i>ypo2720-2733</i> mutation
6 <i>ypo2720-2733V</i>	GGCGAAGAAGCTGCCTTATTCGGTGACGGTT, AGTCCATCGACGTTAACATTTCATGATGTT	PCR verification of <i>ypo2720-2733</i> deletion
7 Kmypo2927-2954	GTAGGTTATGTAAAGTGGAAGCGATGAGATA TGTCATTAAGTGCATGATTTAAAAAGATTAAAA AGGTAAGTTACTGAAGTGTAGGCTGCAGCTGCT <u>TC</u> (FRT sequence), GCGATGTTTAAACATATTCTTCCAATACGACCAC GTCATGCTAAGTCGGGTTATTTAGCATGACGTG ATATCGCTCAAAAA <u>ATTCCGGGGATCCGTCGAC</u> <u>C</u> (FRT sequence)	Construction of a DNA fragment with Km ^r gene cassette and FRT sequence for the <i>ypo2927-2954</i> mutation
8 <i>ypo2927-2954V</i>	CCGTAGCGCGGCGATCTCTTCCAGTACCGC, GGAATGAGCTGTAGATAGGCCCGTTACTGC	PCR verification of <i>ypo2927-2954</i> deletion
9 Kmypo3588-3615	AACAGAACCAAGTTAAGCATTACGACTCATTA AATAAGGGTAGCCCGCGACCACGGGTAAAGCAC AGAGGAGAGCAAAAA <u>GTGTAGGCTGGAGCTGC</u> <u>TTC</u> (FRT sequence), TAGCATACCTATTTTCATATGCAGTTTCAGGAGG GATATTCTCAGTACCATAAATAGCTATAGCCGT ACACATAGTTTCACAT <u>TTCCGGGGATCCGTCGAC</u> <u>C</u> (FRT sequence)	Construction of a DNA fragment with Km ^r gene cassette and FRT sequence for the <i>ypo2927-2954</i> mutation
10 <i>ypo3588-3615V</i>	AAAAAGACGATCTTTACTCCTTGACAGAGAA, AACCACCAAAATCACTTGTGAGAACCCTAA	PCR verification of <i>ypo3588-3615</i> deletion

11	Kmypo2793	GATTATCGGTTTATACTCAGGCTTGAAGTGCCG CCAATTTTGGAAACGACAGCTAACCTCTATTA CATAAGGAATTGTCTGCTAGGCTGGAGCTGCTT C (FRT sequence), AAGCTATGCTCAAGATCATCTTGGATGTCCCCT AATGAATACGTAAAAGATATAAAAGCTATGTCC ATAGTTAACCGCCTCATTCGGGGATCCGTCGA CC (FRT sequence)	Construction of a DNA fragment with Km ^r gene cassette and FRT sequence for the ypo2793 mutation
12	ypo2793V	TCTTTTTTAATAAGAATGGGGTGACATGAT, TGATGTTATTATCTTCTCATGGAAAGTTGG	PCR verification of ypo2793 deletion
13	ypo2793C	GTAAGCTTAACGTCAACGACCAGTAAGTG (HindIII), GCGGATCCGCTATGTCCATAGTTAACCG (BamHI)	Cloning of 2793 in plasmid pBR322
14	Kmypo2868	GTAAGAGACTTATCACTGTGTAAATAACAACCTT TAAATATAAGGAATTGTGTGTAGGCTGGAGCTG CTTC (FRT sequence), TTATGGTTTTTAACGATATAGGGTATATGCCTA TAGCCGTCACCTAAAAAATTCCGGGGATCCGTC GACC (FRT sequence)	Construction of a DNA fragment with Km ^r gene cassette and FRT sequence for the 2868 mutation
15	ypo2868V	ATTCTCTAGCTCCATAGCAATATGC, TGTCGAGGGTATTACGTTGATACGG	PCR verification of ypo2868 deletion
16	ypo2868C	GTAAGCTTTGTTAGCATACGAG (HindIII), CAGGATCCCTATATGCCTATAGCCGTCAC (BamHI)	Cloning of 2868 in plasmid pBR322
17	Kmypo2962	AAGGGCAACTAACCCCTGCATCTTGAAGGCG ACGGGTATATAAGGACATGTGTAGGCTGGAGC TGCTTC (FRT sequence), CGTATGTACACGTAAATAATAAGGGATGGTGTA GGCCATCCCCGAATAAAATTCCGGGGATCCGTC GACC (FRT sequence)	Construction of a DNA fragment with Km ^r gene cassette and FRT sequence for the ypo2962 mutation
18	ypo2962V	TCCCCGCCAGCGATAACGCTCCCGTCAGATA, GTTCAATGGGTCTGTTGGCTGAGTTTTTTG	PCR verification of ypo2962 deletion
19	ypo2962C	ATAAGCTTCCGTCAGATAATAGTAGCGG (HindIII), ATGGATCCCTTAATACACGCGATCATCCCATATG C (BamHI)	Cloning of ypo2962 in plasmid pBR322
20	Kmypo3708	AAGTGACTAACCTTTGATCAAAATCAAATAAAC TATCAAGGATATTAAAAGTGTAGGCTGGAGCTG CTTC (FRT sequence), CGCTTCGATCGGCGCACGCCAGTCATCAGCAC AGAGGTGCCCCGCGGTGGATTCCGGGGATCCGTC GACC (FRT sequence)	Construction of a DNA fragment with Km ^r gene cassette and FRT sequence for the hcp6 mutation
21	ypo3708V	CGAAACTTGGCACTGATAAAAAAGC, TAATATATCCCTGGCGGCGACACAT	PCR verification of hcp6 deletion
22	ypo3708C	CGGGATCCCTTTTGTAACATTTGCGAATTAA (BamHI), ACGCGTCGACTTACGCTTCGATCGGCGCAC (SalI)	Cloning of hcp6 in plasmid pBR322
23	ypo3708R	TCATAGATCTAATGCCAACTCCAGCTTATATCT C (BgIIIIF), GGTCCTCGAGTTACGCTTCGATCGGCGCACG (XhoI)	Cloning of hcp6 in plasmid pET30 vector

24	Kmypo0873	CATCATTATCCCTTACCTTTTTGGGCATATTGCC AAATTGATATTGGCAAACGGATAAATAAGGGA TGATGTGTAGGCTGGAGCTGCTTC (FRT sequence), GGGCAAATTCATAATCCCCAAGATTATCTATT GTTTTTGATCCGCAGCACTGACATGAATATTCA TCACATTCCGGGGATCCGTCGACC (FRT sequence)	Construction of a DNA fragment with Km ^r gene cassette and FRT sequence for the <i>ypo0873</i> mutation
25	<i>ypo0873V</i>	TCTCCTAACCCTACCAATCCCTTA, AAAGCCACTGTTGCTGATAAACCGT	PCR verification of <i>ypo0873</i> deletion
26	Kmypo1484	GGCTAATCGCCCTGCACCCGGCCCGTGCGGCCG TATTATGCGGATAACAGGTGTAGGCTGGAGCTG CTTC (FRT sequence), TCCTAATACGATAAAAATCGTAACAACCATTAT TATTCTTTTCATTACTTTTCCGGGGATCCGTCGA CCTATTCCGGGGATCCGTCGACC (FRT sequence)	Construction of a DNA fragment with Km ^r gene cassette and FRT sequence for the <i>ypo1484</i> mutation
27	<i>ypo1484V</i>	AAGTAATGAAAAGAATAATAATGGTTGTTACG AT, CTTCTCTGTTATCCGCATAATACGGC	PCR verification of <i>ypo1484</i> deletion
28	Kmypo3615	TCATAATTTACGGTCGTTTCGGATAGAGCCACG GCATCAGGAGGATGTTTGTGTAGGCTGGAGCTG CTTC (FRT sequence), TAGCATACCTATTTTCATATGCAGTTTCAGGAGG GATATTCTCAGTACCATAAAATAGCTATAGCCGT ACACATAGTTTCACATTCCGGGGATCCGTCGAC C (FRT sequence)	Construction of a DNA fragment with Km ^r gene cassette and FRT sequence for the <i>ypo3615</i> mutation
29	<i>ypo3615V</i>	AGGCTCTCTGAGCCGGCAATTAAATCACTA, AACCACCAAATCACTTGTGAGAACCCTAA	PCR verification of <i>ypo3615</i> deletion

Appendix B: Names, therapeutic class, and tier of drugs identified from *in vitro* screens against *Y. pestis*

Table 1B: Tier 1 pre- and post-treatment compounds identified using a host cell-based high-throughput drug repurposing screen evaluating viability of macrophages following infection for 12 h. The known functions of drugs have also been indicated.

Tier 1 drugs			
Pre-treatment		Post-treatment	
Drug name	Therapeutic Class	Drug name	Therapeutic class
Beclomethasone dipropionate	Anti-asthmatic, anti-inflammatory	Zafirlukast	Anti-asthmatic
Benazepril	Antihypertensive	Mesalamine	Anti-inflammatory
Betamethasone	Anti-inflammatory, immunosuppressive	Carboplatin	Antineoplastic
Bromfenac	analgesic	Desogestrel	Contraceptive
Brompheniramine maleate	Anti-allergic	Epinastine-HCl	Anti-allergic, antihistamine, mast cell stabilizer
Cisatracurium besylate	Neuromuscular blocking agent	Ethinyl estradiol	Contraceptive
Asenapine maleate**	Antipsychotic	Doxapram-HCl	Respiratory stimulant
Aspirin***	Analgesic	Carglumic acid	Hyperammonaemia treatment
Carmustine**	Antineoplastic	Colchicine***	Natural product used for arthritis
Colchicine***	Natural product used for arthritis	Aspirin***	Analgesic
		Dihydroergotamine mesylate	Antimigraine, vasoconstrictor, analgesic
		Haloperidol	Antipsychotic, schizophrenia agent
		Apomorphine-HCl hemihydrate	Non-selective dopamine agonist and anti-Parkinsonian
		Promethazine-HCl	Anti-allergic, sedative
		Amoxapine	Antidepressant

***Drug identified as Tier 1 in both pre and post treatment

**Drug identified as Tier 1 for one treatment, but Tier 2 for other

Table 2B: Tier 2 pre and post-treatment compounds identified using a host cell-based high-throughput drug repurposing screen evaluating viability of macrophages following infection for 12 h. The known functions of drugs have also been indicated.

Tier 2 drugs			
Pre-treatment		Post-treatment	
Drug name	Therapeutic class	Drug name	Therapeutic class
Amiloride	Diurectic	Asenapine maleate**	Antipsychotic
Amlodipine	Antihypertensive	Estrone	Antineoplastic, estrogen
Bleomycin	Antineoplastic	Etonogestrel	Hormonal contraceptive
Capsaicin	Analgesic	Fenoprofen-Ca	Analgesic
Ethacrynic acid*	Diuretic	Fenofibrate	Antilipidemic
Mepivacaine-HCl	Anesthetic	Finasteride	Benign prostatic hypertrophy treatment
Mometasone furoate	Anti-inflammatory, anti-allergic	Fluorouracil	Antineoplastic
Propranolol-HCl	Antihypertensive, anti-anxiety, anti-arrhythmic	Granisetron-HCl*	Antiemetic
Anastrozole	Antineoplastic	Gemfibrozil	Antilipemic
Budesonide	Anti-inflammatory	Carmustine**	Antineoplastic
Clotrimazole	Antifungal	Danazol	Estrogen antagonist, endometriosis treatment
Fulvestrant	Antineoplastic, hormonal	Mifepristone	Contraceptive
Pentostatin	Antineoplastic	Misoprostol	Anti-ulcer agent, abortifacient agent
Rimantadine	Antiviral	Megestrol acetate	Contraceptive, hormonal, antineoplastic
Terconazole	Antifungal	Mometasone furoate	Anti-inflammatory, antiallergic
Testosterone enanthate	Androgen	Metaxalone	Hypnotic/sedative, muscle relaxant
Trimipramine maleate*	Antidepressant	Methyldopa sesquihydrate	Antihypertensive
Clomiphene citrate	Estrogen modulator, fertility agent	Methylprednisolone	Anti-inflammatory, antiemetic,

			neuroprotective
Dextromethorphan	Antitussive drug	Nabumetone	Non-steroidal anti-inflammatory, antineoplastic
Diclofenac	Non-steroidal anti-inflammatory	Nitisinone*	Hereditary tyrosinemia type 1 treatment
Fexofenadine-HCl	Antihistamine	Orlistat*	Antiobesity agent
Granisetron-HCl*	Antiemetic	Pantoprazole	Treatment for GERD and acute gastritis
Guanidine-HCl	Myasthenia treatment	Paroxetine-HCl	Antidepressant
Hydroxyurea	Antineoplastic	Podofilox	Antineoplastic
Nitisinone*	Hereditary tyrosinemia type 1 treatment	Trimipramine maleate*	Antidepressant
Orlistat*	Anti-obesity agent	Itraconazole	Antifungal
		Levonorgestrel	Contraceptive
		Loratadine	Anti-allergic, antihistamine
		Losartan-K	Antihypertensive, antiarrhythmic
		Mebendazole	Anthelmintic
		Mefenamic acid	Non-steroidal anti-inflammatory, analgesic, antipyretic
		Melphalan	Antineoplastic
		Propafenone-HCl	Antiarrhythmic agent
		Quetiapine Fumarate	Antipsychotic
		Imipramine	Antidepressant
		Entacapone	Antiparkinsonian
		Carvedilol	Antihypertensive, congestive heart failure treatment
		Gefitinib	Antineoplastic
		Nimodipine	Antihypertensive, vasodilator
		Trifluoperazine-HCl	Antipsychotic, antiemetics

		Bromocriptine mesylate	Antiparkinson, antidyskinetic, management of hyperprolactinemia
		Ethacrynic acid*	Diuretic
		Raloxifene-HCl	Antihypocalcemic, osteoporosis prophylactic

**Drug identified as Tier 1 for one treatment, but Tier 2 for other

*Drug1 identified as Tier 2 for both pre- and post-treatment

References

1. Perry RD, Fetherston JD. 1997. *Yersinia pestis* - Etiologic agent of plague. Clin Microbiol Rev.
2. Inglesby T V, Dennis DT, Henderson D a, Bartlett JG, Ascher MS, Eitzen E, Fine a D, Friedlander a M, Hauer J, Koerner JF, Layton M, McDade J, Osterholm MT, O'Toole T, Parker G, Perl TM, Russell PK, Schoch-Spana M, Tonat K. 2000. Plague as a biological weapon: medical and public health management. Working Group on Civilian Biodefense. JAMA 283:2281–2290.
3. Russell P, Eley SM, Green M, Stagg AJ, Taylor RR, Nelson M, Beedham RJ, Bell DL, Rogers D, Whittington D, Titball RW. 1998. Efficacy of doxycycline and ciprofloxacin against experimental *Yersinia pestis* infection. J Antimicrob Chemother 41:301–305.
4. Ligon BL. 2006. Plague: A Review of its History and Potential as a Biological Weapon. Semin Pediatr Infect Dis 17:161–170.
5. Duan R, Liang J, Shi G, Cui Z, Hai R, Wang P, Xiao Y, Li K, Qiu H, Gu W, Du X, Jing H, Wanga X. 2014. Homology analysis of pathogenic *Yersinia* species *Yersinia enterocolitica*, *Yersinia pseudotuberculosis*, and *Yersinia pestis* based on multilocus sequence typing. J Clin Microbiol 52:20–29.
6. Rasmussen S, Allentoft ME, Nielsen K, Orlando L, Sikora M, Sjögren KG, Pedersen AG, Schubert M, Van Dam A, Kapel CMO, Nielsen HB, Brunak S, Avetisyan P, Epimakhov A, Khalyapin MV, Gnuni A, Kriiska A, Lasak I, Metspalu M, Moiseyev V, Gromov A, Pokutta D, Saag L, Varul L, Yepiskoposyan L, Sicheritz-Pontén T, Foley RA, Lahr MM, Nielsen R, Kristiansen K, Willerslev E. 2015. Early Divergent Strains of *Yersinia pestis* in Eurasia 5,000 Years Ago. Cell 163:571–582.
7. Balada-Llasat JM, Meccas J. 2006. *Yersinia* has a tropism for B and T cell zones of lymph nodes that is independent of the type III secretion system. PLoS Pathog 2:0816–0828.
8. Parkhill J, Wren BW, Thomson NR, Titball RW, Holden MT, Prentice MB, Sebahia M, James KD, Churcher C, Mungall KL, Baker S, Basham D, Bentley SD, Brooks K, Cerdeño-Tárraga a M, Chillingworth T, Cronin a, Davies RM, Davis P, Dougan G, Feltwell T, Hamlin N, Holroyd S, Jagels K, Karlyshev a V, Leather S, Moule S, Oyston PC, Quail M, Rutherford K, Simmonds M, Skelton J, Stevens K, Whitehead S, Barrell BG. 2001. Genome sequence of *Yersinia pestis*, the causative agent of plague. Nature 413:523–527.
9. Williamson ED. 2009. Plague. Vaccine 27.
10. Eisen RJ, Gage KL. 2009. Adaptive strategies of *Yersinia pestis* to persist during inter-epizootic and epizootic periods. Vet Res.
11. Oyston PCF, Williamson D. 2011. Plague: Infections of companion animals and

opportunities for intervention. *Animals*.

12. Cornelis GR. 2002. *Yersinia* type III secretion: Send in the effectors. *J Cell Biol*.
13. Plano G V., Schesser K. 2013. The *Yersinia pestis* type III secretion system: Expression, assembly and role in the evasion of host defenses. *Immunol Res* 57:237–245.
14. Pha K, Navarro L. 2016. *Yersinia* type III effectors perturb host innate immune responses. *World J Biol Chem* 7:1–13.
15. Bergsbaken T, Cookson BT. 2009. Innate immune response during *Yersinia* infection: critical modulation of cell death mechanisms through phagocyte activation. *J Leukoc Biol* 86:1153–1158.
16. Dewoody RS, Merritt PM, Marketon MM. 2013. Regulation of the *Yersinia* type III secretion system: traffic control. *Front Cell Infect Microbiol* 3:4.
17. Rosqvist R, Forsberg, Rimpiläinen M, Bergman T, Wolf-Watz H. 1990. The cytotoxic protein YopE of *Yersinia* obstructs the primary host defence. *Mol Microbiol* 4:657–667.
18. Ratner D, Orning MPA, Proulx MK, Wang D, Gavrillin MA, Wewers MD, Alnemri ES, Johnson PF, Lee B, Mecsas J, Kayagaki N, Goguen JD, Lien E. 2016. The *Yersinia pestis* Effector YopM Inhibits Pyrin Inflammasome Activation. *PLoS Pathog* 12.
19. Sha J, Pillai L, Fadl AA, Galindo CL, Erova TE, Chopra AK. 2005. The type III secretion system and cytotoxic enterotoxin alter the virulence of *Aeromonas hydrophila*. *Infect Immun* 73:6446–6457.
20. Rosenzweig JA, Jejelowo O, Sha J, Erova TE, Brackman SM, Kirtley ML, Van Lier CJ, Chopra AK. 2011. Progress on plague vaccine development. *Appl Microbiol Biotechnol*.
21. Feodorova VA, Motin VL. 2012. Plague vaccines: Current developments and future perspectives. *Emerg Microbes Infect* 1:0.
22. Simpson WJ, Thomas RE, Schwan TG. 1990. Recombinant capsular antigen (fraction 1) from *Yersinia pestis* induces a protective antibody response in BALB/c mice. *Am J Trop Med Hyg* 43:389–396.
23. Sha J, Endsley JJ, Kirtley ML, Foltz SM, Huante MB, Erova TE, Kozlova E V., Popov VL, Yeager LA, Zudina I V., Motin VL, Peterson JW, DeBord KL, Chopra AK. 2011. Characterization of an F1 deletion mutant of *Yersinia pestis* CO92, pathogenic role of F1 antigen in bubonic and pneumonic plague, and evaluation of sensitivity and specificity of F1 antigen capture-based dipsticks. *J Clin Microbiol* 49:1708–1715.
24. Hu P, Elliott J, McCready P, Skowronski E, Garnes J, Kobayashi A, Brubaker RR, Garcia E. 1998. Structural organization of virulence-associated plasmids of *Yersinia pestis*. *J Bacteriol* 180:5192–5202.
25. Du Y, Rosqvist R, Forsberg Å. 2002. Role of fraction 1 antigen of *Yersinia pestis*

- in inhibition of phagocytosis. *Infect Immun* 70:1453–1460.
26. Chen TH, Elberg SS. 1977. Scanning electron microscopic study of virulent *Yersinia pestis* and *Yersinia pseudotuberculosis* type 1. *Infect Immun* 15:972–7.
 27. Quenee LE, Cornelius CA, Ciletti NA, Elli D, Schneewind O. 2008. *Yersinia pestis* cafI variants and the limits of plague vaccine protection. *Infect Immun* 76:2025–2036.
 28. Welkos SL, Friedlander AM, Davis KJ. 1997. Studies on the role of plasminogen activator in systemic infection by virulent *Yersinia pestis* strain C092. *Microb Pathog* 23:211–223.
 29. Lathem WW, Price P a, Miller VL, Goldman WE. 2007. A plasminogen-activating protease specifically controls the development of primary pneumonic plague. *Science* 315:509–513.
 30. Van Lier CJ, Sha J, Kirtley ML, Cao A, Tiner BL, Erova TE, Cong Y, Kozlova E V., Popov VL, Baze WB, Chopra AK. 2014. Deletion of braun lipoprotein and plasminogen-activating protease-encoding genes attenuates *Yersinia pestis* in mouse models of bubonic and pneumonic plague. *Infect Immun* 82:2485–2503.
 31. van Lier CJ, Tiner BL, Chauhan S, Motin VL, Fitts EC, Huante MB, Endsley JJ, Ponnusamy D, Sha J, Chopra AK. 2015. Further characterization of a highly attenuated *Yersinia pestis* CO92 mutant deleted for the genes encoding Braun lipoprotein and plasminogen activator protease in murine alveolar and primary human macrophages. *Microb Pathog* 80:27–38.
 32. Robinson JB, Telepnev M V., Zudina I V., Bouyer D, Montenieri JA, Bearden SW, Gage KL, Agar SL, Foltz SM, Chauhan S, Chopra AK, Motin VL. 2009. Evaluation of a *Yersinia pestis* mutant impaired in a thermoregulated type VI-like secretion system in flea, macrophage and murine models. *Microb Pathog* 47:243–251.
 33. Boyer F, Fichant G, Berthod J, Vandenbrouck Y, Attree I. 2009. Dissecting the bacterial type VI secretion system by a genome wide *in silico* analysis: what can be learned from available microbial genomic resources? *BMC Genomics* 10:104.
 34. Filloux A. 2013. The rise of the Type VI secretion system. *F1000 Prime Rep* 5:52.
 35. Records AR. 2011. The type VI secretion system: A multipurpose delivery system with a phage-like machinery. *Mol Plant-Microbe Interact* 24:751–757.
 36. Russell AB, Peterson SB, Mougous JD. 2014. Type VI secretion system effectors: poisons with a purpose. *Nat Rev Microbiol* 12:137–48.
 37. Ponnusamy D, Fitts EC, Sha J, Erova TE, Kozlova E V., Kirtley ML, Tiner BL, Andersson JA, Chopra AK. 2015. High-throughput, signature-tagged mutagenic approach to identify novel virulence factors of *Yersinia pestis* CO92 in a mouse model of infection. *Infect Immun* 83:2065–2081.
 38. Sha J, Agar SL, Baze WB, Olano JP, Fadl AA, Erova TE, Wang S, Foltz SM, Suarez G, Motin VL, Chauhan S, Kumpel GR, Peterson JW, Chopra AK. 2008. Braun lipoprotein (Lpp) contributes to virulence of *Yersinia*: Potential role of Lpp

- in inducing bubonic and pneumonic plague. *Infect Immun* 76:1390–1409.
39. Andam CP, Worby CJ, Chang Q, Campana MG. 2016. Microbial Genomics of Ancient Plagues and Outbreaks. *Trends Microbiol*.
 40. Prentice MB, Rahalison L. 2007. Plague. *Lancet* 369:1196–1207.
 41. Wheelis M. 2002. Biological warfare at the 1346 siege of Caffa. *Emerg Infect Dis*.
 42. Zilinskas R a. 2006. The anti-plague system and the Soviet biological warfare program. *Crit Rev Microbiol* 32:47–64.
 43. Noah DL, Huebner KD, Darling RG, Waeckerle JF. 2002. The history and threat of biological warfare and terrorism. *Emerg Med Clin North Am*.
 44. WHO. 2017. Plague: Fact Sheet.
 45. Centers for Disease Control. 2012. CDC - History - Plague. Plague.
 46. Maher SP, Ellis C, Gage KL, Ensore RE, Peterson AT. 2010. Range-wide determinants of plague distribution in North America. *Am J Trop Med Hyg* 83:736–742.
 47. Adams D a, Jajosky RA, Ajani U, Kriseman J, Sharp P, Onwen DH, Schley AW, Anderson WJ, Grigoryan A, Aranas AE, Wodajo MS, Abellera JP. 2014. Summary of notifiable diseases - United States, 2012. *MMWR Morb Mortal Wkly Rep* 61:1–121.
 48. Hannah Gould L, Pape J, Ettestad P, Griffith KS, Mead PS. 2008. Dog-associated risk factors for human plague. *Zoonoses Public Health* 55:448–454.
 49. Runfola JK, House J, Miller L, Colton L, Hite D, Hawley A, Mead P, Schriefer M, Petersen J, Casaceli C, Erlandson KM, Foster C, Pabilonia KL, Mason G, Douglas JM. 2015. Outbreak of Human Pneumonic Plague with Dog-to-Human and Possible Human-to-Human Transmission - Colorado, June-July 2014. *MMWR Morb Mortal Wkly Rep* 64:429–434.
 50. Kugeler KJ, Staples JE, Hinckley AF, Gage KL, Mead PS. 2015. Epidemiology of human plague in the United States, 1900 - 2012. *Emerg Infect Dis* 21:16–22.
 51. Hinckley AF Biggerstaff BJ Griffith KS Mead PS. 2012. Transmission dynamics of primary pneumonic plague in the USA. *Epidemiol Infect* 140:554–560.
 52. Kwit N, Nelson C, Kugeler K, Petersen J, Plante L, Yaglom H, Kramer V, Schwartz B, House J, Colton L, Feldpausch A, Drenzek C, Baumbach J, DiMenna M, Fisher E, Debess E, Buttke D, Weinburke M, Percy C, Schriefer M, Gage K, Mead P. 2015. Human Plague - United States, 2015. *MMWR Morb Mortal Wkly Rep* 64:918–9.
 53. Stack L. 2017. Plague is found in New Mexico. Again. *New York Times*. New York.
 54. Butler T. 2013. Review article: Plague gives surprises in the first decade of the 21st century in the United States and worldwide. *Am J Trop Med Hyg* 89:788–793.

55. Pechous RD, Sivaraman V, Stasulli NM, Goldman WE. 2016. Pneumonic Plague: The Darker Side of *Yersinia pestis*. Trends Microbiol.
56. Butler T. 2009. Plague into the 21st Century. Clin Infect Dis 49:736–742.
57. Peterson JW, Moen ST, Healy D, Pawlik JE, Taormina J, Hardcastle J, Thomas JM, Lawrence WS, Ponce C, Chatuev BM, Gnade BT, Foltz SM, Agar SL, Sha J, Klimpel GR, Kirtley ML, Eaves-Pyles T, Chopra AK. 2010. Protection afforded by fluoroquinolones in animal models of respiratory infections with *Bacillus anthracis*, *Yersinia pestis*, and *Francisella tularensis*. Open Microbiol J 4:34–46.
58. Boulanger LL, Ettestad P, Fogarty JD, Dennis DT, Romig D, Mertz G. 2004. Gentamicin and tetracyclines for the treatment of human plague: review of 75 cases in new Mexico, 1985-1999. Clin Infect Dis 38:663–669.
59. Guiyoule A, Gerbaud G, Buchrieser C, Galimand M, Rahalison L, Chanteau S, Courvalin P, Carniel E. 2001. Transferable plasmid-mediated resistance to streptomycin in a clinical isolate of *Yersinia pestis*. Emerg Infect Dis 7:43–48.
60. Galimand M, Guiyoule A, Gerbaud G, Rasoamanana B, Chanteau S, Carniel E, Courvalin P, Buchrieser C, Michel P, Chanteau S, Carniel E, Kajdacs B, Costa F, Hyseni C, Porter F, Brown J, Rodrigues G, Farias H, Reis MG, Childs JE, Ko AI, Caccone A, Ramalingaswami V, Riedel S, Sokhey S, Wagle P, Habbu M. 1997. Multidrug resistance in *Yersinia pestis* mediated by a transferable plasmid. Nat Med 22:677–80.
61. Kiefer D, Dalantai G, Damdindorj T, Riehm JM, Tomaso H, Zöller L, Dashdavaa O, Pfister K, Scholz HC. 2012. Phenotypical characterization of Mongolian *Yersinia pestis* strains. Vector Borne Zoonotic Dis 12:183–8.
62. Smiley ST. 2008. Current challenges in the development of vaccines for pneumonic plague. Expert Rev Vaccines 7:209–221.
63. Titball RW, Williamson ED. 2004. *Yersinia pestis* (plague) vaccines. Expert Opin Biol Ther 4:965–73.
64. Williamson ED, Packer PJ, Waters EL, Simpson AJ, Dyer D, Hartings J, Twenhafel N, Pitt MLM. 2011. Recombinant (F1 + V) vaccine protects cynomolgus macaques against pneumonic plague. Vaccine 29:4771–4777.
65. Williamson ED, Flick-Smith HC, LeButt C, Rowland CA, Jones SM, Waters EL, Gwyther RJ, Miller J, Packer PJ, Irving M. 2005. Human immune response to a plague vaccine comprising recombinant F1 and V antigens. Infect Immun 73:3598–3608.
66. Lin J-S, Kummer LW, Szaba FM, Smiley ST. 2011. IL-17 contributes to cell-mediated defense against pulmonary *Yersinia pestis* infection. J Immunol 186:1675–84.
67. Parent MA, Berggren KN, Kummer LW, Wilhelm LB, Szaba FM, Mullarky IK, Smiley ST. 2005. Cell-mediated protection against pulmonary *Yersinia pestis* infection. Infect Immun 73:7304–7310.
68. Tiner BL, Sha J, Ponnusamy D, Baze WB, Fitts EC, Popov VL, Van Lier CJ,

- Erova TE, Chopra AK. 2015. Intramuscular immunization of mice with a live-Attenuated triple mutant of *Yersinia pestis* CO92 induces robust humoral and cell-mediated immunity to completely protect animals against pneumonic plague. *Clin Vaccine Immunol* 22:1255–1268.
69. Tao P, Mahalingam M, Zhu J, Moayeri M, Kirtley ML, Fitts EC, Andersson JA, Lawrence WS, Leppla SH, Chopra AK, Rao VB. 2017. A Bivalent Anthrax–Plague Vaccine That Can Protect against Two Tier-1 Bioterror Pathogens, *Bacillus anthracis* and *Yersinia pestis*. *Front Immunol* 8.
 70. Sha J, Kirtley ML, Klages C, Erova TE, Telepnev M, Ponnusamy D, Fitts EC, Baze WB, Sivasubramani SK, Lawrence WS, Patrikeev I, Peel JE, Andersson JA, Kozlova E V., Tiner BL, Peterson JW, McWilliams D, Patel S, Rothe E, Motin VL, Chopra AK. 2016. A replication-defective human type 5 adenovirus-based trivalent vaccine confers complete protection against plague in mice and nonhuman primates. *Clin Vaccine Immunol* 23:586–600.
 71. Anisimov AP, Dentovskaya S V., Panfertsev EA, Svetoch TE, Kopylov PK, Segelke BW, Zemla A, Telepnev M V., Motin VL. 2010. Amino acid and structural variability of *Yersinia pestis* LcrV protein. *Infect Genet Evol* 10:137–145.
 72. Centers for Disease Control and Prevention (CDC). 2011. Fatal laboratory-acquired infection with an attenuated *Yersinia pestis* Strain--Chicago, Illinois, 2009. *MMWR Morb Mortal Wkly Rep* 60:201–5.
 73. Pukatzki S, Ma AT, Sturtevant D, Krastins B, Sarracino D, Nelson WC, Heidelberg JF, Mekalanos JJ. 2006. Identification of a conserved bacterial protein secretion system in *Vibrio cholerae* using the *Dictyostelium* host model system. *Proc Natl Acad Sci* 103:1528–1533.
 74. Burtnick MN, Brett PJ, Harding S V., Ngugi SA, Ribot WJ, Chantratita N, Scorpio A, Milne TS, Dean RE, Fritz DL, Peacock SJ, Prior JL, Atkins TP, DeShazer D. 2011. The cluster 1 type VI secretion system is a major virulence determinant in *Burkholderia pseudomallei*. *Infect Immun* 79:1512–1525.
 75. Grim CJ, Kozlova E V., Ponnusamy D, Fitts EC, Sha J, Kirtley ML, van Lier CJ, Tiner BL, Erova TE, Joseph SJ, Read TD, Shak JR, Joseph SW, Singletary E, Felland T, Baze WB, Horneman AJ, Chopra AK. 2014. Functional genomic characterization of virulence factors from necrotizing fasciitis-causing strains of *Aeromonas hydrophila*. *Appl Environ Microbiol* 80:4162–4183.
 76. Mougous JD, Cuff ME, Raunser S, Shen A, Zhou M, Gifford CA, Goodman AL, Joachimiak G, Ordoñez CL, Lory S, Walz T, Joachimiak A, Mekalanos JJ. 2006. A virulence locus of *Pseudomonas aeruginosa* encodes a protein secretion apparatus. *Science* 312:1526–30.
 77. Parsons DA, Heffron F. 2005. sciS, an icmF homolog in *Salmonella enterica* serovar Typhimurium, limits intracellular replication and decreases virulence. *Infect Immun* 73:4338–4345.
 78. Rigard M, Bröms JE, Mosnier A, Hologne M, Martin A, Lindgren L, Punginelli C,

- Lays C, Walker O, Charbit A, Telouk P, Conlan W, Terradot L, Sjöstedt A, Henry T. 2016. *Francisella tularensis* IglG Belongs to a Novel Family of PAAR-Like T6SS Proteins and Harbors a Unique N-terminal Extension Required for Virulence. *PLoS Pathog* 12.
79. Schell MA, Ulrich RL, Ribot WJ, Brueggemann EE, Hines HB, Chen D, Lipscomb L, Kim HS, Mrázek J, Nierman WC, DeShazer D. 2007. Type VI secretion is a major virulence determinant in *Burkholderia mallei*. *Mol Microbiol* 64:1466–1485.
 80. Sha J, Rosenzweig JA, Kozlova E V., Wang S, Erova TE, Kirtley ML, van Lier CJ, Chopra AK. 2013. Evaluation of the roles played by Hcp and VgrG type 6 secretion system effectors in *Aeromonas hydrophila* SSU pathogenesis. *Microbiol (United Kingdom)* 159:1120–1135.
 81. Suarez G, Sierra JC, Sha J, Wang S, Erova TE, Fadl AA, Foltz SM, Horneman AJ, Chopra AK. 2008. Molecular characterization of a functional type VI secretion system from a clinical isolate of *Aeromonas hydrophila*. *Microb Pathog* 44:344–361.
 82. Datsenko KA, Wanner BL. 2000. One-step inactivation of chromosomal genes in *Escherichia coli* K-12 using PCR products. *Proc Natl Acad Sci U S A* 97:6640–5.
 83. Fitts EC, Andersson JA, Kirtley ML, Sha J, Erova TE, Chauhan S, Motin VL, Chopra AK. 2016. New insights into autoinducer-2 signaling as a virulence regulator in a mouse model of pneumonic plague. *mSphere* 1:1–16.
 84. Galindo CL, Sha J, Moen ST, Agar SL, Kirtley ML, Foltz SM, McIver LJ, Kozlova E V., Garner HR, Chopra AK. 2010. Comparative global gene expression profiles of wild-type *Yersinia pestis* CO92 and its braun lipoprotein mutant at flea and human body temperatures. *Comp Funct Genomics* 2010.
 85. Suarez G, Sierra JC, Kirtley ML, Chopra AK. 2010. Role of Hcp, a type 6 secretion system effector, of *Aeromonas hydrophila* in modulating activation of host immune cells. *Microbiology* 156:3678–3688.
 86. Andersson JA, Fitts EC, Kirtley ML, Ponnusamy D, Peniche AG, Dann SM, Motin VL, Chauhan S, Rosenzweig JA, Sha J, Chopra AK. 2016. New role for FDA-approved drugs in combating antibiotic-resistant bacteria. *Antimicrob Agents Chemother* 60:3717–3729. *Sections of Chapter 3 and Chapter 4 taken verbatim from this reference.*
 87. Tiner BL, Sha J, Kirtley ML, Erova TE, Popov VL, Baze WB, van Lier CJ, Ponnusamy D, Andersson JA, Motin VL, Chauhan S, Chopra AK. 2015. Combinational deletion of three membrane protein-encoding genes highly attenuates *Yersinia pestis* while retaining immunogenicity in a mouse model of pneumonic plague. *Infect Immun* 83:1318–1338.
 88. Hatcher CL, Mott TM, Muruato LA, Sbrana E, Torresaga AG. 2016. *Burkholderia mallei* CLH001 attenuated vaccine strain is immunogenic and protects against acute respiratory glanders. *Infect Immun* 84:2345–2354.
 89. Qin Y, Polacek N, Vesper O, Staub E, Einfeldt E, Wilson DN, Nierhaus KH. 2006.

The highly conserved LepA is a ribosomal elongation factor that back-translocates the ribosome. *Cell* 127:721–733.

90. Moscoso JA, Mikkelsen H, Heeb S, Williams P, Filloux A. 2011. The *Pseudomonas aeruginosa* sensor RetS switches Type III and Type VI secretion via c-di-GMP signalling. *Environ Microbiol* 13:3128–3138.
91. CDC. 2013. Antibiotic resistance threats in the United States, 2013 | Antibiotic/Antimicrobial Resistance | CDC/CDC.
92. Fernandes P. 2015. The global challenge of new classes of antibacterial agents: An industry perspective. *Curr Opin Pharmacol*.
93. Ashburn TT, Thor KB. 2004. Drug repositioning: identifying and developing new uses for existing drugs. *Nat Rev Drug Discov* 3:673–683.
94. Law GL, Tisoncik-Go J, Korth MJ, Katze MG. 2013. Drug repurposing: a better approach for infectious disease drug discovery? *Curr Opin Immunol*.
95. Czyż DM, Potluri LP, Jain-Gupta N, Riley SP, Martinez JJ, Steck TL, Crosson S, Shuman HA, Gabay JE. 2014. Host-directed antimicrobial drugs with broad-spectrum efficacy against intracellular bacterial pathogens. *MBio* 5:e01534–e01514.
96. Chiu HC, Kulp SK, Soni S, Wang D, Gunn JS, Schlesinger LS, Chen CS. 2009. Eradication of intracellular *Salmonella enterica* serovar Typhimurium with a small-molecule, host cell-directed agent. *Antimicrob Agents Chemother* 53:5236–5244.
97. Wallis RS, Hafner R. 2015. Advancing host-directed therapy for tuberculosis. *Nat Rev Immunol* 15:255–263.
98. Feng J, Wang T, Zhang S, Shi W, Zhang Y. 2014. An optimized SYBR green I/PI assay for rapid viability assessment and antibiotic susceptibility testing for *Borrelia burgdorferi*. *PLoS One* 9.
99. Kouznetsova J, Sun W, Martínez-Romero C, Tawa G, Shinn P, Chen CZ, Schimmer A, Sanderson P, McKew JC, Zheng W, García-Sastre A. 2014. Identification of 53 compounds that block Ebola virus-like particle entry via a repurposing screen of approved drugs. *Emerg Microbes Infect* 3:e84.
100. Zumla A, Rao M, Parida SK, Keshavjee S, Cassell G, Wallis R, Axelsson-Robertsson R, Doherty M, Andersson J, Maeurer MJ. 2015. Inflammation and tuberculosis: Host-directed therapies. *J Intern Med*.
101. Galimand M, Carniel E, Courvalin P. 2006. Resistance of *Yersinia pestis* to antimicrobial agents. *Antimicrob Agents Chemother* 50:3233–3236.
102. Lukaszewski RA, Kenny DJ, Taylor R, Rees DGC, Hartley MG, Oyston PCF. 2005. Pathogenesis of *Yersinia pestis* infection in BALB/c mice: Effects on host macrophages and neutrophils. *Infect Immun* 73:7142–7150.
103. Bi Y, Du Z, Han Y, Guo Z, Tan Y, Zhu Z, Yang R. 2009. *Yersinia pestis* and host macrophages: Immunodeficiency of mouse macrophages induced by YscW.

Immunology 128.

104. Weeks S, Hill J, Friedlander a, Welkos S. 2002. Anti-V antigen antibody protects macrophages from *Yersinia pestis* -induced cell death and promotes phagocytosis. Microb Pathog 32:227–37.
105. Agar SL, Sha J, Baze WB, Erova TE, Foltz SM, Suarez G, Wang S, Chopra AK. 2009. Deletion of Braun lipoprotein gene (lpp) and curing of plasmid pPCP1 dramatically alter the virulence of *Yersinia pestis* CO92 in a mouse model of pneumonic plague. Microbiology 155:3247–3259.
106. Arciszewska LK, Drake D, Craig NL. 1989. Transposon Tn7. J Mol Biol 207:35–52.
107. Box PO. 2004. on the Toxicology and Carcinogenesis Studies of Dipropylene Glycol in F344 / N Rats and B6C3F 1 Mice (Drinking Water Studies) National Toxicology Program.
108. Viyoch J, Ohdo S, Yukawa E, Higuchi S. 2001. Dosing time-dependent tolerance of catalepsy by repetitive administration of haloperidol in mice. J Pharmacol Exp Ther 298:964–9.
109. Inagaki N, Nagao M, Nakamura N, Kawasaki H, Igeta K, Musoh K, Nagai H. 2000. Evaluation of anti-scratch properties of oxatomide and epinastine in mice. Eur J Pharmacol 400:73–79.
110. Malatynska E, Rapp R, Harrawood D, Tunnicliff G. 2005. Submissive behavior in mice as a test for antidepressant drug activity. Pharmacol Biochem Behav 82:306–313.
111. Nasu R, Matsuo H, Takanaga H, Ohtani H, Sawada Y. 2000. Quantitative prediction of catalepsy induced by amoxapine, cinnarizine and cyclophosphamide in mice. Biopharm Drug Dispos 21:129–138.
112. Feng G, Kaplowitz N. 2000. Colchicine protects mice from the lethal effect of an agonistic anti-Fas antibody. J Clin Invest 105:329–339.
113. Senkevitch E, Cabrera-Luque J, Morizono H, Caldovic L, Tuchman M. 2012. A novel biochemically salvageable animal model of hyperammonemia devoid of N-acetylglutamate synthase. Mol Genet Metab 106:160–168.
114. Ward JW, Gilbert DL, Franko B V., Woodard G, Mann GT. 1968. Toxicologic studies of doxapram hydrochloride. Toxicol Appl Pharmacol 13:242–250.
115. Zhidkov N, De Souza R, Ghassemi AH, Allen C, Piquette-Miller M. 2013. Continuous intraperitoneal carboplatin delivery for the treatment of late-stage ovarian cancer. Mol Pharm 10:3315–3322.
116. Agarkov A, Chauhan S, Lory PJ, Gilbertson SR, Motin VL. 2008. Substrate specificity and screening of the integral membrane protease Pla. Bioorganic Med Chem Lett 18:427–431.
117. Peters KN, Dhariwala MO, Hughes Hanks JM, Brown CR, Anderson DM. 2013. Early Apoptosis of Macrophages Modulated by Injection of *Yersinia pestis* YopK

Promotes Progression of Primary Pneumonic Plague. PLoS Pathog 9.

118. Advani MJ, Siddiqui I, Sharma P, Reddy H. 2012. Activity of Trifluoperazine against Replicating, Non-Replicating and Drug Resistant *M. tuberculosis*. PLoS One 7.
119. Rybníček J, Vocat A, Sala C, Busso P, Pojer F, Benjak A, Cole ST. 2015. Lansoprazole is an antituberculous prodrug targeting cytochrome bc1. Nat Commun 6:7659.
120. Bartra SS, Styer KL, O'Bryant DM, Nilles ML, Hinnebusch BJ, Aballay A, Plano G V. 2008. Resistance of *Yersinia pestis* to complement-dependent killing is mediated by the ail outer membrane protein. Infect Immun 76:612–622.
121. Schwegmann A, Brombacher F. 2008. Host-directed drug targeting of factors hijacked by pathogens. Sci Signal 1:re8.
122. Euba B, Moleres J, Segura V, Viadas C, Morey P, Moranta D, Leiva J, De-Torres JP, Bengoechea JA, Garmendia J. 2015. Genome expression profiling-based identification and administration efficacy of host-directed antimicrobial drugs against respiratory infection by nontypeable *Haemophilus influenzae*. Antimicrob Agents Chemother 59:7581–7592.
123. Steth SD, Steh V. 2009. Textbook of PharmacologyTextbook of Pharmacology.
124. Caspar M, Florin I, Thelestam M. 1987. Calcium and calmodulin in cellular intoxication with *Clostridium difficile* toxin B. J Cell Physiol 132:168–172.
125. Mazumder R, Ganguly K, Dastidar SG, Chakrabarty AN. 2001. Trifluoperazine: A broad spectrum bactericide especially active on *Staphylococci* and *Vibrios*. Int J Antimicrob Agents 18:403–406.
126. Hendricks O, Butterworth TS, Kristiansen JE. 2003. The in-vitro antimicrobial effect of non-antibiotics and putative inhibitors of efflux pumps on *Pseudomonas aeruginosa* and *Staphylococcus aureus*. Int J Antimicrob Agents 22:262–264.
127. Gadre D V, Talwar V, Gupta HC, Murthy PS. 1998. Effect of trifluoperazine, a potential drug for tuberculosis with psychotic disorders, on the growth of clinical isolates of drug resistant *Mycobacterium tuberculosis*. Int Clin Psychopharmacol 13:129–131.
128. Conway KL, Kuballa P, Song JH, Patel KK, Castoreno AB, Yilmaz OH, Jijon HB, Zhang M, Aldrich LN, Villablanca EJ, Peloquin JM, Goel G, Lee IA, Mizoguchi E, Shi HN, Bhan AK, Shaw SY, Schreiber SL, Virgin HW, Shamji AF, Stappenbeck TS, Reinecker HC, Xavier RJ. 2013. Atg16l1 is required for autophagy in intestinal epithelial cells and protection of mice from *Salmonella* infection. Gastroenterology 145:1347–1357.
129. O'Donnell J, Shelton R. 2011. Drug therapy of depression and anxiety disorders, p. 397–416. In Goodman and Gilman's pharmacological basis of therapeutics., 12th ed. McGraw-Hill, New York.
130. Kong R, Liu T, Zhu X, Ahmad S, Williams AL, Phan AT, Zhao H, Scott JE, Yeh LA, Wong STC. 2014. Old drug new use - Amoxapine and its metabolites as

- potent bacterial β -glucuronidase inhibitors for alleviating cancer drug toxicity. *Clin Cancer Res* 20:3521–3530.
131. Gloux K, Berteau O, El Oumami H, Béguet F, Leclerc M, Doré J. 2011. A metagenomic β -glucuronidase uncovers a core adaptive function of the human intestinal microbiome. *Proc Natl Acad Sci U S A* 108 Suppl:4539–4546.
 132. Palmeira A, Rodrigues F, Sousa E, Pinto M, Vasconcelos MH, Fernandes MX. 2011. New uses for old drugs: Pharmacophore-based screening for the discovery of P-glycoprotein inhibitors. *Chem Biol Drug Des* 78:57–72.
 133. Bose T, Cieřlar-Pobuda A, Wiechec E. 2015. Role of ion channels in regulating Ca^{2+} homeostasis during the interplay between immune and cancer cells. *Cell Death Dis* 6:e1648.
 134. Eijkelkamp N, Linley JE, Baker MD, Minett MS, Cregg R, Werdehausen R, Rugiero F, Wood JN. 2012. Neurological perspectives on voltage-gated sodium channels. *Brain*.
 135. Ferguson LR, Cooper GJS, Loisselle DS, Robertson AM. 1989. A possible mechanism of toxicity by the antidepressant amoxapine based on its effects in three in vitro models. *Toxicol Vitr* 3:285–291.
 136. Lunsford CD, Cale AD, Ward JW, Franko B V, Jenkins H. 1964. 4-(beta-substituted ethyl)-3,3-diphenyl-2-Pyrrolidinone. A new series of CNS stimulants. *J Med Chem* 7:302–10.
 137. Yost CS. 2003. Update on tandem pore 2P domain K^+ channels. *Curr Drug Targets* 4:347–351.
 138. Chokshi RH, Larsen AT, Bhayana B, Cotten JF. 2015. Breathing stimulant compounds inhibit TASK-3 potassium channel function likely by binding at a common site in the channel pore. *Mol Pharmacol* 88:926–934.
 139. Cotten JF, Keshavaprasad B, Laster MJ, Eger EI, Yost CS. 2006. The ventilatory stimulant doxapram inhibits TASK tandem pore (K^+ 2P) potassium channel function but does not affect minimum alveolar anesthetic concentration. *Anesth Analg* 102:779–785.
 140. Kim D, Cavanaugh EJ, Kim I, Carroll JL. 2009. Heteromeric TASK-1/TASK-3 is the major oxygen-sensitive background K^+ channel in rat carotid body glomus cells. *J Physiol* 587:2963–75.
 141. Martins M, Viveiros M, Amaral L. 2008. Inhibitors of Ca^{2+} and K^+ transport enhance intracellular killing of *M. tuberculosis* by non-killing macrophages. *In Vivo (Brooklyn)* 22:69–76.
 142. Contreras RG, Flores-Maldonado C, Lázaro A, Shoshani L, Flores-Benitez D, Larré I, Cereijido M. 2004. Ouabain binding to Na^+ , K^+ -ATPase relaxes cell attachment and sends a specific signal (NACos) to the nucleus. *J Membr Biol* 198:147–158.
 143. Neu HC. 1992. The crisis in antibiotic resistance. *Science* 257:1064–73.

144. Threlfall EJ. 2002. Antimicrobial drug resistance in *Salmonella*: Problems and perspectives in food- and water-borne infections. FEMS Microbiol Rev 26:141–148.
145. Parry CM, Threlfall EJ. 2008. Antimicrobial resistance in typhoidal and nontyphoidal *Salmonellae*. Curr Opin Infect Dis 21:531–538.
146. Ananthakrishnan AN. 2011. *Clostridium difficile* infection: epidemiology, risk factors and management. Nat Rev Gastroenterol Hepatol 8:17–26.
147. DuPont HL. 2011. The search for effective treatment of *Clostridium difficile* infection. N Engl J Med 364:473–475.
148. Spigaglia P. 2016. Recent advances in the understanding of antibiotic resistance in *Clostridium difficile* infection. Ther Adv Infect Dis 3:23–42.
149. Shah D, Dang M-D, Hasbun R, Koo HL, Jiang Z-D, DuPont HL, Garey KW. 2010. *Clostridium difficile* infection: update on emerging antibiotic treatment options and antibiotic resistance. Expert Rev Anti Infect Ther 8:555–64.
150. Huang H, Weintraub A, Fang H, Nord CE. 2009. Antimicrobial resistance in *Clostridium difficile*. Int J Antimicrob Agents.
151. Chen X, Katchar K, Goldsmith JD, Nanthakumar N, Cheknis A, Gerding DN, Kelly CP. 2008. A mouse model of *Clostridium difficile*-associated disease. Gastroenterology 135:1984–1992.
152. Sorg JA, Dineen SS. 2009. Laboratory maintenance of *Clostridium difficile*. Curr Protoc Microbiol.
153. Liu T, König R, Sha J, Agar SL, Tseng CTK, Klimpel GR, Chopra AK. 2008. Immunological responses against *Salmonella enterica* serovar Typhimurium Braun lipoprotein and lipid A mutant strains in Swiss-Webster mice: Potential use as live-attenuated vaccines. Microb Pathog 44:224–237.
154. Kuo S-Y, Castoreno AB, Aldrich LN, Lassen KG, Goel G, Dančík V, Kuballa P, Latorre I, Conway KL, Sarkar S, Maetzel D, Jaenisch R, Clemons PA, Schreiber SL, Shamji AF, Xavier RJ. 2015. Small-molecule enhancers of autophagy modulate cellular disease phenotypes suggested by human genetics. Proc Natl Acad Sci U S A 112:E4281-7.
155. Tanida I, Ueno T, Kominami E. 2008. LC3 and autophagy. Methods Mol Biol 445:77–88.
156. Grant AJ, Oshota O, Chaudhuri RR, Mayho M, Peters SE, Clare S, Maskell DJ, Mastroeni P. 2016. Genes required for the fitness of *Salmonella enterica* serovar Typhimurium during infection of immunodeficient gp91^{-/-} phox mice. Infect Immun 84:989–997.
157. Spigaglia P. 2016. Recent advances in the understanding of antibiotic resistance in *Clostridium difficile* infection. Ther Adv Infect Dis 3:23–42.
158. Shah D, Dang M-D, Hasbun R, Koo HL, Jiang Z-D, DuPont HL, Garey KW. 2010. *Clostridium difficile* infection: update on emerging antibiotic treatment

- options and antibiotic resistance. *Expert Rev Anti Infect Ther* 8:555–64.
159. Kuo S-Y, Castoreno AB, Aldrich LN, Lassen KG, Goel G, Dančák V, Kuballa P, Latorre I, Conway KL, Sarkar S, Maetzel D, Jaenisch R, Clemons PA, Schreiber SL, Shamji AF, Xavier RJ. 2015. Small-molecule enhancers of autophagy modulate cellular disease phenotypes suggested by human genetics. *Proc Natl Acad Sci U S A* 112:E4281-7.
160. Mizushima N. 2007. Autophagy: Process and function. *Genes Dev*.
161. Levine B, Mizushima N, Virgin HW. 2011. Autophagy in immunity and inflammation. *Nature* 469:323–335.

Vita

Jourdan Alexandra Olga Andersson was born on October 31, 1989 in Gretna, Louisiana to Matts and Tammy Andersson. After graduating from Cy-Fair High School in Cypress, Texas in 2008, she attended Rensselaer Polytechnic Institute in Troy, NY, to pursue a bachelor's degree in biochemistry and biophysics. After receiving her B.S. in 2012, she returned to Texas to join the Human Pathophysiology and Translational Medicine doctoral program at the University of Texas Medical Branch in Galveston, TX to pursue a Ph.D. in the area of microbiology.

Permanent address: 14318 Spanish River Lane, Cypress, TX 77429

This dissertation was typed by Jourdan Andersson.

